Probing Asphaltenes Aggregation with Fluorescence Techniques

by

Hui Ting Zhang
B.Sc., University of Victoria, 2008

A Thesis Submitted in Partial Fulfillment
of the Requirements for the Degree of

MASTER OF SCIENCE

in the Department of Chemistry

© Hui Ting Zhang, 2010
University of Victoria

All rights reserved. This thesis may not be reproduced in whole or in part, by photocopy or other means, without the permission of the author.

Supervisory Committee

Probing Asphaltene Aggregation with Fluorescence Techniques

by

Hui Ting Zhang
B.Sc., University of Victoria, 2008

Supervisory Committee

Dr. Cornelia Bohne (Department of Chemistry)
Supervisor

Dr. Matthew Moffitt (Department of Chemistry)
Departmental Member

Dr. David Sinton (Department of Mechanical Engineering)
Outside Member

Abstract

Supervisory Committee
Dr. Cornelia Bohne (Department of Chemistry)
Supervisor
Dr. Matthew Moffitt (Department of Chemistry)
Departmental Member
Dr. David Sinton (Department of Mechanical Engineering)
Outside Member

Asphaltenes correspond to the fraction of oil that is insoluble in heptane but is soluble in toluene. The aggregates of asphaltene are of interest because they cause serious problems in the production of oil. Asphaltenes contain fluorescent moieties, and as such they can be studied by fluorescence techniques.

The first objective of this work was to develop methodologies to study the fluorescence of asphaltenes, and to investigate the fluorescence of asphaltenes at various concentrations. Time-resolved fluorescence studies indicate that asphaltenes have different chromophores with different lifetimes. The average lifetime of the asphaltene emission decreased when the asphaltene concentration was increased because of quenching processes occurring within the aggregates. The measurement of lifetimes at different excitation and emission wavelengths demonstrated that different components of asphaltene aggregate at different concentrations.

The second objective of this work was to investigate how accessible the asphaltene aggregate is to small molecules by fluorescence quenching experiments. Nitromethane was the quencher used in the fluorescence of asphaltenes. The quenching efficiencies were found to be independent of the concentration of asphaltenes. However, the quenching efficiencies differed for different chromophores, suggesting a selective

quenching for nitromethane of the excited states for the different chromophores of asphaltenes.

The third objective of this thesis was to investigate the fluorescence of externally added probes that might be incorporated in asphaltene aggregates through π–π stacking. Pyrene was chosen as the probe because its fluorescence properties are strongly affected by its surroundings. The pyrene emission was quenched by nitromethane. The quenching efficiencies determined for pyrene in the absence or the presence of asphaltene aggregates were the same. This suggests that pyrene is located in an open environment, where the asphaltene aggregates do not offer any protection for pyrene from nitromethane.

Table of Contents

List of Tables

List of Figures

List of Schemes

List of Abbreviations

A	absorbance
AA-5	50% heptane-insoluble Athabasca asphaltene
A_i	pre-exponential factor for species, i
Ant	anthracene
Å	angstrom
ca.	approximately
cm	centimetre
CMC	critical micelle concentration
CNAC	critical nanoaggregate concentration
^oC	degree Celsius
E	energy
F	fluorescence
g	gram
h	Plank's constant (6.63×10^{-34} J·s)
HPLC	high performance liquid chromatography
I	intensity
I_0	initial intensity
IC	internal conversion
IRF	instrument response function
ISC	intersystem crossing
k_0	intrinsic decay rate constant
k_f	fluorescence rate constant
k_{IC}	internal conversion rate constant
k_{ISC}	intersystem crossing rate constant
k_{obs}	observed rate constant
k_q	quenching rate constant
K_{eq}	equilibrium constant
L	litre
λ	wavelength (nm)

λ_{em}	emission wavelength
λ_{ex}	excitation wavelength
M	molar
$MeNO_2$	nitromethane
mg	milligram
mL	millilitre
mm	millimetre
mM	millimolar
mol	mole
μL	microlitre
μm	micrometre
μM	micromolar
μs	microsecond
N	nitrogen
Ni	nickel
nm	nanometre
ns	nanosecond
O	oxygen
P	phosphorescence
PAH	polyaromatic hydrocarbon
PRODEN	6-propionyl-2-(N,N-dimethylamino) naphthalene
Py	pyrene
Q	quencher
Φ_f	fluorescence quantum yield
s	second
S	sulphur
S_0	ground state
S_1	singlet excited state
SPC	single photon counting
t	time
T_1	triplet excited state

TRES	time resolved emission spectra
$<\tau>$	average lifetime
τ_0	fluorescence lifetime
$\tau_{obs,}$ τ_i	observed lifetime (of component, i)
V	vanadium
Vis-NIR	visible-near infrared
VR	vibrational relaxation
v	frequency (s^{-1})
UV	ultraviolet
UV-Vis	ultraviolet-visible

Acknowledgments

I would like to thank my supervisor, Dr. Cornelia Bohne, for her encouraging guidance and assistance throughout my graduate study time.

Special thanks to Luis Netter, for all the technical support; Hao Tang, who gave me great help when I started the work in the lab and the latter work throughout these three years; Tamara Pace, Rui Li and Cerize Santos, for their great professional help. I would also like to thank many colleagues in Bohne's research group and in the chemistry department.

Finally, I would like to thank COSI for the funding and provide the study opportunities.

Dedication

To my dear family

1. INTRODUCTION

1.1 Asphaltenes

1.1.1 The importance of asphaltenes

Asphaltenes correspond to the heaviest portion of crude oil, and solubility properties are used to separate them from the lighter portions of crude oils. Asphaltenes have applications as construction materials, such as for road pavement, and for roofing. Other lighter fractions of crude oils, such as butanes, gasoline, naphtha, and kerosene, are used as fuels or as industrial materials. These lighter fractions have higher commercial value as compare to asphaltenes.[1]

Crude oil has been used as an energy source for over one hundred years and it accounts for a large percentage of the energy consumption around the world. Crude oil can be classified into two categories: conventional oil and unconventional oil.[2] The oil extracted using methods for traditional oil well extraction is normally classified as conventional oil. On the other hand, unconventional oil refers to crude oil extracted using techniques other than oil well methods. Conventional oil is generally less dense and easy to refine compare to unconventional oil. Unconventional oil contains heavy oil, extra heavy oil and oil sands.[3] Unconventional oils are very viscous and some of them are solids, and for this reason they cannot be processed using traditional extraction and refining methods. Alternative methods have to be established in order to process unconventional oil, which increases the cost and lowers the economic value of these oil sources. Thus, conventional oil used to be the predominant oil source in the oil industry. However, the total world oil reserves include 30% of conventional oil and 70% of other

heavier oil sources.[3] As the demand for crude oil has risen continuously, conventional oil sources are declining, and for this reason the focus has moved to find substitution resources for oil production, such as extracting oil from oil sands.

Oil sands are sands coated with dense and sticky oil.[4] Canada has large reserves of oil sands, and oil sands production has grown in recent years. The crude oil produced from oil sands contributed to one-half of the Canadian oil production in 2009.[5] Oil sands contain large amounts of asphaltenes. For example, Athabasca crude oil, which comes from one of the largest deposits of oil sands in Canada, contains about 16.9% per weight of asphaltenes.[6] Research on asphaltenes is of interest to the oil industry because asphaltenes negatively impact oil production. For example, asphaltenes form precipitates that clog pipelines and surface facilities. Asphaltenes also contain a significant amount of contaminants that decrease the efficiency of oil refining, by for example poisoning catalysts used in hydrogenation processes. Therefore, the evaluation of the properties of asphaltenes and the understanding of the mechanism for asphaltene aggregation are very important to make the production of oil more effective from the economical and environmental points of view.[7]

1.1.2 Definition and composition of asphaltenes

The operational definition of asphaltenes is based on the solubility of the material in defined solvents.[7-9] In the laboratory, asphaltenes are precipitated from crude oil by adding n-alkanes. The light components of crude oil soluble in n-alkane are called maltenes. Maltenes can be further fractionated into saturated hydrocarbons, aromatic hydrocarbons, and resins based on their solubility in defined solvents. Asphaltenes are

insoluble in n-alkane but soluble in toluene. The separation of asphaltenes from crude oil is summarized in Scheme 1.1.

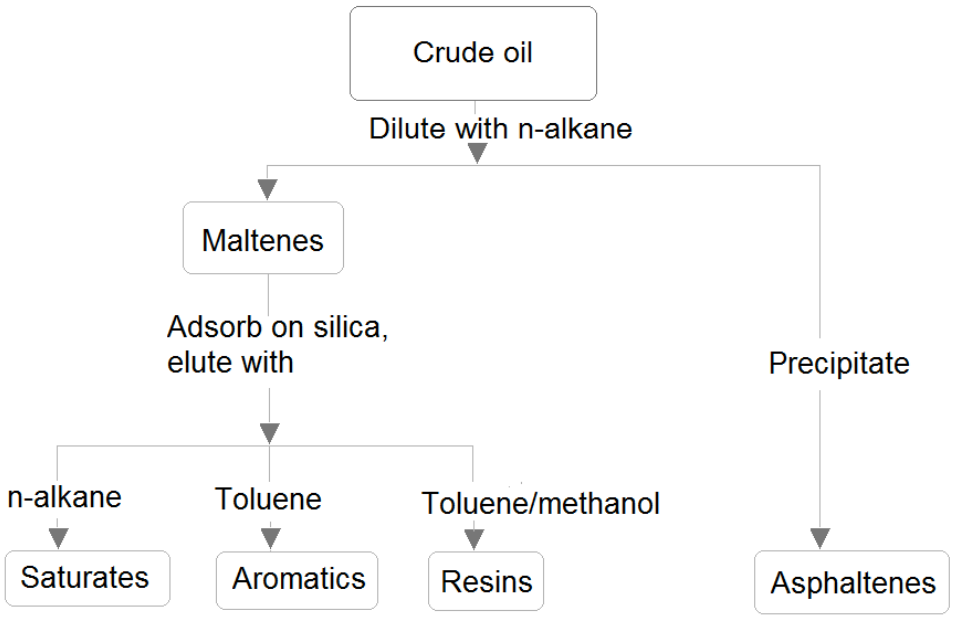

Scheme 1.1 Separation of crude oil into saturates, aromatics, resins and asphaltenes based on their solubility (adapted from reference 7).

The chemical composition is relatively easy to be determined in the light fractions of crude oils. For example, butane is one of the saturated compounds in maltenes, and it is easily distilled from crude oil because of its low boiling point (-0.5 ^{o}C).[1] The boiling points of the components of oil increase as the sizes of the molecules in the oil become larger and the molecular weights increase. For example, most hydrocarbons found in gasoline contain 4-12 carbons, and they have boiling points between 40-220 ^{o}C.[10] Compounds in asphaltenes have big molecular sizes containing up to 30 carbon atoms, and they usually have boiling points higher than 500 ^{o}C,[11] which leave asphaltenes as residues in the commercial distillation of crude oil.

Since asphaltenes are defined by their solubility and correspond to a class of molecules with similar solubility in a defined solvent, asphaltenes are not composed of one kind of compound but different kinds of compounds. Asphaltenes contain mainly polyaromatic hydrocarbons (PAHs) with pendant and branched alkyl chains. Asphaltenes are enriched in heteroatoms, such as N, O, and S, which can be part of the aromatic or aliphatic moieties. These heteroatoms introduce polarities into the asphaltene framework,[7] by for example inducing charge separation in the fused ring systems.[12] In addition, asphaltenes contain metals, such as V and Ni. These metals form complexes with porphyrins, which are responsible for poisoning the catalysis processes during the upgrading of crude oil.[11,13] The identification of the molecular components in asphaltenes is complex[8,11,14] and is still poorly understood.

The understanding of the molecular structure of asphaltenes has changed over time based on the results from different experimental techniques and the development of different theories. There are two parameters that are important to define the structures of asphaltene molecules, one is the molecular weight, and the other one is the size of the fused ring systems. To date, many attempts have been made to establish an average value for the asphaltene molecular weight. Over a long period of time, from the 1930's to 1980's, the reported range for the molecular weight of asphaltenes was very broad. The molecular weight was reported to be as high as 300,000 g/mol based on ultracentrifugation experiments.[15] At the same time, lower values (600-6,000 g/mol) were also reported using different techniques, such as cryoscopic methods, viscosity determinations, light adsorption coefficients measurements, pressure osmometry experiments and by using the isotonic vapor pressure method.[15] As a result of the high

molecular weight determination the structure of asphaltene was proposed to have large aromatic systems with up to 70 aromatic rings containing heteroatoms (S, O, and N).[11] The broad range of molecular weights and unrealistic big aromatic ring systems are controversial for a single asphaltene molecule. In the past two decades, the molecular weight of asphaltenes has been narrowed down to a range of 500-1,000 g/mol by using advanced techniques, such as mass spectrometry[16] and fluorescence spectroscopy.[14,17-19] A consensus value for the average molecule weight is 750 g/mol. Also, a small distribution (4-10) of fused rings have been reported using scanning tunnelling microscopy,[20] transmission electron microscopy,[21] and molecular simulations.[19,22]

1.1.3 Asphaltene aggregates

Asphaltenes are known to self-associate in solution to form aggregates, which upon further aggregation form precipitates. The self-association behaviour is attributed primarily to π–π stacking interactions involving fused aromatic rings. In addition, acid-base interactions and hydrogen bonding are also proposed to be important in the aggregation of asphaltene molecules.[23]

One attempt to rationalize the mechanism of asphaltene aggregation is to relate it to well-known concepts of aggregation, such as micellization.[24] The concept of micelles is widely used to describe asphaltene aggregates. However, the conventional definition for micelles is an aggregate of surfactant molecules in solution.[25] Surfactant molecules have defined structures that contain a hydrophilic region and a hydrophobic region. In aqueous solution, the hydrophobic effect is the driving force for the formation of micelles. Conventional micelles are formed spontaneously from monomers as the critical

micelle concentration (CMC) is reached. However compared to surfactants, asphaltene molecules are polydisperse and the mechanism of asphaltene aggregation is likely to be more complex than for the formation of micelles. Therefore, in the description below I am using the term "micelle" in quotation marks for literature reports that employed this concept in order to differentiate asphaltene aggregates from conventional micelles.

Currently, there are three major models to describe the association of asphaltene molecules.[23,24,26] These models are based on different model structures for asphaltene monomers. One model is the "Yen model", in which different stages of aggregation in asphaltenes were proposed.[26] The Yen model is constructed based on asphaltene monomers that contain large fused aromatic rings with short alkyl chains on the periphery (Scheme 1.2a). This molecular structure is frequently referred to as the continental model.[27] The large planar rings are unit sheets that are proposed to stack via π–π interactions. The results from X-ray diffraction studies supported the concept of condensed aromatic sheets, and these sheets tend to stack together.[28,29] The asphaltene stacks were called particles in Yen's model and he proposed that two or more particles can cluster further to form "micelles".[26] Recently, Mullins proposed a "modified Yen model",[12] in which the term nanoaggregates was used for the smallest unit of asphaltene aggregates. Mullins proposed that the condensed aromatic rings stack in the interior of the aggregates and the alkane chains reside on the exterior (Scheme 1.2b). The attractive force between these aromatic rings makes asphaltene monomers associate with each other, while the repulsive force between the peripheral alkane chains caused by steric hindrance limits the size of the nanoaggregates. Thus, asphaltene monomers form nanoaggregates with a small aggregation numbers of around 6, where the additional

asphaltene monomers are not able to stack onto the aromatic rings in the nanoaggregate. Mullins defined that the asphaltene "critical nanoaggregate concentration" (CNAC) as a concentration at which the nanoaggregates stop to growth. Mullins also proposed that the asphaltene nanoaggregates could form "clusters".

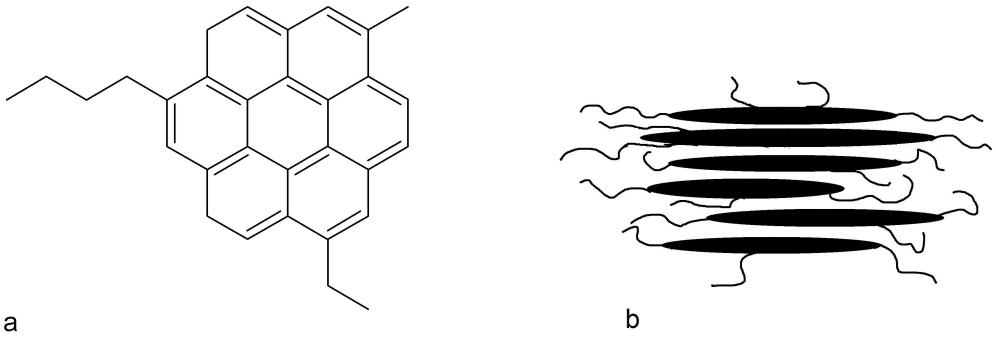

Scheme 1.2 (a) Hypothetical continental model for an asphaltene molecule and (b) a cartoon representation of asphaltene stacks. The aggregation number and the relative positioning of the monomers are arbitrary (adapted from reference 12).

A different molecular structure for asphaltenes, frequently refers to as archipelago model, was proposed by Strausz,[30,31] where the aromatic rings are dispersed but are linked by side chains within the asphaltene molecule (Scheme 1.3a). Yarranton proposed a model where specific interactions of active sites in the asphaltene molecule are responsible for the aggregation. These interactions could be π–π stacking, acid-base interactions, hydrogen bonding, and van der Walls interactions.[32,33] Some large asphaltene molecules contain multiple sites and act as propagators in an oligomerization-like reaction, while other small asphaltene molecules have a single site that link with the propagators and therefore terminate the oligomerization.[6,23,32] Asphaltenes can form linear aggregates (Scheme 1.3b), or branched aggregates (Scheme 1.3c).[23] A recent study

on asphaltene aggregation using single molecule force spectroscopy indicated that asphaltene aggregates appear as worm-like chain structures.[33] Finally, Sheu proposed another model of asphaltene aggregates based on the archipelago structure. In this model the asphaltene monomers form spherical aggregates as "micelles" (Scheme 1.3d).[24] It is clear that the "micelles" from Yen's model is different from the "micelles" proposed by Sheu. In Sheu's model, "micelles" refers to the smallest unit of asphaltene aggregates, but "micelles" corresponds to the cluster of asphaltene aggregates in Yen's paper.

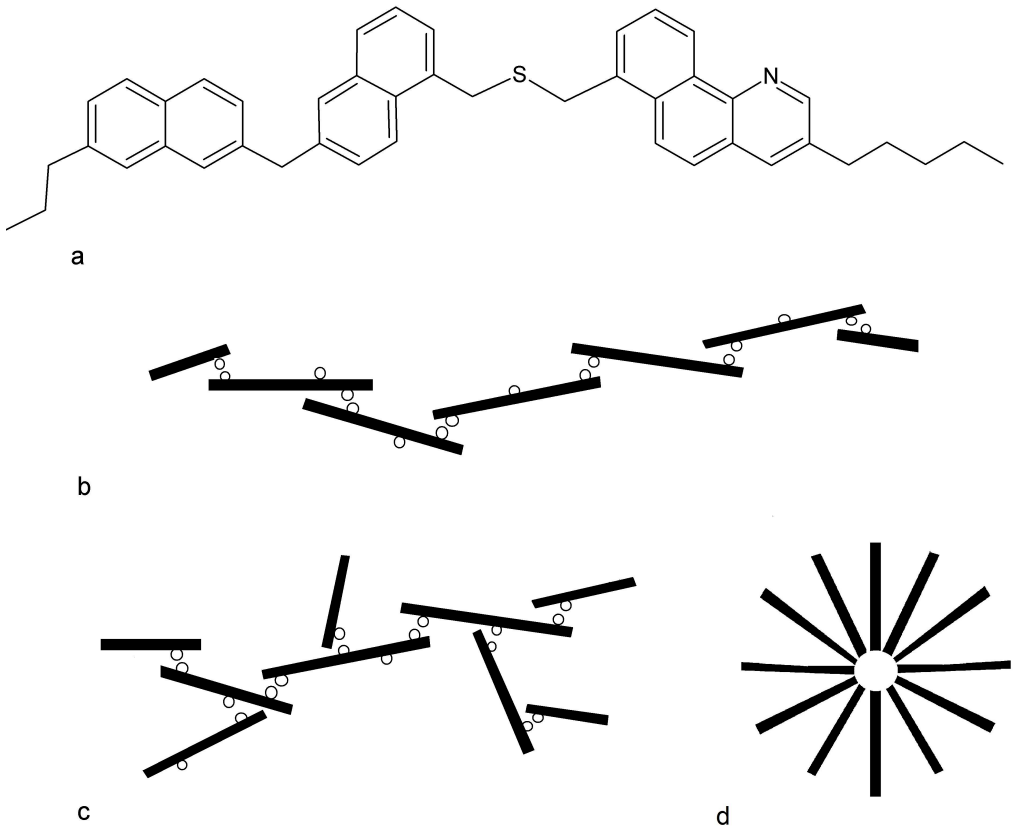

Scheme 1.3 (a) Hypothetical archipelago model for an asphaltene molecule and a cartoon representation of (b) asphaltene linear "oligomer", (c) asphaltene branched "oligomer", where the active sites of asphaltene molecules are present as open circles, and (d) asphaltene "micelles" as described by Sheu. The aggregation number and the relative positioning of the monomers are arbitrary (adapted from reference 23 and 33).

As mention above, the term of "micelle" is defined differently based on different theories. In some studies of asphaltene the concept of "micelles" is employed where the description of their properties is the same as for conventional micelles. For example, the measurement of surface tension, a traditional method for CMC determination in aqueous solutions, was employed to determine the "CMC" for asphaltene.[34,35] However, some studies use "micelles" to describe a phenomenon where the presence of asphaltene aggregates is supported by their experimental evidences. For example, the size of "micelles" of 10-30 μm in diameter was suggested using the electron micrograph technique and this size corresponded to a "micelle" with a weight of 37,000-10,000,000 g/mol.[26] In such case, the size and the weight of these "micelles" is much larger than the sum of several (up to 1000) asphaltene monomers. This reported "micelles" is more in line with the size of clusters. As the term of "micelles" has been used indiscriminately from different perspectives, the "CMC" of asphaltenes have been reported over a broad range of concentrations (mg/L-g/L) and the differences between these values is probably due to the different detection techniques and/or different measurable physical parameters measured. In recent studies the term "nanoaggregates" have been used to avoid the confusion around the use of "micelles". The asphaltene CNAC have been reported to be in the range of mg/L by using different techniques, such as centrifugation,[36] high-*Q* ultrasonics,[37] electrical conductivity measurements,[38] gas chromatography,[39] mass spectroscopy,[39] NMR diffusion measurement,[40] and fluorescence measurements.[41,42]

The aggregation behaviour of asphaltenes depends on the solvent that is used to solubilize it. For example, some studies of asphaltene aggregation are performed in toluene, while other studies are carried out in crude oil. In toluene, asphaltene molecules

are believed to be dispersed as a true solution at very low concentrations (ca. ~0.2-2 mg/L).[43] Previous work reported the formation of asphaltene aggregates at concentrations as low as 50-80 mg/L in toluene.[17,44-46] In crude oil, asphaltene molecules are believed to start to aggregate at higher concentrations than in toluene because of the presence of resins, which can stabilize the asphaltenes in solution.[6,11] Resins have similar structures to asphaltenes but they have lower molecular weights and a smaller fraction of aromatic carbons.[11,32] Resins dissolve in alkanes because they contain alkane chains and they are relatively small in size. Resins also contain aromatic rings that can have π–π interactions with asphaltene molecules. Thus, resins can be adsorbed on the surface of asphaltenes and stabilize asphaltenes in solution.[11]

1.1.4 Fluorescence of asphaltenes

Asphaltenes are colored solids, either brown or black depending on the separation method employed. Many of the asphaltene components are fluorescent and they are photochemically stable under near-visible and visible light.[47] Therefore, photophysical properties, such as fluorescence, can be used to study asphaltenes. Compared to other techniques, fluorescence is a very sensitive technique to detect analytes at very low concentrations, even at a single molecule level.[48] The fluorescence properties of many molecules are sensitive to the molecules' surrounding environment.[25,49,50] Therefore, it is possible to use fluorescent probes to fingerprint the various environments present in microheterogeneous media.[25] The background information about fluorescence and related photophysical techniques will be introduced next before the discussion of the previous fluorescence studies on asphaltenes.

1.2 Photophysical techniques

1.2.1 Unimolecular photophysical processes

Photophysical processes are processes related to a molecule gaining energy by absorbing a photon, or losing energy by releasing heat or emitting a photon. The transitions between energy levels are divided into two categories: the processes that involve the absorption or emission of photons are called radiative transitions, while the processes that involve the release of heat in the deactivation of the excited state molecule are non-radiative transitions. In particular, absorption (A), fluorescence (F) and phosphorescence (P) are the possible radiative transitions. Internal conversion (IC), intersystem crossing (ISC) and vibrational relaxation (VR) are the possible non-radiative transitions. The various photophysical processes are summarized in the Jablonski diagram and are represented in Scheme 1.4.

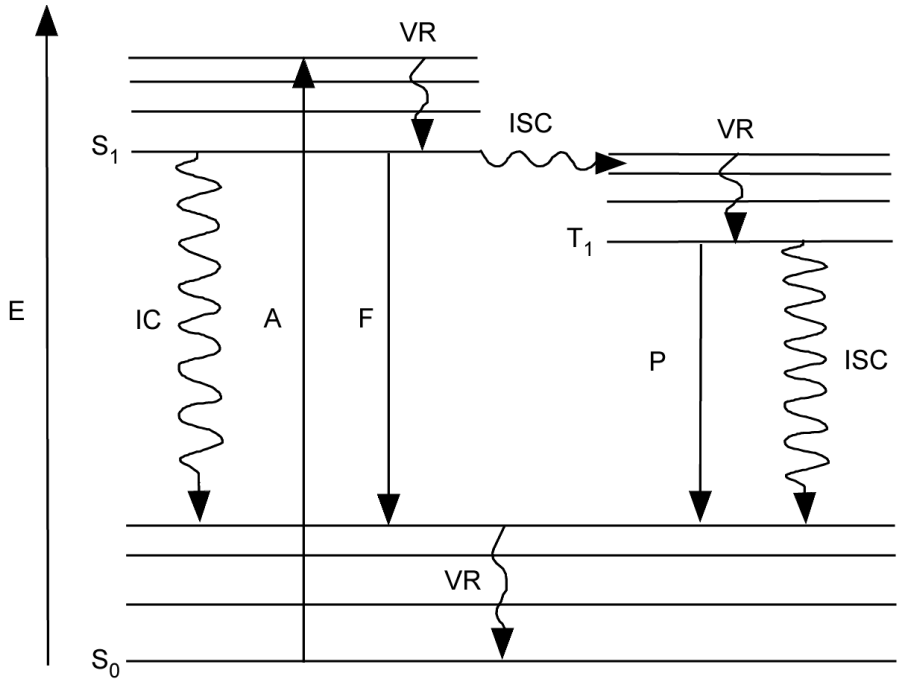

Scheme 1.4 Jablonski diagram. Radiative transitions are depicted with straight arrows, and non-radiative transitions are depicted with curly arrows. E, S_0, S_1 and T_1 represent energy, the ground state, singlet excited state and triplet excited state, respectively.

Absorption (A) is a phenomenon where the energy of an electromagnetic radiation is absorbed by a molecule. During this process, the molecule is excited from the ground state to one of its electronic excited states. The excited state molecule is unstable and will return to its ground state through various deactivation pathways. IC is the non-radiative transition between electronic states with the same spin state, while ISC is the non-radiative transition between electronic states with different spin states. Fluorescence (F) is the radiative transition between electronic states with the same spin multiplicity ($S_1 \rightarrow S_0 + h\nu$), while phosphorescence (P) is the radiative transition between electronic states with the different spin multiplicity ($T_1 \rightarrow S_0 + h\nu$). VR is a rapid transition ($<10^{-12}$ s)[48] between vibrational levels in the same electronic state in solution phase, and the

fluorescence and phosphorescence are always from the lowest vibrational energy level of the excited state to the ground states.

In this thesis, the fluorescence properties of asphaltenes were investigated, and for this reason the deactivation processes from the triplet excited states (T_1) are not discussed. Fluorescence (F), IC, and ISC are competitive intramolecular photophysical processes for the deactivation of S_1. These deactivation processes correspond to first-order reactions with rate constant of k_f, k_{IC}, and k_{ISC} (Scheme 1.5).

$$S_1 \xrightarrow{k_f} S_0 + h\nu$$
$$S_1 \xrightarrow{k_{IC}} S_0 + \text{heat}$$
$$S_1 \xrightarrow{k_{ISC}} T_1$$

Scheme 1.5 Competitive deactivation pathways for S_1.

The intrinsic decay rate constant (k_0) is the sum of all deactivation rate constants for the singlet excited state, as shown in Equation 1.1.

$$k_0 = k_f + k_{IC} + k_{ISC}$$

Equation 1.1

The rate law for the deactivation of S_1 is expressed as the sum of all the deactivation pathways, as shown in Equation 1.2.

$$-\frac{d[S_1]}{dt} = (k_f + k_{IC} + k_{ISC})[S_1] = k_0[S_1]$$

Equation 1.2

The concentration of the singlet excited state molecule [S_1] at time t is expressed as a mono-exponential function (Equation 1.3),

$$[S_1] = [S_1]_0 e^{-k_0 t}$$

Equation 1.3

where $[S_1]_0$ is the initial concentration of the singlet excited state molecule (S_1).

The fluorescence lifetime of a molecule (τ_0) is defined as the amount of time it takes for the concentration of the singlet excited state molecule to decrease to 1/e of the initial value. Therefore, the fluorescence lifetime is expressed as the inverse of the intrinsic decay rate constant, as shown in Equation 1.4.

$$\tau_0 = \frac{1}{k_0}$$

Equation 1.4

Typical timescales for fluorescence lifetimes are of the order of 10^{-12} to 10^{-8} s.[51] The fluorescence quantum yield (Φ_f), is given by the number of photons emitted as fluorescence relative to the total number of photons absorbed by the molecule (Equation 1.5).

$$\Phi_f = \frac{k_f}{k_0} = k_f \tau_0$$

Equation 1.5

1.2.2 Steady-state fluorescence emission spectra

The steady-state fluorescence emission spectrum corresponds to the distribution of emission intensities as a function of wavelength. Experimentally, the emission spectrum is obtained by exciting a sample with a continuous irradiation at a certain wavelength and monitoring the intensity at various emission wavelengths.

1.2.3 Time-resolved fluorescence decay measurements: single photon counting

Fluorescence lifetimes are measured using a single photon counting (SPC) technique. In this technique, the fluorescence emission intensity is measured as a function of time. Experimentally, a pulsed light source excites the sample and causes the sample to emit photons. The time for the first photon detected after the excitation pulse is measured. For each photon detected a count is stored in an array that contains 1,000 channels, which correspond to incrementally longer time intervals. The distribution of counts stored in the 1,000 channels after repeating the pulsed experiment many times represents the time dependence of the fluorescence emission, which is a fluorescence decay profile.[48]

When one type of fluorophore with a single fluorescence lifetime is present in the sample, the fluorescence decays correspond to a mono-exponential decay and fit to Equation 1.3, where the concentration of singlet excited state molecules is proportional to the fluorescence intensity. When the sample contains more than one fluorophore with different lifetimes, the decay follows a sum of exponentials (Equation 1.6),

$$I(\mathrm{t}) = \sum_{1}^{\mathrm{i}} A_{\mathrm{i}} \mathrm{e}^{-(\frac{\mathrm{t}}{\tau_{\mathrm{i}}})}$$

Equation 1.6

where I(t) is the emission intensity or the number of counts, and τ_{i} is the lifetime of the emitting species, i and t is time. A_{i} is the pre-exponential factor of the emitting species, i, with the sum of all pre-exponential factors normalized to unity. The pre-exponential factor of each emitting species corresponds to the abundance of that component in the total emission.

1.2.4 Time-resolved emission spectra

Time-resolved emission spectra (TRES) are the emission spectra collected at specific time windows after the excitation pulse. The steady-state fluorescence emission spectra are related to all chromophores in solution, while TRES are related the species that emit within a particular time window. Experimentally, fluorescence decays are collected at different emission wavelengths for the same amount of time. TRES are constructed by integrating the decay intensities for each emission wavelength between defined delays windows after the excitation pulse. At short delays long lived and short lived species contribute to the TRES, while at long delays after excitation the short lived species have decayed and only the spectrum for the long lived species is measured.

1.2.5 Bimolecular photophysical processes

The intramolecular deactivation pathways of the excited states discussed so far are unimolecular processes. The intermolecular deactivation of the excited state molecules by another molecule (the same molecule or different molecule) is a bimolecular process, called quenching,[48] as shown in Scheme 1.6,

$$S_1 + Q \xrightarrow{k_q} S_0 + Q$$

Scheme 1.6 Deactivation of S_1 by quenching.

where quencher (Q) refers to a substance that can accelerate the deactivation of the excited state molecule and k_q is the quenching rate constant. The overall rate law for the deactivation of S_1 is expressed as the sum of the rate of the unimolecular and bimolecular processes, as shown in Equation 1.7.

$$-\frac{d[S_1]}{dt} = k_0[S_1] + k_q[S_1][Q]$$

Equation 1.7

Quenching studies are usually carried out as pseudo first order reactions, where the quencher concentration is in excess over the S_1 concentration. Therefore, [Q] is considered as a constant and Equation 1.7 can be integrated as Equation 1.8,

$$[S_1] = [S_1]_0 e^{-(k_0 + k_q[Q])t}$$

Equation 1.8

where the decay of S_1 follows a first-order function. The observed rate constant (k_{obs}) and the observed fluorescence lifetime (τ_{obs}) are expressed in Equation 1.9:

$$\frac{1}{\tau_{obs}} = k_{obs} = k_0 + k_q[Q]$$

Equation 1.9

Quenching can be static or dynamic. Static quenching takes place if there is the formation of nonfluorescent complexes (S_0Q) between the ground state molecules (S_0) and quenchers (Q) with equilibrium constant K_{eq} (Scheme 1.7).

$$S_0 + Q \overset{K_{eq}}{\rightleftharpoons} S_0Q$$

Scheme 1.7 Complexation of S_0 and Q.

The complexes S_0Q normally absorb light, but the quenching in the complex is immediate and no fluorescence occurs. An increase in the quencher concentration leads to a decrease of the concentration of the excited state molecules S_1 formed because a larger amount of the ground state is tied up in the non-fluorescent complex S_0Q. Therefore, static quenching decreases the emission intensity of S_1, while static quenching has no influence on fluorescence lifetime of S_1,[48] as shown in Equation 1.10 and 1.11:

$$\frac{I_0}{I} = 1 + K_{eq}[Q]$$

Equation 1.10

$$\frac{\tau_0}{\tau_{obs}} = 1$$

Equation 1.11

Dynamic quenching is also called collisional quenching. The collision happens between a quencher molecule and the singlet excited state (S_1) to form an encounter complex, where quenching occurs. The static quenching does not rely on diffusion or molecular collisions, but dynamic quenching does.[48] Static and dynamic quenching both decrease the concentration of excited state molecules (S_1), so they lower the emission intensity. However, dynamic quenching shortens the fluorescence lifetime and the fluorescence intensity at the same time[48] because quenching is an additional deactivation process for the excited states. The ratio of the fluorescence lifetimes and intensities in the absence and presence of the quencher is given by Equation 1.12 in the case of dynamic quenching.

$$\frac{\tau_0}{\tau_{obs}} = \frac{I_0}{I} = 1 + k_q \tau_0 [Q]$$

Equation 1.12

1.3 Pyrene

Externally added probe, such as Pyrene (Py, Scheme 1.8), might interact with a subset of the components of asphaltene. The quenching experiments of probes in the presence of asphaltene aggregates by quenchers will determine if the probes are located inside the aggregates or free in the solution. Probes in the interior of the aggregates are

expected to have lower quenching rate constants than probes that are exposed in the solution.

Py is a common probe used in fluorescence studies of organized systems.[25,49] The dimensions of Py are 10.4 Å long and 8.2 Å wide.[52] Its size is relatively small compared to the size of asphaltene aggregates.

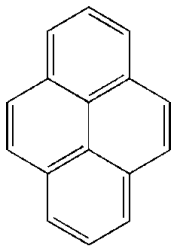

Scheme 1.8 Structure of pyrene.

Py is a very popular fluorescent probe because it has a very long fluorescence lifetime (190 ns in non-polar solvent and 650 ns in polar solvent)[53] and a high fluorescence quantum yield (0.65 in non-polar solvent and 0.72 in polar solvent).[53] More importantly, the fluorescence spectrum and fluorescence lifetime of Py are very sensitive to the surroundings of the excited state Py. [49,54-57]

Py has limited solubility (1.6 x 10^{-6} M) in water.[58] Its solubility in water can be enhanced when Py is incorporated into a hydrophobic cavity of a host system. For this reason Py was used as probe on study several organized systems in the aqueous solutions.[25,49,54] Also, Py can be employed to study aromatic systems in the organic phase,[59] since Py has a conjugated aromatic system and it can bind with other aromatic systems via π–π interactions. For this reason, Py was employed as probes to study the polydisperisty of aggregates present in asphaltene solutions.

1.4 Review of the fluorescence studies with asphaltenes

Fluorescence has been employed to study crude oils and asphaltenes, either by exploring the intrinsic emission spectra,[17,19,41-45,47,60-67] or by measuring the fluorescence lifetimes.[46,47,62,63,68-70] The emission spectra[41,42,44,45,47,65] and lifetimes[46,47,62] for asphaltenes and oil samples are dependent on the concentration of the samples.

The studies involving the measurement of steady-state fluorescence emission spectra showed that the intensity of the emission decreased when the concentration of asphaltenes or oil samples were increased. Some authors interpreted that the intensity decreases were due to quenching inside the asphaltene aggregates.[42,45,65] Other authors rationalized that these decreases were due to the high optic density of the solutions.[41] In addition, red shifts of the emission spectra for asphaltenes were observed with the increase in the concentration of the samples, which was also attributed to aggregation.[41,42,45]

The CMC or CNAC determined from the steady-state fluorescence experiments have been reported over a broad concentration range from 50 mg/L to 1.6 g/L.[41,42,44,45,47,65] The differences in these values are due to different experimental conditions, such as the solvent, the excitation wavelengths and the way the fluorescence measurement are carried out for the concentrated solutions. The solvent dependence of the CMC or CNAC values is reasonable since asphaltene is defined as a solubility class. The wavelength dependence on the asphaltene aggregation behaviour can be rationalized by the fact that the chromophores with different excited state energies may start to aggregate at different concentrations. The red shift observed at high asphaltene concentrations could be related to self-absorption, which is an artifact that will be discussed in the Experimental section (2.3.5). Front-face detection[41,65] or short light

pathlength[42,45] were employed to solve the self-absorption problem. However, no systematic procedure has been established to test how well the self-absorption was diminished.

Time-resolved fluorescence experiments have been used recently to investigate the lifetimes for the intrinsic emission of crude oils and asphaltenes.[46,47,62,63,68,70] Wang *et al.* found that an increase of the fluorescence lifetimes for oil samples was observed with an increase in the dilution of the crude oil.[47] Ryder *et al.* studied the fluorescence lifetimes for oil samples that contain a known content of aromatic compounds. The results showed that the fluorescence lifetimes were increased as the concentration of aromatic compounds in oils decreased.[63,70] Both results suggest that high concentrations of chromophores lead to efficient collisional quenching and energy transfer in the oil samples. Similarly, the fluorescence lifetimes of asphaltenes also showed a dependence on the concentration,[46,62] in which the lifetimes decrease as the concentrations of asphaltenes increase. This observation suggests the formation of aggregates.

Some experiments were carried out at different excitation and/or emission wavelengths. At a fixed excitation wavelength, the lifetimes for the emission of crude oils increased as the emission wavelength became longer.[47] Ryder *et al.* confirmed these observations; however, he noticed that this increase occurred for a certain wavelength range. A maximum lifetime was obtained between 600 and 700 nm for various oil samples, and the lifetimes decreased for emission wavelengths longer than 700 nm.[63,70] This observation was assigned to the interplay between collisional energy transfer and quenching processes.

Beside the possible quenching between the chromophores in the asphaltene solution, the quenching of the fluorescence of asphaltenes by an externally added quencher, such as *o*- and *p*-chloranil, was observed.[69] In this experiment, the lifetimes for the excited state of asphaltenes remained the same with the addition of quencher, indicating that a static quenching mechanism involving ground-state complexation of asphaltene with the quencher occurs.

As mentioned earlier in section 1.1.4, externally added probes can be employed to characterize the various environments present in microheterogeneous media. The use of 6-propionyl-2-(N,N-dimethylamino) naphthalene (PRODEN) as an external probe showed a slightly red shift of its emission with the addition of asphaltenes.[41] The authors concluded that the probe was incorporated into a polarizable site in the asphaltene aggregates. On the other hand, fluorescence lifetimes of probe molecules were measured with the addition of crude oils.[71] It was found that a significant quenching of the lifetime for the excited state probes occurred by the aromatic moieties present in crude oil. Analysis of these results indicates that the observed lifetime decay rate constant is linearly correlated to the concentration of crude oil.

1.5 Thesis objectives

Asphaltenes are usually considered a problem because they form aggregates easily and further form precipitates that clog the pipelines and surface facilities in the oil industry. Thus, asphaltenes aggregation is an active area of research.[12,14,33,36,37,42,45,72,73] The intrinsic fluorescence properties of asphaltenes have been studied, but the mechanism of asphaltene aggregation is still poorly understood. Probe molecules have

been previously employed to study the asphaltene aggregation, but no successful characterization of the asphaltene aggregates has yet been achieved.

The primary objective of this work was to establish appropriate methodologies to be used for the characterization of the intrinsic fluorescence of asphaltenes by measuring steady-state emission spectra, time-resolved fluorescence decays and time-resolved emission spectra. The combination of the use of complementary fluorescence techniques was employed to study the aggregation of asphaltenes by exploring the intrinsic emission from asphaltene solutions at different concentrations.

The second objective of this work was to quench the intrinsic asphaltene emission to determine the accessibility of quenchers to the asphaltene aggregates. This work can be used to determine how accessible the interior of the asphaltene aggregate is to small molecules, and also determine if the accessibility of the small molecule is different for the aggregates formed from different asphaltene components.

The third objective of this thesis was to quench externally added probes that might be incorporated in asphaltene aggregates. The probe molecule employed was Py, because it has a long fluorescence lifetime that can be well distinguish from the asphaltene lifetime. Also, Py has a high fluorescence quantum yield and for this reason only a low concentration is required to give sensitive fluorescence measurements. In addition, Py was employed as a fluorescent probe to study the aggregation of asphaltenes because Py might interact with a subset of the components of asphaltenes through π–π stacking. If the π–π interactions between the Py and the subset of the aromatic components of asphaltene exist, Py should have a different fluorescence lifetime in the aggregates. A lower quenching efficiency would be expected for the Py inside the asphaltene aggregates

when they are less accessible to the quencher molecules. In this respect, the information obtained from the quenching experiments using externally added Py would complement the studies from the intrinsic asphaltene fluorescence, in which the the ability of small molecules to enter the particular binding sites that form through π–π interactions would be investigated.

2. EXPERIMENTAL

Some of the results presented in this chapter have been published in the Photochemical & Photobiological Sciences. Reproduced by permission of The Royal Society of Chemistry (RSC) on behalf of the European Society for Photobiology, the European Photochemistry Association, and RSC. This open access article can be accessed via the website (at http://pubs.rsc.org/en/content/articlelanding/2014/pp/c4pp00069b).

2.1 Materials

Athabasca asphaltene (AA-5, 50% heptane-insoluble asphaltene, obtained from Dr. Murray Gray's group, University of Alberta),[74] nitromethane ($MeNO_2$, 99+%, Aldrich), anthracene (Ant, 99+%, Aldrich), and toluene (Caledon, spectroscopic grade) were used as received. Pyrene (Py, 99%, Aldrich) was recrystalized once from 95% ethanol. The purity of Py was checked using single photon counting (SPC) experiments to measure the fluorescence decay of Py in aerated aqueous solutions. For pure Py a mono-exponential decay (τ = ~130 ns) was obtained,[54] while impure samples showed a fast decay in addition of the long decay due to the Py emission.

2.2 Sample preparations

Stock solutions of AA-5 (1 g/L or 10 g/L) were prepared by dissolving appropriate amounts of the AA-5 solid in toluene. A series of dilutions (0.1 mg/L to 5 g/L) were prepared by adding the stock solution into toluene using an Eppendorf® pipette. A stock solution of Py (2-5 mM) was prepared by dissolving appropriate amounts of Py solid in toluene. Py samples (20 μM) were prepared by injecting appropriate amounts of the Py stock solution into toluene or AA-5/toluene solutions. A stock solution

of Ant (1.35 mM) was prepared by dissolving appropriate amounts of Ant solid in toluene. Ant samples (20 μM) were prepared by injecting the Ant stock solution into toluene.

$MeNO_2$ was used as a quencher and its stock solutions (~1 M) were prepared daily by injecting appropriate volumes of neat $MeNO_2$ into toluene. Appropriate volumes of the quencher stock solution were added to 2.5 mL of AA-5 or Py solutions using a Hamilton gastight glass syringe.

All samples were contained in 10 x 10 mm quartz cells. Oxygen is an efficient quencher of singlet excited states,[75] and Py has a long excited state lifetime. For these reasons, all Py samples used for SPC experiments and the quencher solutions used for the quenching of excited state Py were deaerated. Samples were bubbled with nitrogen for at least 30 min. The Ant samples used for SPC experiments were aerated solutions, since Ant has a short excited state lifetime (ca. ~4 ns) in toluene.

Oxygen quenches the lifetime of the excited states in AA-5 samples. In preliminary studies, the SPC experiments for AA-5 samples were performed under different conditions: (i) aerated solutions, (ii) deaerated solutions by bubbling nitrogen for at least 30 min and (iii) oxygen saturated solutions by bubbling oxygen for at least 30 min. Unless otherwise stated, lifetimes measurements for AA-5 samples at different concentrations and quenching experiments for the excited states of AA-5 were done with aerated solutions.

Two or more independent experiments were performed to check the reproducibility of data (refer to section 3.2.2.1). Independent experiments for AA-5 lifetime measurements means that the experiments were done with solutions prepared

separately by dissolving a new portion of AA-5 solid in toluene, and measuring lifetimes on different days. Independent experiments for Py lifetime measurements means that the experiments were done with the solutions prepared with the same or different stock solutions of Py but deaeration of the solutions were done on different days.

2.3 Instrumentation

2.3.1 UV-Vis absorption spectroscopy

Absorption spectra were recorded with a Varian Cary 1 UV-Visible spectrophotometer at room temperature, and the spectra were collected between 250 nm and 600 nm. Correction of spectra was done by subtracting the absorption spectrum of solvent (toluene) from the absorption spectrum of sample solutions.

2.3.2 Steady-state fluorescence spectroscopy

Steady-state fluorescence emission spectra were collected with a Photon Technology International® (PTI) QuantaMaster^{TM} (QM-2) fluorimeter. The excitation light source was a Xenon lamp. Excitation and emission slits were set to correspond to a bandwidth between 2 and 3 nm, depending on the sample's fluorescence intensity. The step size and integration time were 0.5 nm and 0.25 s, respectively. All measurements were done at room temperature. Unless otherwise stated, corrected spectra were obtained by subtracting the spectra for the solvent (toluene) from the spectra for the samples. This correction procedure is required to remove the Raman scattering from the solvent.

2.3.3 Time-resolved fluorescence decay measurements using single photon counting (SPC)

Time-resolved fluorescence decay measurements were performed with an Edinburgh OB 920 SPC system. The excitation light sources were an Edinburgh EPLED-330 light emitting diode and an Edinburgh EPL-405 laser diode, where the excitation wavelengths were centered at 335 nm and at 405 nm, respectively. When the excitation wavelength was 335 nm, the lifetime measurements for the emission of AA-5 samples were collected at emission wavelengths of 391 nm, 420 nm or 520 nm. When the excitation wavelength was 405 nm, the lifetime measurements for the emission of AA-5 samples were collected at 520 nm. The lifetime measurements for the emission of Py in the absence or in the presence of AA-5 were done by exciting the samples at 335 nm and by collecting the emission at 391 nm. Unless stated otherwise the detection monochromator width was set to 2 mm which corresponds to a bandwidth of 16 nm. Unless stated otherwise the total number of accumulation counts was 10,000 at the channel of maximum emission intensity. The instrument response function (IRF) was collected with an aqueous Ludox (Aldrich) solution to scatter light at the excitation wavelength. The shapes of the IRF are as expected from the profiles for the EPLED-330 and EPL-405 supplied by Edinburgh Instrument.[76,77] All the SPC measurements were done at room temperature.

The emission decays were fit to a sum of exponentials (Equation 1.6) using the software provided by Edinburgh. The lifetimes for the emission of AA-5 samples were short ($\leq$ 20 ns), the IRF was deconvoluted from the decays to obtain the fit curve. This procedure eliminates both the noise and the effects of the exciting light pulse. In the case

of Py emission, its lifetime was long (ca. 305 ns) and the decay were fit using a "tail" fit in which no deconvolution was performed, because the IRF was collected over too narrow a window of time, i.e. it was collected in too small a number of channels. χ^2 is called the "reduced chi-square", its values are used to scale the "goodness of fit". In addition, the residuals between the orignal data and the fitting curve were used to evaluate the goodness of the fits. The fits with χ^2 values between 0.9 and 1.2 and a random distribution of residuals around 0 were considered to be acceptable.[50]

2.3.4 Time-resolved emission spectra (TRES)

TRES were constructed from time-resolved fluorescence decays with the same SPC system mentioned above. The experiments were done by exciting a sample at a fixed wavelength and collecting the decays at different emission wavelengths for the same amount of time. TRES were constructed using the Edinburgh software by integrating the intensities between defined time windows. TRES were usually normalized at the wavelengths of maximum intensity in order to compare changes in the shape of the spectra with time.

The excitation wavelength was 335 nm for AA-5 samples. Raman scattering of toluene was detected at 360 and 380 nm as an emission with the same time profile as the IRF. The Raman scattering emission was visible in some spectra ([AA-5] $\leq$ 10 mg/L). Therefore, the emission decays for AA-5 samples were collected from 400 nm to 600 nm at each 20 nm to construct the TRES. The excitation wavelength was 335 nm for Py samples, where the intensity of Raman scattering emission was very low compared to the

emission intensity of 20 μM Py; therefore, the emission decays for Py samples were collected from 360 nm to 450 nm at each 5 nm.

2.3.5 The usage of the front-face sample holder

The fluorescence intensity of a sample is directly related to the fluorescence quantum yield of a particular molecule and the concentration of excited states formed in the absorption process. In principle, a linear relationship exists between the fluorescence intensity and the absorbance of a sample. However, depending on the geometry employed between the excitation beam and the emission detection this relationship only holds at low absorbance values at the excitation wavelength. Fluorescence is normally measured at a 90 degree angle between the excitation and emission optics. In this case, at high absorbance values the number of photons reaching the sample volume from which emission is collected is not directly related to the concentration of fluorophore and smaller emission intensities are observed than predicted from the absorbance values. This decrease in intensity is proportionally the same for the whole emission spectrum.

The fluorescence of a sample is also affected by self-absorption when the emission and absorption spectra overlap and the emission pass through the solution before being detected. This situation occurs with the 90 degree arrangement between the excitation source and the emission detection where the excitation normally occurs in the centre of the cell. Self-absorption is increased with an increase in the pathlength and it is more prominent at wavelengths where the molar absorptivity of the sample is higher. Therefore, self-absorption leads to a distortion of the emission spectrum with a larger decrease of the emission intensity being observed where the absorption of the sample is

higher. The solution to the self-absorption problem is to use a front-face illumination set-up where the excitation and emission occur at the same surface of the solution.

Triangular cells are traditionally used for front-face measurements, but specular reflections can lead to artifacts. A sample holder (Figure 2.1 from Edinburgh) was employed which holds 10 x 10 mm cell in which the sample is titled backwards by 30 degrees and there is a 52 degree angle with respect to the normal for excitation beam and emission optics.

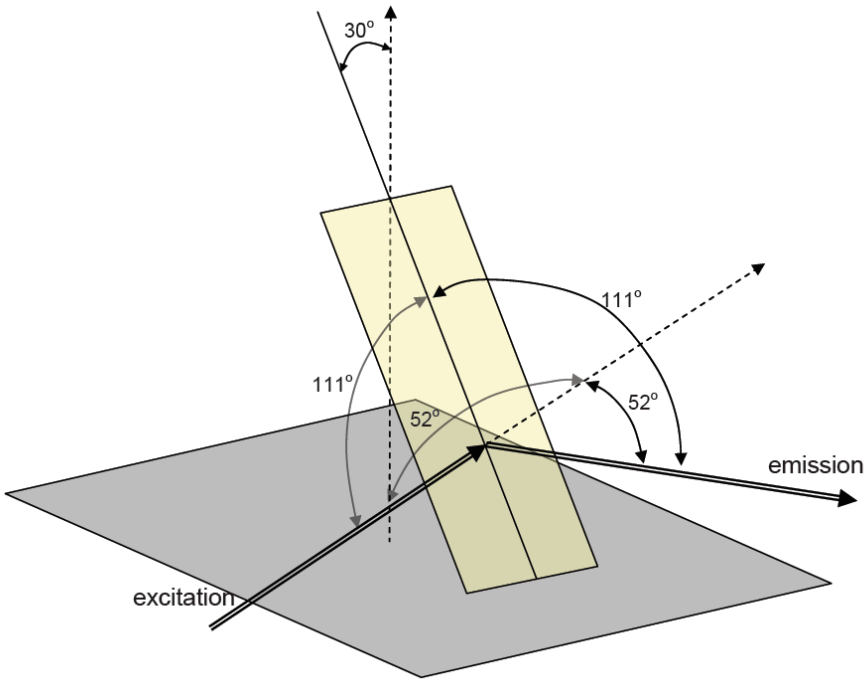

Figure 2.1 Geometry for the front-face sample holder from Edinburgh (Diagram provided by Edinburgh Instruments Ltd.)

In this thesis, the front-face sample holder was employed to measure the fluorescence for samples with high concentrations, and a sample holder with the common arrangement of a 90 degree angle between the excitation beam and the detection optics

was employed for diluted samples. The switch of two sample holders between concentrated and diluted samples will be illustrated in section 3.2.1.1.

3. INVESTIGATION OF THE ASPHALTENE AGGREGATION AND THE ACCESSIBILITY OF QUENCHERS TO ASPHALTENE AGGREGATES USING FLUORESCENCE STUDIES

Some of the results presented in this chapter have been published in the Photochemical & Photobiological Sciences. Reproduced by permission of The Royal Society of Chemistry (RSC) on behalf of the European Society for Photobiology, the European Photochemistry Association, and RSC. This open access article can be accessed via the website (at http://pubs.rsc.org/en/content/articlelanding/2014/pp/c4pp00069b).

3.1 Introduction

Asphaltenes are black or brown solids that absorb light in the near visible and visible region of the spectrum. In general, the fluorescence properties of molecules, such as their emission spectra and their singlet excited state lifetimes, are related to the molecules' surrounding environment.[25] As the asphaltene molecules form aggregates, the environment where the molecules are located is different from the environment when the molecules are free in solution. The fluorescence of asphaltenes has been previously employed with some success to investigate asphaltene aggregation.[17,19,41-45,47,60-67] The purpose of the current work was to provide a more comprehensive use of complementary fluorescence techniques. The combination of the use of steady-state fluorescence emission spectra, time-resolved fluorescence lifetime and time-resolved emission spectra (TRES) measurements was employed to study the aggregation of asphaltenes by exploring the intrinsic emission from asphaltene solutions at different concentrations.

Additional information can be obtained from quenching studies. Fluorescence quenching is a bimolecular process and quenching experiments can be used to investigate the accessibility of small molecules to fluorophores located in the asphaltene aggregates. A lower quenching efficiency is expected when the accessibility of the quencher to the chromophores inside the aggregates is decreased. In this work, the quenching efficiency was obtained from time-resolved fluorescence experiments because the data from steady-state spectra were difficult to interpret due to self-absorption of the asphaltene emission at high asphaltene concentrations.`

3.2. Results

3.2.1 Steady-state fluorescence of AA-5 asphaltene

3.2.1.1 Self-absorption of the AA-5 asphaltene emission at high asphaltene concentrations

The fluorescence for diluted samples was measured with a 90 degree arrangement between the excitation source and the detection optics (see section 2.3.5). As the concentration of asphaltene was increased, the fluorescence of samples with high absorbance values at the excitation wavelength cannot be measured correctly using a 90 degree arrangement because of the absorption of the emitted light by the sample, i.e. self-absorption. The front-face sample holder was employed at high fluorophore concentrations. To use the front-face sample holder one needs to define the transition between diluted and concentrated samples where self-absorption becomes a problem to accurately determine the fluorescence intensity. In a control experiment, the fluorescence spectra of a series of concentrations of AA-5 samples from 10 mg/L to 10 g/L in toluene

were collected using both a 90 degree arrangement between the excitation beam and the detection optics and the front face sample holder. It was found that the fluorescence spectra for the samples with absorbance values around 1 or higher than 1 at the excitation wavelengths, obtained using a 90 degree arrangement for the excitation/emission optics were red shift in comparison to the spectra obtained when using the front-face sample holder. Two samples, 10 mg/L and 50 mg/L AA-5 in toluene were chosen to show this effect. The absorption spectra of the two samples are shown in Figure 3.1. At 310 nm, the absorbance was about 0.25 for the sample containing 10 mg/L AA-5 and was about 1.3 for the sample with 50 mg/L AA-5.

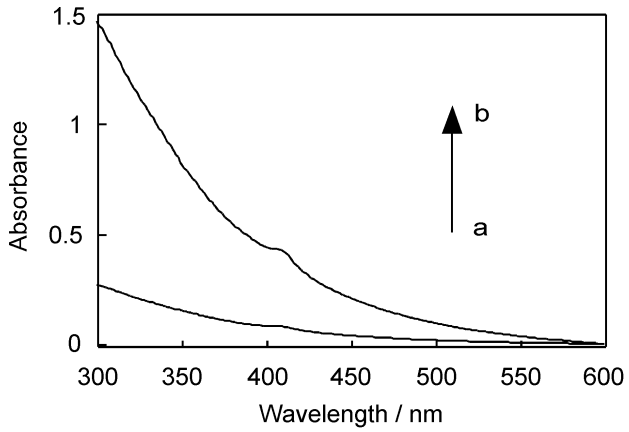

Figure 3.1 Absorption spectra for 10 mg/L AA-5 (a) and 50 mg/L AA-5 (b) in toluene.

The normalized fluorescence emission spectra excited at 310 nm for the two samples are shown in Figure 3.2. A red shift was observed for the spectrum of the solution with 50 mg/L AA-5 obtained using a 90 degree arrangement between the excitation and emission optics compare to the spectrum obtained with the front-face sample holder. The relative decrease of the emission at the shorter wavelength using a 90 degree arrangement was due to self-absorption. The self-absorption effect was minimal for the fluorescence of the solution with 10 mg/L AA-5.

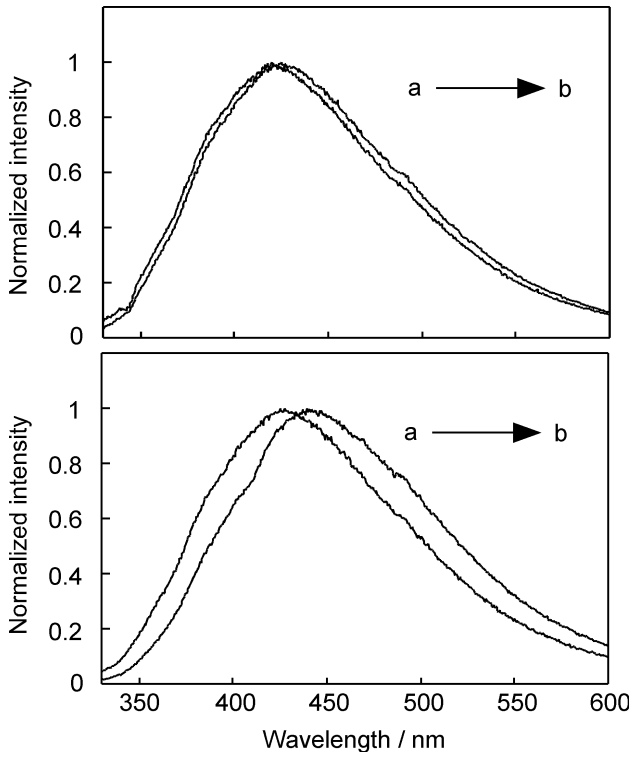

Figure 3.2 Normalized steady-state fluorescence spectra for AA-5 (top: 10 mg/L in toluene; bottom: 50 mg/L in toluene) excited at 310 nm obtained using the front-face arrangement between the excitation source and the detection system (a) or using a 90 degree arrangement between the excitation source and the detection optics (b).

The spectra in Figure 3.2 showed that significant distortions of spectra occurred when the absorbance at the emission wavelengths were high. In such cases the front-face sample holder was employed.

3.2.1.2 Steady-state fluorescence of AA-5 asphaltene for different excitation wavelengths

Different chromophores have different energy gaps between the ground states and the excited states, and for this reason they absorb and emit light at different wavelengths.

The emission spectrum is the same at different excitation wavelengths when a solution contains only one kind of chromophore. In contrast, a mixture with different chromophores has different emission spectra when the solution is excited at different wavelengths.

Previous studies have showed that asphaltenes contain many different chromophores that absorb light from the UV to Vis-NIR range.[17,41,42,45,61,65,68] The steady-state fluorescence spectra of AA-5 samples obtained at different excitation wavelengths may be useful to characterize the different chromophores in the samples.[14,62] An example of steady-state fluorescence spectra for an AA-5 solution in toluene obtained at different excitation wavelengths is shown in Figure 3.3. Other AA-5 solutions at different concentrations have similar spectra to those shown in Figure 3.3.

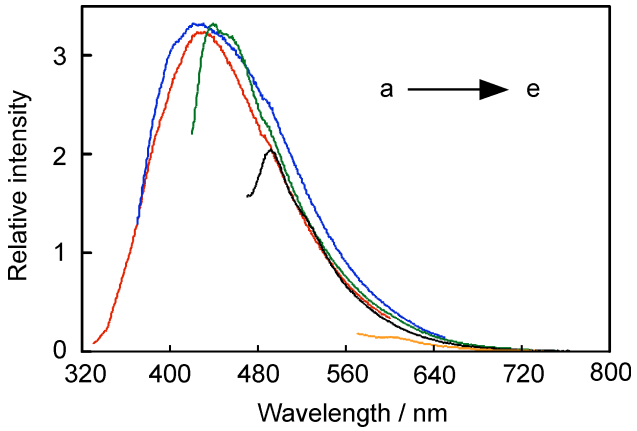

Figure 3.3 Fluorescence spectra for 8 mg/L AA-5 in toluene obtained at different excitation wavelengths: 310 nm (a, red), 350 nm (b, blue), 400 nm (c, green), 450 nm (d, black) and 550 nm (e, orange). Spectra were collected using a 90 degree arrangement between the excitation source and the detection optics.

The emission spectra were different in shape for the various excitation wavelengths used, confirming that AA-5 is a mixture that contains a variety of

chromophores with distinguishable fluorescence properties. At a particular excitation wavelength the emission comes from all the chromophores that absorb light at this wavelength. Therefore, a combined emission from all chromophores is always obtained in the steady-state fluorescence spectra for AA-5.

The dependence of the fluorescence emission spectra for AA-5 with the AA-5 concentration is shown in Figure 3.4. A slight red shift was observed with the increase of the concentration of AA-5, but the shape of the spectra did not change substantially. Similar results were obtained for these samples excited at 350, 400, 450 and 550 nm.

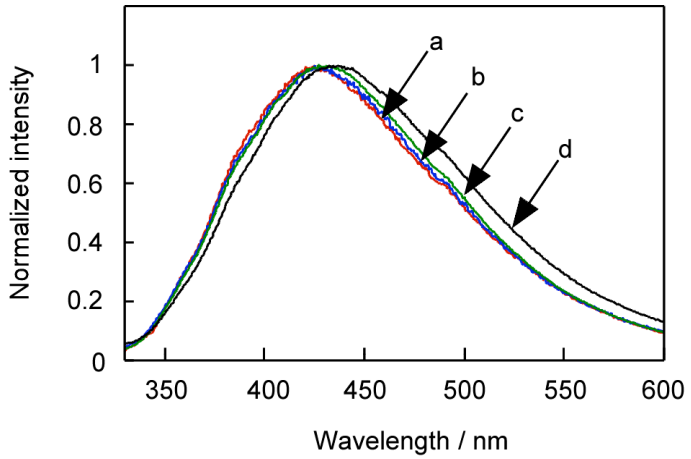

Figure 3.4 Normalized fluorescence spectra for AA-5 in toluene at different concentrations: 10 mg/L (a, red), 50 mg/L (b, blue), 1 g/L (c, green), and 10 g/L (d, black). The excitation wavelength was 310 nm. A 90 degree arrangement between the excitation and detection optics was employed to collect the spectra for the solution with 10 mg/L AA-5 and the front-face arrangement was employed for the other samples.

3.2.2 Time-resolved fluorescence decay experiments

Time-resolved single photon counting (SPC) experiments correspond to fluorescence studies in the time domain rather than the energy domain as is the case for

the steady-state fluorescence experiment. Since AA-5 is a heterogeneous sample, SPC experiments make it possible to differentiate species with similar fluorescence emission spectra but different singlet excited state lifetimes.

3.2.2.1 Determination of the experimental conditions for time-resolved fluorescence studies

Several experimental parameters need to be defined for SPC experiments, such as the fitting method, oxygen quenching, accumulation counts, and data reproducibility. These parameters had to be established for studies with asphaltenes because of the mixture of chromophores in these samples and their high absorbance at the concentrations of interest.

A compound with one type of chromophore shows a mono-exponential fluorescence decay (i.e. a straight line in a semi-log plot). An example of the time-resolved fluorescence decay for a pure compound is shown in Figure 3.5.

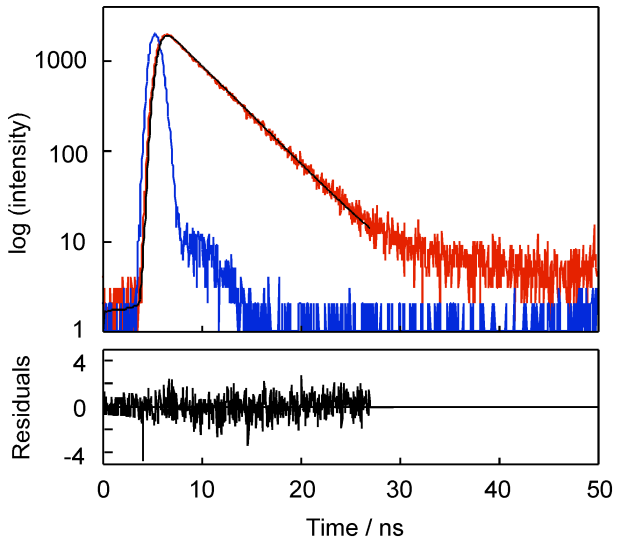

Figure 3.5 Time-resolved fluorescence decay for Ant in toluene (red). The excitation and the emission wavelengths were 335 and 403 nm, respectively. The instrument response function (IRF) is shown in blue. The data are fit to a mono-exponential function (black, $\chi^2 = 0.988$) and the residuals between the fit and the experimental data are shown in the panel below the decay. A 90 degree arrangement between the excitation and detection optics was employed to collect this decay.

In Figure 3.4, the decay was fit to a mono-exponential function (Equation 1.6), yielding one lifetime for the Ant emission with a pre-exponential factor (*A)* value equal to 1. The residuals were randomly distributed and the χ^2 value was between 0.9 and 1.2. These parameters indicate that the mono-exponential function is adequate for the fit of the fluorescence decay for Ant in toluene. The recovered lifetime for Ant in toluene was 3.9 ns, which was in accordance with the literature value of 4.2 ns in toluene.[75]

A mixture with several different chromophores shows a multi-exponential decay if these chromophores have distinguishable lifetimes. An example of the time-resolved fluorescence decay for an AA-5 sample is shown in Figure 3.6.

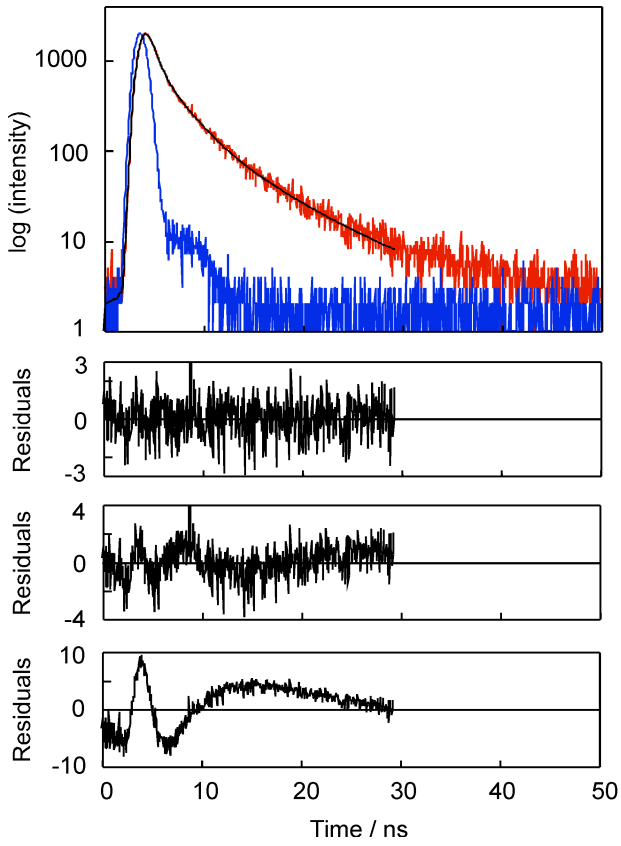

Figure 3.6 Time-resolved fluorescence decay for 10 mg/L AA-5 in toluene (red). The excitation and the emission wavelengths were 335 and 420 nm, respectively. The IRF is shown in blue. The fit of the experimental data to a sum of three-exponentials is shown in black. The residuals between the fit and the experimental data are shown in the panels below the decay, the top panel corresponds to the fit for a sum of three-exponentials with $\chi^2 = 0.989$, the middle panel corresponds to the fit for a sum of two-exponentials with $\chi^2 = 1.359$, and the bottom panel corresponds to the fit for a mono-exponential function with $\chi^2 = 13.468$. A 90 degree arrangement between the excitation and detection optics was employed to collect this decay.

A non-exponential decay was observed for the emission of AA-5 in toluene because AA-5 contains several chromophores which have different lifetimes. The emission decay was fit to a sum of exponentials (Equation 1.6), and the number of exponentials was increased until an acceptable fit was observed. In Figure 3.6, the decay was fit to a mono-exponential and a sum of two-exponentials. In both cases the residuals for the fits of the data significantly deviated from a random distribution, and the χ^2 values

were greater than 1.2, indicating that both functions are not adequate to fit the fluorescence decay. On the other hand, the decay could be fit to a sum of three-exponentials with random residuals and an acceptable χ^2 value. With further increase of the number of exponentials no change in the residuals or improvement of the χ^2 values was observed.

The number of exponentials is related to the number of chromophores with distinguishable lifetimes in a sample. For example, three lifetimes, 0.53 ns, 1.95 ns and 6.19 ns, were recovered from the decay of an AA-5 sample that was fit to a sum of three exponentials (Figure 3.5). Moreover, three *A* values, 0.59, 0.34, and 0.07 were obtained for these three lifetimes. Clearly, AA-5 contains many different chromophores, each lifetime is recovered for a group of chromophores with similar lifetimes, and the *A* value is related to the population of chromophores for each lifetime in the sample.

Oxygen quenches the singlet excited states of most hydrocarbon molecules efficiently,[75] leading to a shortening of the lifetimes for the excited states of these molecules. The singlet excited states of chromophores in asphaltenes are also quenched by oxygen. The time-resolved fluorescence decays for an AA-5 sample were collected for aerated solutions and solutions deaerated by purging them with nitrogen or oxygenated solutions by purging them with oxygen. A summary of the lifetimes recovered under these conditions is shown in Table 3.1.

Table 3.1 Recovered lifetimes and pre-exponential factors for the emission of 100 mg/L AA-5 in toluene with different oxygen content. ($\lambda_{ex/em}$ = 335/420 nm).[a, b, c]

Samples	τ_1 / ns (A_1)	τ_2 / ns (A_2)	τ_3 / ns (A_3)	χ^2
deaerated	0.88 ± 0.04 (0.71 ± 0.05)	3.6 ± 0.1 (0.24 ± 0.02)	15.1 ± 0.5 (0.046 ± 0.004)	1.145
aerated	0.40 ± 0.06 (0.61 ± 0.07)	1.76 ± 0.09 (0.32 ± 0.03)	6.3 ± 0.2 (0.069 ± 0.007)	1.124
oxygenated	0.39 ± 0.08 (0.5 ± 0.1)	1.2 ± 0.1 (0.4 ± 0.1)	2.9 ± 0.2 (0.08 ± 0.02)	1.026

a, the decays were collected with 2,000 counts in the channel of the maximum intensity.
b, errors are obtained from the fit of the experiment decays with the Edinburgh software.
c, all experiments were performed once using the front-face sample holder.

All lifetimes were shortened with the increase in the concentration of oxygen. The longest lifetime (τ_3) was significantly affected by oxygen compared with the shorter lifetimes (τ_1 and τ_2). The larger degree for the shortening of the longest lifetime at a particular oxygen concentration is expected (Equation 1.9). The decrease in the lifetimes between the aerated samples and deaerated samples is moderate and all lifetime measurements for AA-5 samples were performed under aerated condition to avoid working at slightly different concentrations of oxygen, which would introduce a lower degree of precision for the recovered lifetime values.

A control experiment was performed to find the adequate number of counts to be accumulated in the channel of maximum intensity in order to obtain reliable lifetimes for the excited states in the AA-5 samples. Under the same experimental conditions (concentration, temperature, excitation and emission wavelengths), the decays for an AA-5 sample were collected for different numbers of total counts (between 2,000 and 20,000 counts) in the channel with the maximum intensity (Table 3.2).

Table 3.2 Recovered lifetimes and pre-exponential factors for the emission of 15 mg/L AA-5 in toluene with a different number of counts for the channel with maximum intensity ($\lambda_{ex/em}$= 335/420 nm).[a, b]

Counts	τ_1 / ns (A_1)	τ_2 / ns (A_2)	τ_3 / ns (A_3)	τ_4 / ns (A_4)	χ^2
2,000	0.69 ± 0.06 (0.64 ± 0.03)	2.3 ± 0.2 (0.29 ± 0.03)	7.0 ± 0.2 (0.069 ± 0.006)	-	1.171
10,000	0.78 ± 0.02 (0.69 ± 0.01)	2.77 ± 0.06 (0.27 ± 0.01)	8.5 ± 0.1 (0.042 ± 0.002)	-	1.138
	0.47 ± 0.06 (0.48± 0.04)	1.5 ± 0.1 (0.37 ± 0.04)	4.0 ± 0.3 (0.13 ± 0.02)	9.9 ± 0.5 (0.025 ± 0.004)	1.071
20,000	0.81 ± 0.01 (0.69 ± 0.01)	2.77 ± 0.04 (0.26 ± 0.01)	8.54 ± 0.09 (0.042 ± 0.001)	-	1.217
	0.39 ± 0.05 (0.44 ± 0.03)	1.30 ± 0.08 (0.40 ± 0.03)	3.7 ± 0.2 (0.13 ± 0.01)	9.5 ± 0.3 (0.024 ± 0.003)	1.081

a, errors are obtained from the fit of the experimental decays with the Edinburgh software. b, all experiments were performed once using a 90 degree arrangement between the excitation and detection optics.

As the number of accumulation counts in the channel with the maximum intensity was increased, the ability to distinguish between lifetimes was also increased. In Table 3.2, three lifetimes were recovered from the decay collected for 2,000 counts, while four lifetimes could be recovered from the decays collected for 10,000 and 20,000 counts. In addition, the decays with 10,000 counts and 20,000 counts were fit to the sum of four exponentials, yielding better χ^2 values than for the fits of the decays to the sum of three exponentials. This experiment showed that the accumulation of 10,000 counts was sufficient to obtain reliable lifetimes for AA-5 samples because the recovered lifetimes were the same and no improvement of χ^2 value was observed with a further increase of the accumulation counts to 20,000.

Table 3.3 Recovered lifetimes and pre-exponential factors for the emission of AA-5 in toluene at different concentrations ($\lambda_{ex/em}$= 335/420 nm).[a, b]

[AA-5] mg/L	τ_1 / ns (A_1)	τ_2 / ns (A_2)	τ_3 / ns (A_3)	τ_4 / ns (A_4)	χ^2
0.1[c]	0.86 ± 0.02 (0.71 ± 0.01)	3.02 ± 0.06 (0.26 ± 0.01)	9.0 ± 0.2 (0.029 ± 0.002)	-	1.147
0.1[c]	0.33 ± 0.07 (0.41 ± 0.05)	1.24 ± 0.08 (0.43 ± 0.04)	3.7 ± 0.2 (0.14 ± 0.01)	9.8 ± 0.4 (0.024 ± 0.003)	1.042
0.5[c]	0.82 ± 0.02 (0.69 ± 0.01)	2.82 ± 0.06 (0.27 ± 0.01)	8.5 ± 0.1 (0.042 ± 0.002)	-	1.055
0.5[c]	0.33 ± 0.08 (0.40 ± 0.04)	1.19 ± 0.09 (0.42 ± 0.04)	3.5 ± 0.2 (0.15 ± 0.02)	9.3 ± 0.3 (0.024 ± 0.003)	0.992
1[c]	0.83 ± 0.02 (0.70 ± 0.01)	2.86 ± 0.06 (0.25 ± 0.01)	8.5 ± 0.1 (0.042 ± 0.002)	-	1.096
1[c]	0.4 ± 0.1 (0.35 ± 0.05)	1.1 ± 0.1 (0.45 ± 0.07)	3.3 ± 0.2 (0.18 ± 0.02)	9.0 ± 0.3 (0.025 ± 0.003)	1.060
10[c]	0.78 ± 0.02 (0.69 ± 0.01)	2.72 ± 0.06 (0.27 ± 0.01)	8.2 ± 0.1 (0.041 ± 0.001)	-	1.085
10[c]	0.48 ± 0.06 (0.49 ± 0.04)	1.5 ± 0.2 (0.36 ± 0.04)	3.9 ± 0.4 (0.13 ± 0.02)	9.5 ± 0.5 (0.025 ± 0.005)	1.023
50[d]	0.61 ± 0.02 (0.68 ± 0.01)	2.40 ± 0.04 (0.27 ± 0.01)	7.82 ± 0.09 (0.052 ± 0.001)	-	1.187
50[d]	0.30 ± 0.04 (0.56 ± 0.04)	1.31 ± 0.09 (0.32 ± 0.02)	3.6 ± 0.3 (0.11 ± 0.01)	9.1 ± 0.3 (0.021 ± 0.003)	1.082
100[d]	0.63 ± 0.02 (0.69 ± 0.01)	2.45 ± 0.04 (0.27 ± 0.01)	7.95 ± 0.09 (0.039 ± 0.001)	-	1.207
100[d]	0.18 ± 0.04 (0.7 ± 0.2)	1.25 ± 0.05 (0.26 ± 0.03)	3.8 ± 0.2 (0.08 ± 0.01)	9.7 ± 0.4 (0.015 ± 0.002)	0.994
500[d]	0.57 ± 0.02 (0.68 ± 0.02)	2.42 ± 0.04 (0.27 ± 0.01)	7.85 ± 0.09 (0.049 ± 0.001)	-	1.230
500[d]	0.22 ± 0.04 (0.61 ± 0.09)	1.16 ± 0.08 (0.27 ± 0.03)	3.3 ± 0.2 (0.11 ± 0.01)	8.8 ± 0.2 (0.018 ± 0.002)	1.101
1000[d]	0.67 ± 0.02 (0.71 ± 0.01)	2.60 ± 0.05 (0.25 ± 0.01)	8.0 ± 0.1 (0.040 ± 0.001)	-	1.126
1000[d]	0.23 ± 0.06 (0.5 ± 0.1)	1.07 ± 0.08 (0.33 ± 0.04)	3.2 ± 0.1 (0.13 ± 0.01)	8.7 ± 0.2 (0.019 ± 0.003)	1.028

a, errors are obtained from the fit of the experimental decays with the Edinburgh software. b, all experiments were performed once on the same day. c, experiments were performed using a 90 degree arrangement between the excitation source and the detection optics. d, experiments were performed using the front-face sample holder.

From the description above, the number of exponentials that is used to fit the decay is related to the numbers of distinguishable lifetimes in the sample and the accumulation counts for the decay. In order to compare the excited state lifetimes recovered from AA-5 samples at different concentrations, all the decays were fit to the same number of exponentials. In Table 3.3, the decays for AA-5 at 100 and 500 mg/L could be only fit to the sum of four-exponentials with acceptable χ^2 values. While the decays at other concentrations could be fit to either three- or four-exponentials, comparisons for different AA-5 concentrations were done for the data from the fit to the sum of four exponentials.

AA-5 is an inhomogeneous mixture containing different chromophores, which potentially could lead to reproducibility problems. The reproducibility of the recovered lifetimes was tested by measuring ten decays for the same AA-5 solution under the same experimental conditions (temperature, excitation and emission wavelengths, and accumulation counts) and analyzing these decays with the same fitting method. Based on the data shown in Table 3.4, inconsistent results were obtained among some trials. For example, the highest recovered value for τ_1 was 0.42 ± 0.04 ns (trial 4), while the lowest recovered value for τ_1 was 0.26 ± 0.05 ns (trial 5). These values did not overlap within errors. However, none of them could be discarded when the Dixon's Q test with a 90% confidence was applied on the data set of these ten trials. Therefore the data from the ten trials were averaged.

Table 3.4 Recovered lifetimes and pre-exponential factors for the emission of 50 mg/L AA-5 in toluene where the experiment was repeated 10 times for the same sample ($\lambda_{ex/em}$ = 335/420 nm).[a, b]

Trial	τ_1 / ns (A_1)	τ_2 / ns (A_2)	τ_3 / ns (A_3)	τ_4 / ns (A_4)	χ^2
1	0.27 ± 0.04 (0.56 ± 0.06)	1.30 ± 0.08 (0.32 ± 0.02)	3.7 ± 0.2 (0.10 ± 0.01)	9.0 ± 0.4 (0.020 ± 0.003)	1.027
2	0.34 ± 0.06 (0.52 ± 0.04)	1.2 ± 0.1 (0.31 ± 0.03)	3.2 ± 0.2 (0.13 ± 0.02)	8.5 ± 0.3 (0.033 ±0.004)	1.064
3	0.30 ± 0.04 (0.56 ± 0.05)	1.3 ± 0.1 (0.31 ± 0.02)	3.5 ± 0.3 (0.11 ± 0.01)	8.8 ± 0.3 (0.020 ± 0.003)	0.999
4	0.42 ± 0.04 (0.58 ± 0.03)	1.6 ± 0.1 (0.31 ± 0.02)	4.3 ± 0.4 (0.09 ± 0.01)	9.6 ± 0.7 (0.023 ± 0.006)	1.113
5	0.26 ± 0.05 (0.54 ± 0.07)	1.19 ± 0.08 (0.33 ± 0.03)	3.4 ± 0.2 (0.11 ± 0.01)	8.7 ± 0.03 (0.020 ± 0.003)	1.050
6	0.28 ± 0.05 (0.53 ± 0.06)	1.19 ± 0.08 (0.33 ± 0.03)	3.5 ± 0.2 (0.13 ± 0.01)	9.2 ± 0.3 (0.020 ± 0.002)	1.047
7	0.37 ± 0.04 (0.58 ± 0.03)	1.49 ± 0.09 (0.30 ± 0.02)	4.2 ± 0.3 (0.10 ± 0.01)	10.0 ± 0.06 (0.022 ± 0.003)	1.063
8	0.33 ± 0.05 (0.55 ± 0.04)	1.2 ± 0.2 (0.29 ± 0.03)	3.0 ± 0.3 (0.13 ± 0.02)	8.1 ± 0.2 (0.032 ± 0.004)	1.190
9	0.41 ± 0.05 (0.53 ±0.03)	1.4 ± 0.1 (0.33 ± 0.03)	3.7 ± 0.3 (0.12 ± 0.02)	9.4 ± 0.4 (0.024 ± 0.004)	1.106
10	0.36 ± 0.04 (0.58 ± 0.03)	1.53 ± 0.09 (0.32 ± 0.02)	4.4 ± 0.3 (0.09 ± 0.01)	10.5 ± 0.7 (0.011 ± 0.003)	1.050
Mean[c]	0.33 ± 0.06 (0.55 ± 0.02)	1.3 ± 0.2 (0.31 ± 0.01)	3.7 ± 0.5 (0.11 ± 0.02)	9.2 ± 0.7 (0.023 ± 0.006)	-

a, experiments were performed using the front-face sample holder, all experiments were performed on the same sample on the same day. b, errors are obtained from the fit of the experimental decays with the Edinburgh software. c, errors correspond to the standard deviation.

In this thesis, at least five decays were collected for each AA-5 sample and the Dixon's Q test was employed to discard any outlier from a data set with a 90% confidence. The average values of the recovered lifetimes and their *A* values were considered as one result for one independent experiment. At least two independent measurements were done for the data reported below.

To conclude, unless otherwise stated the following procedures were employed for the SPC experiments: aerated samples were used, at least five decays were collected for each sample and all decays were collected with 10,000 counts in the channel with the maximum intensity.

3.2.2.2 Time-resolved fluorescence decays of AA-5 asphaltene at different asphaltene concentrations

Asphaltene aggregates can bring two chromophores into close proximity facilitating energy transfer between them, which leads to a shortening of the lifetimes for the excited states of these chromophores. Therefore, we monitored the changes for the lifetimes of the excited states in AA-5 samples at different AA-5 concentrations. An example for the time-resolved fluorescence decays at different AA-5 concentrations is shown in Figure 3.7.

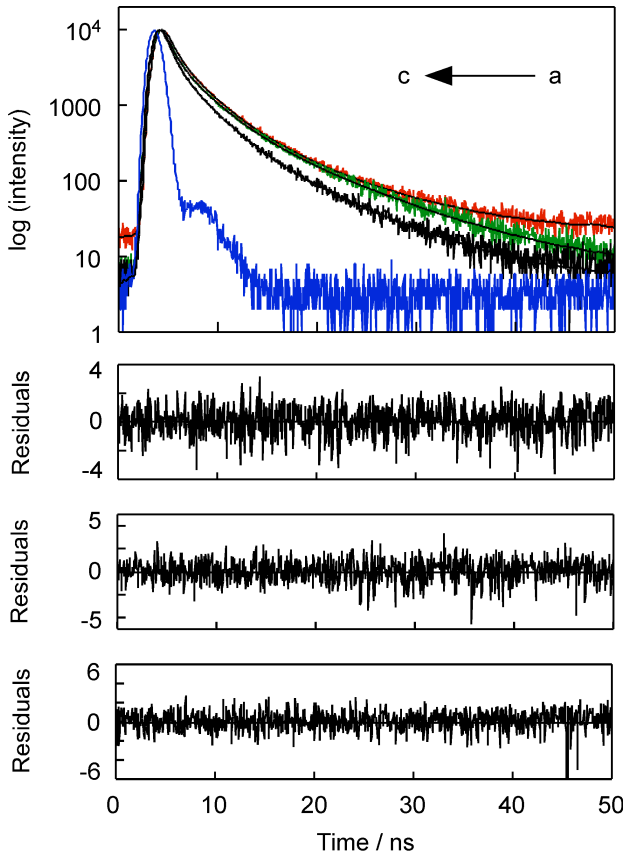

Figure 3.7 Time-resolved fluorescence decays for AA-5 in toluene at different concentrations when the excitation and the emission wavelengths were 335 and 420 nm, respectively. The IRF is shown in blue. The concentrations for AA-5 are: 0.1 mg/L (a, red), 50 mg/L (b, green) and 10 g/L (c, black) and the fits of the experimental data to a sum of four exponentials are shown in black. The residuals between the fits and the experimental data are shown in the panels below the decays (top: 0.1 mg/L, $\chi^2 = 1.083$, middle: 50 mg/L, $\chi^2 = 0.995$, and bottom: 10 g/L, $\chi^2 = 1.051$). A 90 degree arrangement between the excitation and detection optics was employed to collect the decay for the solution with 0.1 mg/L AA-5 and the front-face sample holder was employed for the other samples.

Visually, the decays became faster when the concentration of AA-5 was increased. Numerically, the four lifetimes recovered from these decays were shortened and their pre-exponential factors were changed when the concentration of AA-5 was increased (Table 3.5).

Table 3.5 Recovered lifetimes and pre-exponential factors for the emission of AA-5 in toluene at different AA-5 concentrations ($\lambda_{ex/em}$= 335/420 nm).[a]

[AA-5] mg/L	τ_1 / ns (A_1)	τ_2 / ns (A_2)	τ_3 / ns (A_3)	τ_4 / ns (A_4)	$<\tau>$ / ns
0.1 (2)[b, c]	0.41 ± 0.08 (0.44± 0.03)	1.4 ± 0.1 (0.39 ± 0.04)	3.7 ± 0.2 (0.14 ± 0.02)	9.7 ± 0.4 (0.025 ± 0.003)	1.48 ± 0.09
0.5 (2)[b, c]	0.42 ± 0.09 (0.40 ± 0.05)	1.3 ± 0.1 (0.41± 0.05)	3.5 ± 0.2 (0.16 ± 0.02)	9.2 ± 0.3 (0.025 ± 0.003)	1.5 ± 0.1
1 (6)[b, c]	0.48 ± 0.09 (0.44 ± 0.07)	1.4 ± 0.2 (0.39 ± 0.04)	3.8 ± 0.6 (0.14 ± 0.03)	10 ± 1 (0.026 ± 0.008)	1.51 ± 0.07
10 (9)[b, c]	0.50 ± 0.03 (0.47 ± 0.02)	1.45 ± 0.07 (0.38 ± 0.01)	3.9 ± 0.2 (0.13 ± 0.01)	9.5 ± 0.4 (0.024 ± 0.003)	1.50 ± 0.03
10 (2)[b, d]	0.39 ± 0.09 (0.52 ± 0.03)	1.4 ± 0.1 (0.36 ± 0.02)	4.2 ± 0.2 (0.10 ± 0.01)	10.2 ± 0.4 (0.017 ± 0.002)	1.31 ± 0.06
25 (2)[b, c]	0.50 ± 0.05 (0.49 ± 0.03)	1.5 ± 0.1 (0.36 ± 0.03)	4.0 ± 0.2 (0.12 ± 0.01)	9.9 ± 0.4 (0.023 ± 0.004)	1.51 ± 0.06
25 (2)[b, d]	0.37 ± 0.04 (0.53 ± 0.02)	1.4 ± 0.1 (0.34 ± 0.01)	4.0 ± 0.4 (0.11 ± 0.01)	10.1 ± 0.8 (0.018 ± 0.005)	1.28 ± 0.05
50 (4)[b, c]	0.41 ± 0.07 (0.47 ± 0.02)	1.4 ± 0.1 (0.37 ± 0.01)	3.7 ± 0.3 (0.13 ± 0.01)	9.3 ± 0.5 (0.025 ± 0.003)	1.41 ± 0.07
50 (4)[b, d]	0.31 ± 0.05 (0.55 ± 0.02)	1.30 ± 0.07 (0.32 ± 0.02)	3.6 ± 0.2 (0.11 ± 0.01)	9.2 ± 0.3 (0.022 ± 0.001)	1.17 ± 0.09
100 (4)[b, d]	0.21 ± 0.03 (0.60 ± 0.04)	1.23 ± 0.01 (0.29 ± 0.02)	3.6 ± 0.1 (0.10 ± 0.01)	9.2 ± 0.3 (0.018 ± 0.002)	1.0 ± 0.1
250 (2)[b, d]	0.22 ± 0.05 (0.61 ± 0.02)	1.2 ± 0.1 (0.27 ± 0.02)	3.5 ± 0.3 (0.10 ± 0.01)	9.1 ± 0.3 (0.018 ± 0.003)	0.97 ± 0.09
500 (2)[b, d]	0.25 ± 0.04 (0.59 ± 0.05)	1.24 ± 0.08 (0.29 ± 0.02)	3.6 ± 0.3 (0.10 ± 0.01)	9.4 ± 0.6 (0.018 ± 0.002)	1.04 ± 0.09
1000 (6)[b, d]	0.28 ± 0.05 (0.58 ± 0.05)	1.3 ± 0.1 (0.29 ± 0.03)	3.5 ± 0.2 (0.11 ± 0.02)	8.9 ± 0.3 (0.019 ± 0.003)	1.1 ± 0.1
2500 (2)[b, d]	0.17 ± 0.02 (0.67 ± 0.02)	1.12 ± 0.06 (0.23 ± 0.02)	3.2 ± 0.2 (0.09 ± 0.01)	8.3 ± 0.3 (0.017 ± 0.002)	0.78 ± 0.05
5000 (2)[b, d]	0.16 ± 0.02 (0.69 ± 0.02)	1.10 ± 0.06 (0.22 ± 0.01)	3.2 ± 0.2 (0.08 ± 0.01)	8.2 ± 0.4 (0.013 ± 0.002)	0.70 ± 0.06
10000 (5)[b, d]	0.17 ± 0.01 (0.71 ± 0.02)	1.06 ± 0.01 (0.21 ± 0.01)	2.92 ± 0.09 (0.073 ± 0.003)	7.3 ± 0.2 (0.013 ± 0.002)	0.65 ± 0.03

a, errors for the average of two independent experiments correspond to the average deviation or the propagation of individual error values, whichever is larger. Errors for more than two independent experiments correspond to the standard deviation. b, values in parenthesis correspond to the number of independent experiments. c, experiments were performed by using the sample in a 90 degree arrangement between the excitation beam and the detection optics. d, experiments were performed using the front-face sample holder.

A parameter $<\tau>$ corresponding to the average lifetime for a sample is given by Equation 3.1,

$$<\tau>=\sum_{1}^{i} A_i \tau_i$$

Equation 3.1

where A_i is the pre-exponential factor of component i and τ_i is the lifetime of component i. The average lifetime expressed in Equation 3.1 is an "amplitude average lifetime" that is related to the total integrated area under the decay trace.[48]

The concentration range studied was between 0.1 mg/L and 10 g/L of AA-5. The front-face sample holder was employed to measure the decays for the concentrated samples. The consistency of the results obtained by using the front-face sample holder and a 90 degree arrangement between the excitation and detection optics was tested by measuring decays with both sample holders for three AA-5 concentrations (10, 25, and 50 mg/L), where the absorbance values at the 335 nm were 0.2, 0.6, and 1.0. The average lifetime when using the front-face sample holder was systematically shorter ($\leq$ 0.2 ns) than the $<\tau>$ values obtained from the 90 arrangement. This shortening could be due to the contribution of a small amount of light reflection from the front face sample holder. For this reason, the fluorescence lifetimes for some samples were measured with both sample holders in order identify the trends for the average lifetimes with the AA-5 concentration.

The average lifetimes decreased with the increase of the AA-5 concentrations (Figure 3.8), and this change for the average lifetimes did not depend linearly on the AA-

5 concentration. There were four distinct regions for this dependence (Figure 3.8), where two platform regions with a constant average lifetime were observed, and two different regions where the shortening of the average lifetimes was observed.

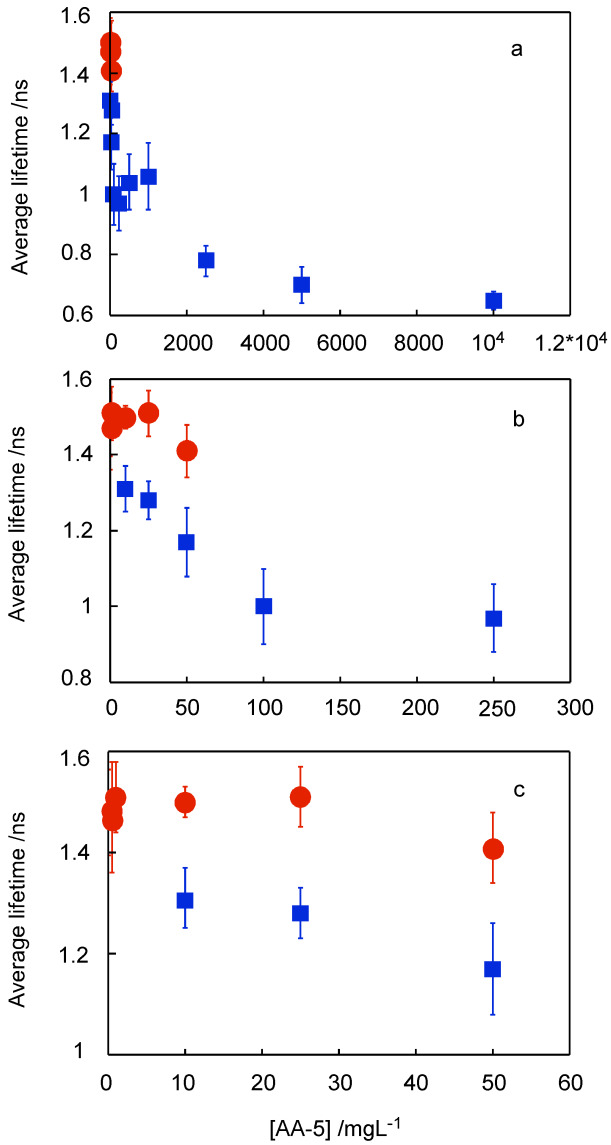

Figure 3.8 Dependence of the average lifetimes for the emission of AA-5 with the AA-5 concentration when the excitation and the emission wavelengths were 335 and 420 nm, respectively: a, [AA-5] = 0.1 mg/L to 10 g/L; b, [AA-5] = 0.1 mg/L to 250 mg/L; c, [AA-5] = 0.1 mg/L to 50 mg/L (red dots: experiments performed using a 90 degree arrangement between the excitation source and the detection system; blue squares: experiments performed using a front-face sample holder).

The average lifetimes were the same within experimental errors for the AA-5 samples with concentrations between 0.1 and 50 mg/L. The individual lifetimes and their *A* values remained the same in this region (Table 3.5). The shortening of the average lifetime for the AA-5 samples started at the AA-5 concentration of 50 to 100 mg/L. In this concentration range, the values for τ_1 were shortened while the other lifetimes (τ_2, τ_3, and τ_4) remained fairly constant. Also, the pre-exponential factor A_1 increased when the AA-5 concentration was raised, while the A_2, A_3 and A_4 values decreased as the AA-5 concentration was increased. This result suggests that some of the chromophores that have longer lifetimes at low AA-5 concentrations have shorter lifetimes at the higher concentrations. The second region with constant average lifetimes occurred between the concentrations of 100 mg/L and 1 g/L of AA-5. In this region, the individual lifetimes and their *A* values did not change. A further shortening of the average lifetimes was observed at AA-5 concentrations higher than 1 g/L, where the four individual lifetimes were shortened but their *A* values did not change significantly with the increase of the AA-5 concentrations.

The fluorescence decays were measured for different combinations of excitation and emission wavelengths to determine if the features for the changes in the average lifetimes with the AA-5 concentration described above were general. The time-resolved fluorescence decays for AA-5 samples at different AA-5 concentrations with excitation and emission wavelengths at 405 nm and 520 nm, respectively, are shown in Figure 3.9.

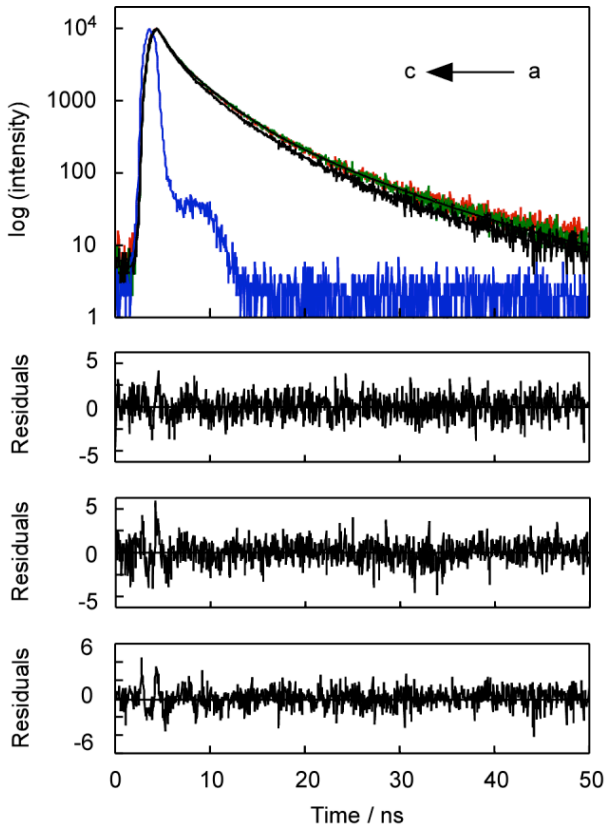

Figure 3.9 Time-resolved fluorescence decays for AA-5 in toluene with different AA-5 concentrations when the excitation and the emission wavelengths were 405 and 520 nm, respectively. The IRF is shown in blue. The concentration of AA-5 is 1 mg/L (a, red), 1 g/L (b, green) and 10 g/L (c, black) and the fits of the experimental data to a sum of three exponentials are shown in black. The residuals between the fits and the experimental data are shown in the panels below the decays (top: 1 mg/L, $\chi^2 = 1.144$, middle: 1 g/L, $\chi^2 = 1.152$, and bottom: 10 g/L, $\chi^2 = 1.106$). A 90 degree arrangement between the excitation and detection optics was employed to collect the decay for the solution with 1 mg/L AA-5 and the front-face arrangement was employed for the other samples.

In contrast to the decays in Figure 3.7 ($\lambda_{ex/em}$ = 355/420 nm) where large changes were observed at different AA-5 concentrations, only small differences were observed when the excitation and the emission wavelengths were 405 and 520 nm, respectively. A similar result was obtained when the excitation and the emission wavelengths were 335 and 520 nm, respectively. The decays collected at 520 nm with both excitation wavelengths were adequately fit to the sum of three exponentials.

Table 3.6 Recovered lifetimes and pre-exponential factors for the emission of AA-5 in toluene at different AA-5 concentrations ($\lambda_{ex/em}$ = 405/520 nm).[a]

[AA-5] mg/L	τ_1 / ns (A_1)	τ_2 / ns (A_2)	τ_3 / ns (A_3)	$<\tau>$ / ns
1 (3)[b, c]	1.26 ± 0.02 (0.60 ± 0.01)	3.51 ± 0.06 (0.35 ± 0.01)	9.5 ± 0.2 (0.051 ± 0.005)	2.46 ± 0.01
10 (4)[b, c]	1.21 ± 0.04 (0.60 ± 0.02)	3.5 ± 0.1 (0.35 ± 0.01)	9.4 ± 0.2 (0.050 ± 0.004)	2.41 ± 0.02
25 (2)[b, c]	1.23 ± 0.03 (0.60 ± 0.02)	3.5 ± 0.1 (0.35 ± 0.01)	9.5 ± 0.3 (0.050 ± 0.006)	2.43 ± 0.02
50 (3)[b, c]	1.23 ± 0.04 (0.61 ± 0.01)	3.50 ± 0.05 (0.35 ± 0.01)	9.4 ± 0.1 (0.051 ± 0.003)	2.42 ± 0.04
100 (3)[b, d]	1.24 ± 0.03 (0.61 ± 0.01)	3.50 ± 0.06 (0.34 ± 0.01)	9.3 ± 0.1 (0.052 ± 0.002)	2.43 ± 0.01
250 (2)[b, d]	1.15 ± 0.03 (0.57 ± 0.01)	3.43 ± 0.08 (0.37 ± 0.01)	9.3 ± 0.2 (0.057 ± 0.005)	2.45 ± 0.02
500 (2)[b, d]	1.22 ± 0.03 (0.58 ± 0.01)	3.53 ± 0.06 (0.36 ± 0.01)	9.4 ± 0.1 (0.059 ± 0.003)	2.54 ± 0.03
1000 (5)[b, d]	1.12 ± 0.08 (0.57 ± 0.02)	3.4 ± 0.2 (0.38 ± 0.01)	9.1 ± 0.3 (0.059 ± 0.004)	2.43 ± 0.07
2500 (2)[b, d]	1.05 ± 0.03 (0.54 ± 0.01)	3.29 ± 0.06 (0.39 ± 0.01)	8.9 ± 0.2 (0.064 ± 0.005)	2.43 ± 0.05
5000 (2)[b, d]	1.0 ± 0.1 (0.54 ± 0.01)	3.2 ± 0.1 (0.39 ± 0.01)	8.6 ± 0.2 (0.065 ± 0.003)	2.32 ± 0.09
10000 (4)[b, d]	1.02 ± 0.09 (0.59 ± 0.02)	3.1 ± 0.1 (0.35 ± 0.02)	8.2 ± 0.1 (0.057 ± 0.005)	2.18 ± 0.08

a, errors for the average of two independent experiments correspond to the average deviation or the propagation of individual error values, whichever is larger. Errors for more than two independent experiments correspond to the standard deviation. b, values in parenthesis correspond to the number of independent experiments. c, experiments were performed by using a 90 degree arrangement between the excitation beam and the detection optics. d, experiments were performed using the front-face sample holder.

In general, the average lifetimes obtained for the excited states in AA-5 that emit at 520 nm were longer than the lifetimes obtained for the detection at 420 nm (Table 3.5, Table 3.6 and Appendix A, Table A.1). Moreover, the average lifetimes obtained for the excited states in AA-5 when the excitation and the emission wavelengths were 405 and

520 nm, respectively, were slightly shorter than that the lifetimes obtained when the excitation and the emission wavelengths were 335 and 520 nm, respectively (Table 3.6 and Appendix A, Table A.1). These observations suggest that the different chromophores are monitored at different combinations of excitation and emission wavelengths. However, the chromophores that emit at 520 nm show some similarities on the trend for the shortening of the average lifetimes with the increase of the AA-5 concentrations. In Figure 3.10 and Figure 3.11, the average lifetimes decreased with the increase of the AA-5 concentrations and this change for the average lifetimes did not dependent linearly on the AA-5 concentration. There were two distinct regions for this dependence, containing one platform region where a constant average lifetime was observed and one region where the shortening of the average lifetime was observed.

At 520 nm, a constant average lifetime was observed over a wide range of AA-5 concentrations from 1 mg/L to 1 g/L. The individual lifetimes and their *A* values remained the same in this region. The shortening of the average lifetimes was observed at AA-5 concentrations higher than 1 g/L, where the three individual lifetimes were shortened but their *A* values did not change significantly with the increase of AA-5 concentrations.

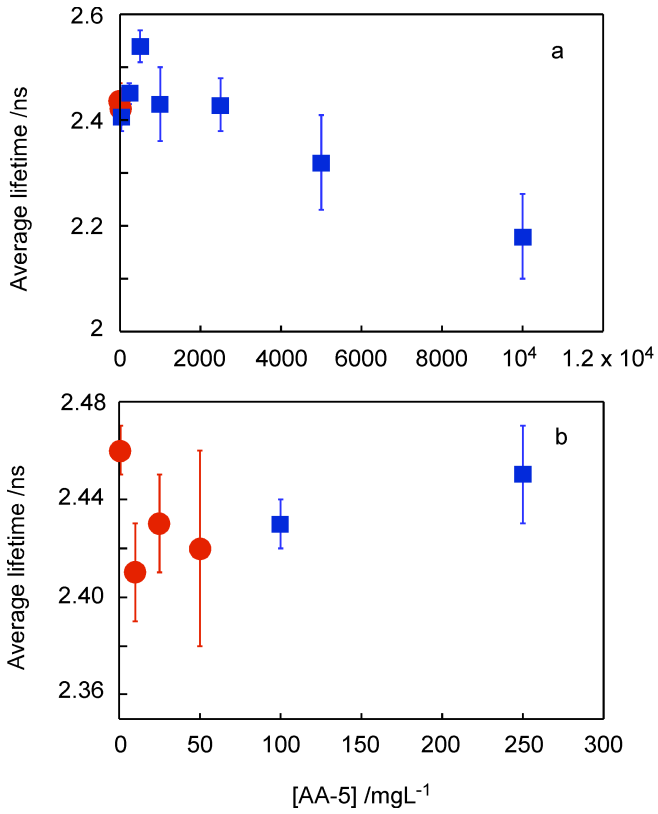

Figure 3.10 Dependence of the average lifetimes for the emission of AA-5 with the AA-5 concentrations when the excitation and the emission wavelengths were 405 and 520 nm, respectively: a, [AA-5] = 1 mg/L to 10 g/L; b, [AA-5] = 1 mg/L to 250 mg/L (red dots: experiments performed using a 90 degree arrangement between the excitation source and the detection system; blue squares: experiments performed using the front-face sample holder).

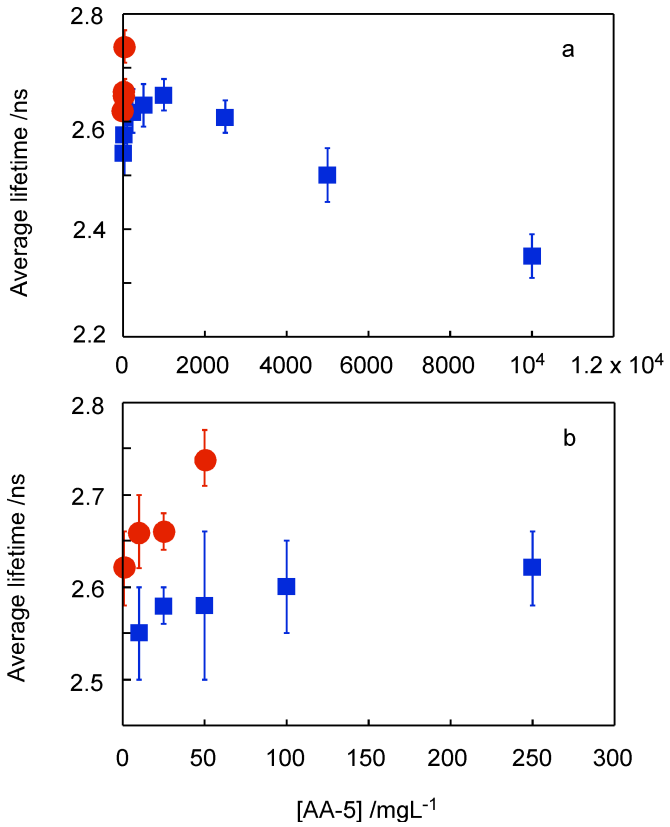

Figure 3.11 Dependence of the average lifetimes for the emission of AA-5 with the AA-5 concentrations when the excitation and the emission wavelengths were 335 and 520 nm, respectively: a, [AA-5] = 1 mg/L to 10 g/L; b, [AA-5] = 1 mg/L to 250 mg/L. (red dots: experiments performed using a 90 degree arrangement between the excitation source and the detection system; blue squares: experiments performed using the front-face sample holder).

3.2.3. Time-resolved emission spectra for AA-5 asphaltene

Time-resolved emission spectra (TRES) are the recovered emission spectra from the time resolved fluorescence decays, where the intensities at specific wavelengths are obtained from integrating the decays between different time intervals. TRES measurements have the advantage over steady state fluorescence measurements that the fluorescence spectrum for particular species at specific time intervals after the excitation pulse is obtained. In the case of the steady-state spectrum the combined emission of all

species in solution is always obtained. An example of the time-resolved fluorescence decays and TRES for an AA-5 sample is shown in Figure 3.12.

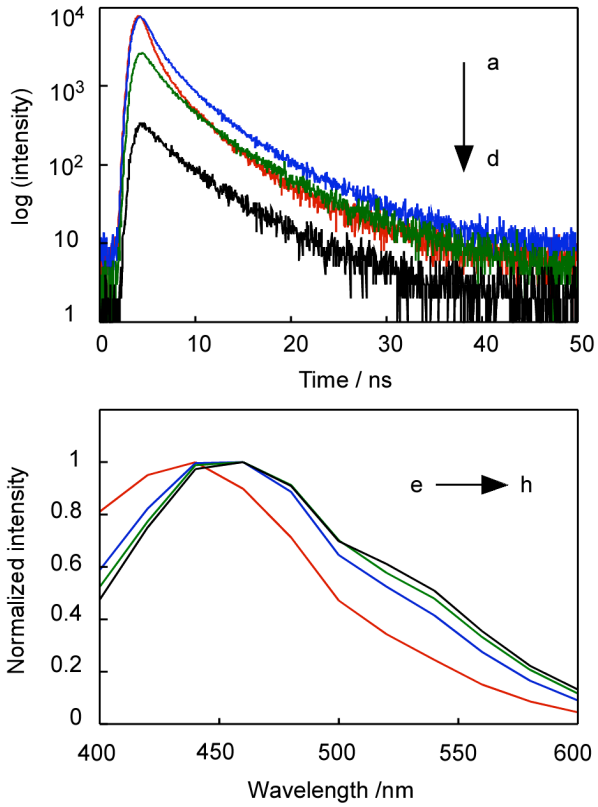

Figure 3.12 Time-resolved fluorescence decays (top) for 10 g/L AA-5 in toluene collected at 400 nm (a, red), 460 nm (b, blue), 520 nm (c, green) and 600 nm (d, black) when the excitation wavelength was 335 nm. The normalized TRES (bottom) obtained from integration for different time intervals: 0-5 ns (e, red), 5-10 ns (f, blue), 10-15 ns (g, green) and 15- 20 ns (h, black). The decays were collected with the front-face sample holder.

The time-resolved fluorescence decays for AA-5 samples were collected from 400 nm to 600 nm. Selected decays are shown in the upper panel of Figure 3.12 in order to show the major differences between the decays. For example the decay collected at 400 nm showed a significantly faster decay than the decay collected at 460 nm. The bottom panel of Figure 3.12 shows the spectra up to a time interval for which no further changes

in the TRES were observed. Integration at longer times led to the same TRES as the last time interval shown in the figure.

The TRES obtained at short delays after excitation pulse corresponds to the combined spectra for the long-lived and the short-lived species. At long delays, the short-lived species had decayed and only the spectra for the long-lived species were collected. Therefore, two typical time intervals, (0-5 ns) and (15-20 ns) are representative for the spectra for short and long delays for samples at different AA-5 concentrations.

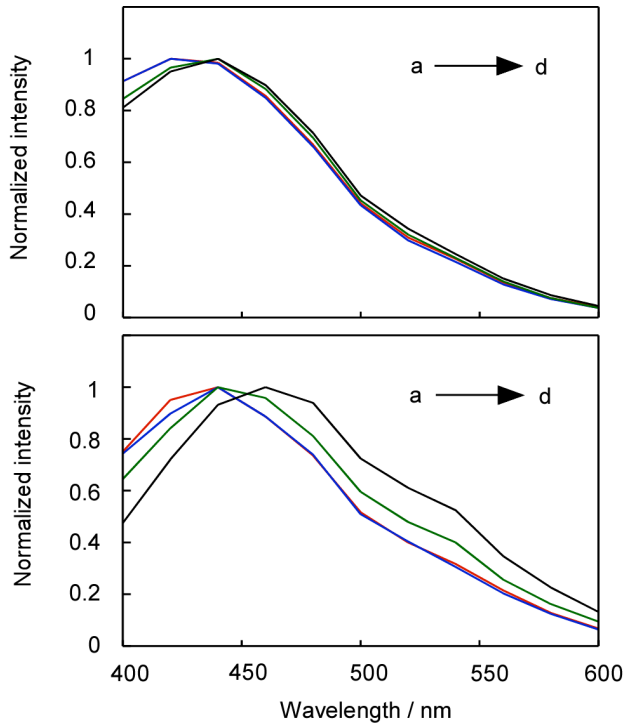

Figure 3.13 Normalized TRES for the AA-5 emission in toluene with an excitation wavelength of 335 nm obtained for different time intervals: 0-5 ns (top) and 15-20 ns (bottom). The concentration of AA-5 was 1 mg/L (a, red), 10 mg/L (b, blue), 1 g/L (c, green), and 10 g/L (d, black). A 90 degree arrangement between the excitation and detection optics was employed to collect the decay for the TRES on the samples with 1 and 10 mg/L AA-5 and the front-face arrangement was employed for the other samples.

When the concentration of AA-5 was increased, the changes observed for the TRES at different concentrations for different time intervals showed different trends. In Figure 3.13, the TRES from the 0-5 ns time interval were slightly red shifted, while the TRES from the 15-20 ns time interval had larger red shifts for the concentrated samples.

3.2.4 Quenching studies by nitromethane of the AA-5 asphaltene emission

$MeNO_2$ is an organic molecule with a small size. It has low excitation energy and has been used as a quencher to quench the excited states of PAHs.[78] Figure 3.14 shows an example of time-resolved fluorescence decays for AA-5 samples with the addition of $MeNO_2$. The decays became faster with the increase of quencher concentrations.

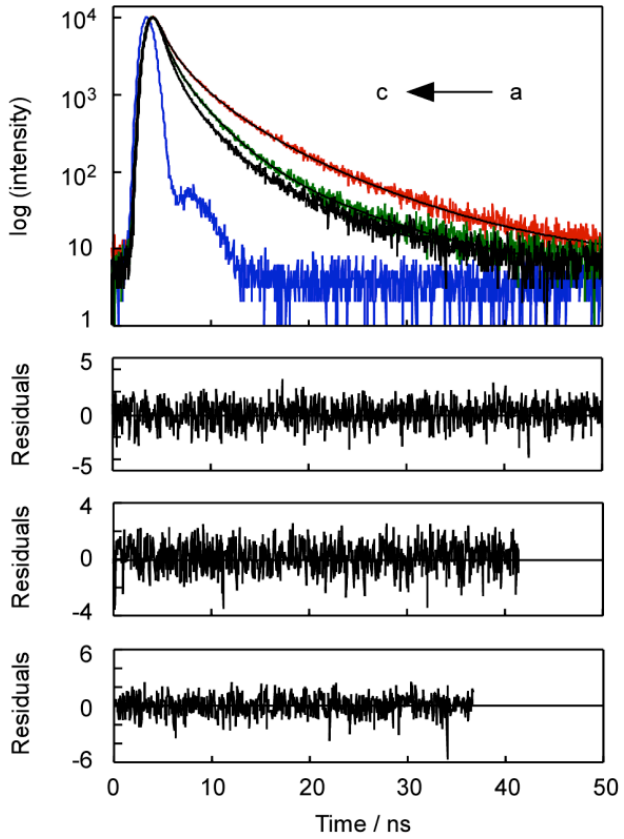

Figure 3.14 Time-resolved fluorescence decays for 1 g/L AA-5 in toluene with the addition of 0 mM (a, red), 28.2 mM (b, green), 71.7 mM (c, black) of $MeNO_2$ when the excitation and emission wavelengths were 335 and 420 nm, respectively. The IRF is shown in blue. The fits of the experimental data to a sum of three exponentials are shown in black. The residuals between the fits and the experimental data are shown in the panels below the decays (top: 0 mM $MeNO_2$, χ^2= 1.134, middle: 28.2 mM $MeNO_2$, χ^2= 1.111, and low: 71.7 mM $MeNO_2$, χ^2= 1.098). The decays were collected with the front-face sample holder.

All decays were fit to the sum of three exponentials. An example of the changes in individual lifetimes and their *A* values for 10 mg/L AA-5 with the addition of $MeNO_2$ is shown in Figure 3.15 and Table B.1 in Appendix B. The similar changes in individual lifetimes and their *A* values were obtained for 1 g/L AA-5 with the addition of $MeNO_2$ (Appendix B, Table B.2).

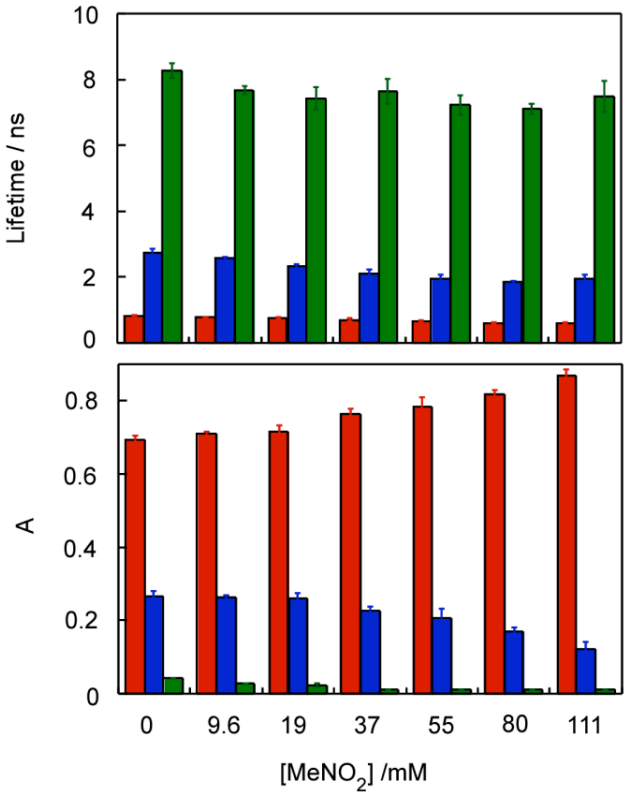

Figure 3.15 Dependence of the lifetimes (top) and their *A* values (bottom) with the concentration of $MeNO_2$ for a 10 mg/L AA-5 solution in toluene. The excitation and emission wavelengths were 335 and 420 nm, respectively (red: the shortest lifetime; blue: the medium lifetime; and green: the longest lifetime).

Individual lifetimes for the excited states of AA-5 were slightly shortened, and the A_1 value was increased at the expense of the other *A* values when the concentration of $MeNO_2$ was increased. The quenching plots were obtained by plotting the decay rate constant (k_{obs}) against the concentrations of $MeNO_2$ (Equation 1.9). The slope of this plot corresponds to the quenching rate constant, k_q, and k_{obs} is equal to the inverse of the average lifetime. The quenching plots for AA-5 at two different concentrations are shown in Figure 3.16.

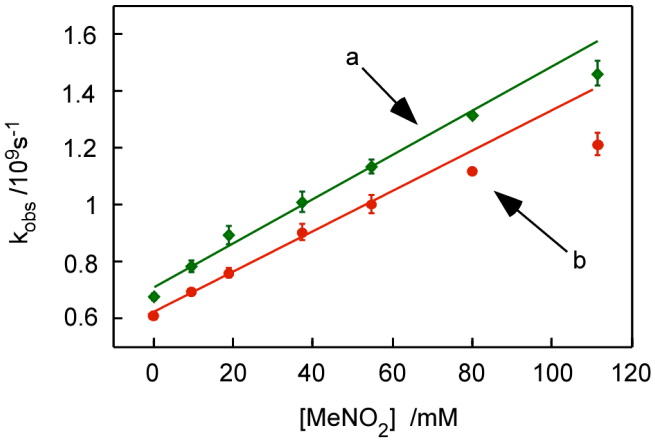

Figure 3.16 Quenching plots for the emission of 1 g/L AA-5 in toluene (a, green) and 10 mg/L AA-5 in toluene (b, red) by $MeNO_2$ when the excitation and emission wavelengths were 335 and 420 nm, respectively.

Slightly curved quenching plots were obtained. This curvature could indicate that the time resolution of the single photon counter was reached at the higher quencher concentrations. For this reason the k_q values were obtained only from the linear portion ([$MeNO_2$] = 0-55mM) of the quenching plots. The k_q values obtained at different excitation and emission wavelengths are summarized in Table 3.7.

Table 3.7 Quenching rate constants for AA-5 by $MeNO_2$. [a, b]

[AA-5]	k_q /10^9 $M^{-1}s^{-1}$		
	$\lambda_{ex/em}$ = 335/420 nm	$\lambda_{ex/em}$ = 335/520 nm	$\lambda_{ex/em}$ = 405/520 nm
10 mg/L	7.3 ± 0.4	1.2 ± 0.2	0.87 ± 0.06
1 g/L	8.1 ± 0.4	1.2 ± 0.1	1.04 ± 0.09

a, quenching rate constants were obtained from the concentration range of $MeNO_2$ between 0 and 55 mM. b, two independent experiments were performed. Errors for the average of two experiments correspond to the average deviation or the propagation of individual errors, whichever is larger.

No difference in the quenching efficiency was observed for AA-5 samples at two different concentrations. Higher quenching rate constants were observed for the

chromophores that emit at 420 nm, suggesting that the $MeNO_2$ quenches the chromophores with high excited state energies more efficiently than those with low excited state energies.

An example of TRES for the AA-5 emission in the absence and presence of $MeNO_2$ is shown in Figure 3.17.

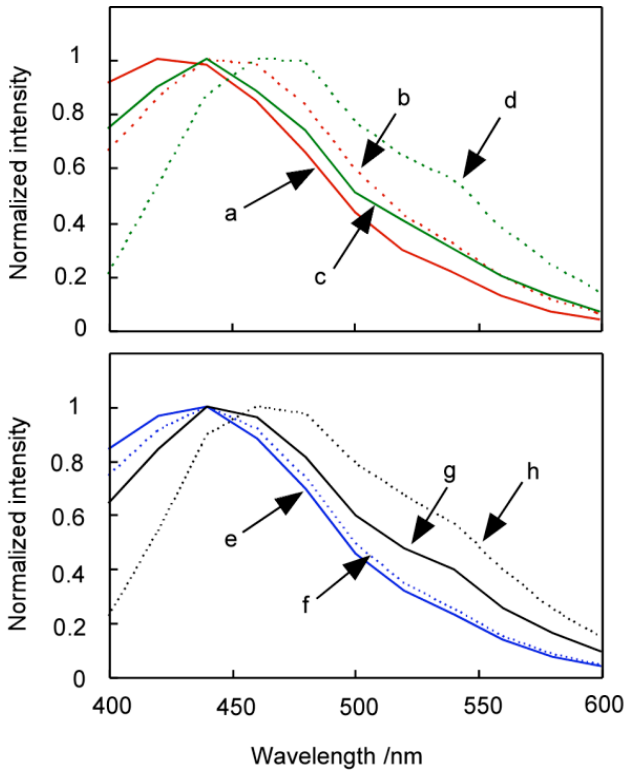

Figure 3.17 Normalized TRES for 10 mg/L AA-5 in toluene (top panel) in the absence of $MeNO_2$ for different time interval: 0-5 ns (a, red solid line) and 15-20 ns (c, green solid line); and in the presence 37 mM $MeNO_2$ for different time intervals: 0-5 ns (b, red dash line) and 15-20 ns (d, green dash line). Normalized TRES for 1 g/L AA-5 in toluene (bottom panel) in the absence of $MeNO_2$ for different time interval: 0-5 ns (e, blue solid line) and 15-20 ns (f, black solid line); and in the presence 19 mM $MeNO_2$ for different time intervals: 0-5 ns (f, blue dash line) and 15-20 ns (g, black dash line). A 90 degree arrangement between the excitation and detection optics was employed to collect the decay for the TRES on the 10 mg/L AA-5 and the front-face sample holder was employed for 1 g/L AA-5.

When the relative intensities were compared, the emission intensities of chromophores that emit at shorter wavelengths (e.g. 400 nm) were quenched more efficiently than the chromophores that emit at longer wavelengths (e.g. 540 nm). Also, the chromophores with long lifetimes (15-20 ns) were quenched more efficiently than those with short lifetimes (0-5 ns). Therefore, the TRES results confirmed that $MeNO_2$ quenches chromophores in AA-5 solutions selectively.

3.3 Discussion

3.3.1 The dependence of fluorescence spectra of AA-5 asphaltene on the asphaltene concentration

The fluorescence spectra for asphaltenes and oil samples were found to be dependent on the concentration of the samples.[41,42,45,47,60,65] A red shift of the fluorescence spectra was observed when the concentration of the samples was increased.

A red shift in the fluorescence spectra is expected due to the energy transfer or quenching of the chromophores in the asphaltenes or oil samples as the concentration of chromophores is increased. At high concentrations, chromophores with different excited state energies are close to each other and the electronic excitation energy can be transferred from the chromophores with higher excited state energies to the chromophores with the lower excited state energies. The latter chromophores emit at longer wavelengths compared to the chromophores with high excited state energies. The electronic excitation energy from the chromophores with high excited state energies can be also quenched by non-fluorescent compounds. Both the energy transfer and quenching

will decrease the emission intensity for the chromophores emitting at short wavelengths, resulting in a red shift of the fluorescence spectra.

A red shift of the fluorescence spectra can also be caused by self-absorption as discussed in section 2.3.5. In Figure 3.2, a red shift of the fluorescence spectrum for 50 mg/L AA-5 was observed using a 90 degree arrangement between the excitation and detection optics compared to the spectrum obtained using the front-face sample holder. Therefore, the red shift might be an artifact for experiments done with a 90 degree arrangement between the excitation and detection optics.[42,45] In several literature reports, the problem of self-absorption was pointed out and alternative methods, such as the use of front face measurements, were employed to avoid this problem in the measurements of fluorescence for concentrated crude oils or asphaltene samples.[41,47,60,65] Front face measurements can be achieved in different ways. First, a square cell can be orientated at an angle other than 90 degree relative to the incident beam. Albuquerque *et al.* worked at a 22 degree angle for the front face measurement.[65] Second, front face measurement can also be archived by using triangular cells, like the one that was employed in Pietraru *et al.*'s work.[41] In Albuquerque *et al.*'s and Pietraru *et al.*'s work, the shape of the fluorescence emission spectra did not change substantially with the increase of the asphaltene concentrations. "Front-surface mode" was mentioned to be used in the fluorescence measurements of oil samples in some works.[47,60] However, the authors did not explain in detail how the "front-surface mode" operates. In these studies a large red shifted and broad spectra were observed for the neat oils samples compare to the diluted oil ones. However, without a detailed description of the experimental set-up one cannot be assure that these red shifts are not due to the self-absorption artifact.

In the present work, the problem of self-absorption was solved by the usage of the front-face sample holder. This design is different from other devices used in the literature reports since not only the angle between the normal and incident beam is changed from 90 degree to 52 degree, but also the reflection of light is minimized by tilting the cell backwards (Figure 2.1). As a result, the self-absorption effect was eliminated and the shape of the fluorescence emission spectra did not change substantially with the increase of the AA-5 concentrations (Figure 3.4). Only a slight red shift of the spectra was observed for concentrated solutions (10 g/L). These results were consistent with Albuquerque *et al.*'s and Pietraru *et al.*'s work.[41,65]

3.3.2 The dependence of fluorescence lifetimes on the concentration of AA-5

Time-resolved fluorescence experiments have been widely used to study crude oils and asphaltenes, but different methods were used to analyze the fluorescence decays. Wang *et al.*[47] and Ralston *et al.*[62] recovered individual lifetimes for the excited states in crude oils or asphaltenes at different dilutions, and the individual lifetimes increased significantly with the increase in dilution. In their experiments, the decays were fit to mono- or the sum of two-exponentials with χ^2 values of approximately 2. The authors mentioned that the increase of the number of exponentials to three did not significantly change the χ^2 values, but they did not show the residuals for the fits. In the present work, three or four lifetimes were required to achieve the acceptable χ^2 values between 0.9 and 1.2. In Figure 3.6, the χ^2 values were 1.359 and 0.989 for the decays were fit to the sum of two- or three-exponentials, respectively. The trends observed in the previous reports[47,62] and in this work are comparable from the qualitative point of view, but the method used

in this work provides more detailed information because of the appropriate χ^2 values obtained.

A different method used is the calculation of the average lifetimes based on the individual lifetimes and their pre-exponential factors. This method is used to study the fluorescence emission of all chromophores in crude oils or asphaltenes. For example, crude oils with different concentrations of aromatic compounds were compared by their average lifetimes.[70] In this work, the average lifetimes of oil samples were increased as the concentration of aromatic components decreased. The content of aromatic components in this case was measured by high performance liquid chromatography (HPLC). Thus, average lifetime measurements were employed to predict the concentration of aromatic compounds in oil samples. In comparison, the analysis of individual lifetimes is not comprehensive because some of the chromophores that have longer lifetimes at low chromophore concentrations have shorter lifetimes at the higher concentrations. Therefore, the average lifetime, which incorporates the emission of all chromophores in asphaltenes, is particularly useful to study the aggregation behaviour at various concentrations of asphaltenes.

A distribution of lifetimes was also used to analyze the fluorescence decays of asphaltene.[46] In this case, the fluorescence decays were fit to a series of exponential functions, and up to 100 lifetime values were recovered. Histograms of lifetime distribution were plot over the range of 0.1-10 ns, and the distribution maximums of lifetime were reported. At similar experimental conditions, the present results (the average lifetime) were comparable with the results obtained from distribution maximum of lifetimes for asphaltenes. For example, at low concentration (16 mg/L asphaltenes),

one distribution maximum of lifetime was observed around 2.3 ns when the excitation and emission wavelength were 467 and 511 nm, respectively.[46] An average lifetime of (2.41 ± 0.02) ns for the 10 mg/L AA-5 was obtained when the excitation and emission wavelengths were 405 and 520 nm, respectively. The difference might be caused by different asphaltene samples and the different excitation and emission wavelengths employed. At high concentrations of asphaltene, ca. 80 mg/L asphaltene, two distribution maximums of lifetime were reported around 0.4 and 2.3 ns.[46] The short lived component was attributed to the asphaltene aggregates by the authors. However, the author ignored a local maximum around 10 ns, which was presented as a small shoulder peak in the lifetime distribution. In the present work, a lifetime around 9 ns was always recovered.

The dependence of fluorescence lifetimes on the concentrations of crude oils or asphaltenes has been reported by several researchers.[14,46,47,62] Different analysis methods lead to the similar results that the lifetimes of excited states in crude oils or asphaltenes increase with increased dilution. Ralston *et al.* pointed out that asphaltenes had a dilution limit of about 10 mg/L and the fluorescence lifetimes did not change with further dilution.[62] Qualitatively the present results agree with this report, where the individual lifetimes and their *A* values were found to be constants for all the dilutions below 10 mg/L for all the emission wavelengths investigated. From these experiments one can conclude that energy transfer is minimal between AA-5 molecules when the concentration of AA-5 is below 10 mg/L. Thus, AA-5 molecules that fluoresce are dispersed as a true solution at these low concentrations.

The shortening of lifetimes for the emission of asphaltene solutions are probably due to two reasons. First, quenching can occur between the chromophores in close

proximity (inside asphaltene aggregates). The term intra-aggregate quenching is employed to describe the quenching that happens between the chromophores located inside the asphaltene aggregates. Intra-aggregate quenching does not rely on diffusion or molecular collisions. Moreover, bimolecular quenching is always possible in solutions with sufficiently high concentrations. This bimolecular reaction corresponds to a different mechanism from intra-aggregate quenching. Bimolecular quenching happens by the collision of two molecules and it is a diffusion controlled process. These two quenching are illustrated in Scheme 3.1.

Scheme 3.1 Intra-aggregates quenching and bimolecular quenching (Shaded stars: excited chromophores, open ellipse: quenchers, and open stars: unexcited chromophores).

The average lifetime for the chromophores emitting at 420 nm had two different AA-5 concentration regions for which a shortening of the average lifetime was observed. This result suggests the involvement of two different quenching mechanisms. The quenching rate constant for bimolecular quenching can be calculated based on the concentration of chromophores (Equation 1.9). Assuming all AA-5 molecules can absorb light, the concentration of chromophores was calculated from the average molecular weight of asphaltene (750 g/mol [14,17]). The quenching rate constant for the region that the average lifetime was shortened from 1.5 ns for 10 mg/L AA-5 to 1.0 ns for 100 mg/L AA-5 was ~10^{12} $M^{-1}s^{-1}$. This value is two orders of magnitude higher than the diffusion control rate constant in toluene (~10^{10} $M^{-1}s^{-1}$ [53]). A bimolecular reaction cannot be faster

than the rate for the encounter of the reagents. Therefore, the quenching that happened at low concentrations of AA-5 is not caused by a collision between two molecules and could only be due to two molecules in close contact at the time of excitation. The only possibility is that the chromophores are quenched by other components inside the AA-5 aggregates.

The same calculation was employed for the lifetime shortening observed at higher AA-5 concentrations (1 g/L-10 g/L). The estimated rate constant is of the same order of magnitude as the diffusional rate constant and for this reason the data were plotted according to Equation 1.9 (Figure B.1 in Appendix B). This reaction is likely to be due to bimolecular quenching and it occurred for the entire excitation/emission wavelength combinations studied (Table 3.8)

Table 3.8 Bimolecular quenching rate constants for the emission of AA-5 quenched by ground state AA-5.[a]

$\lambda_{ex/em}$	335/420 nm	335/520 nm	405/520 nm
k_q / $M^{-1}s^{-1}$	$(3 \pm 1) \times 10^{10}$	$(4.2 \pm 0.5) \times 10^{9}$	$(4.2 \pm 0.2) \times 10^{9}$

a, errors were obtained from linear fit from Appendix B, Figure B.1.

3.3.3 Wavelength dependent aggregation pattern of AA-5 asphaltene

A difference in the shape of steady-state fluorescence spectra of AA-5 samples was observed at different excitation wavelengths, confirming that AA-5 contains different chromophores with different excited state energies (Figure 3.3). Therefore, the behaviour of different chromophores with the increase in the AA-5 concentration can be

investigated by varying the excitation and emission wavelengths in the SPC measurements.

Wang *et al.* measured the fluorescence lifetimes for crude oils at different dilutions and different emission wavelengths with a fixed excitation wavelength.[47] In their results, the dependence of lifetimes on the emission wavelengths was found. In general, the fluorescence lifetimes for a certain dilution were increased as the emission wavelength became longer. Wang *et al.* also found that the relative decrease of the emission lifetimes with crude oil concentration was larger at the shorter wavelengths. Wang *et al.* mentioned that energy transfer could only occur from excited states with higher energies to chromophores with lower energies and therefore energy transfer would lead to emissions at longer wavelengths. As a consequence, the chromophores emitting at short wavelength have higher collisional decay rates compared to those emitting at long wavelengths, resulting in a more significant decrease for the lifetimes collected at short wavelengths than those collected at long wavelengths.

The dependence of the lifetimes on the concentration of AA-5 was studied at different excitation and emission wavelength combinations in this thesis. The results showed that the concentration dependence of the average lifetimes was remarkably different for the emission collected at different wavelengths. For the chromophores emitting at 420 nm, aggregation led the shortening of the average lifetime at low concentrations through intra-aggregate quenching and bimolecular quenching led to another shortening of the average lifetime at high concentrations (Figure 3.8). For the chromophores emitting at 520 nm, the shortening of the average lifetime only happened at high concentrations where the bimolecular quenching was seen to occur (Figure 3.10

and 3.11). Either, these latter chromophores never form aggregates, or not all singlet excited state lifetimes are shortened when the chromophores are aggregated. It is more likely that these chromophores do not form aggregates because not only the average lifetimes but also the individual lifetimes and their *A* values did not change with the increase of the AA-5 concentrations. If some excited state lifetimes were shortened due to the aggregation but some were not, the *A* values should have changed.

As a summary, some components of AA-5 form aggregates easily at low concentrations (i.e. chromophores emitting at 420 nm). Other components of AA-5 may form aggregates at higher concentrations or may not form aggregates for the concentration range investigated. These results are inconsistent with the concept of a critical concentration for aggregate formation. Therefore, the use of parameters such as "CMC" or "CNAC" are not relevant to understand the mechanism for asphaltene aggregation; asphaltenes do not have one concentration at which all its components start to form aggregates.

3.3.4 The accessibility of nitromethane to different chromophores in AA-5 asphaltene aggregates

Ghosh *et al.* reported a fluorescence quenching experiment of asphaltene by chloranil.[69] They found that static quenching between chloranil and asphaltenes occurred, in which only the fluorescence emission intensity was decreased with the increase of quencher concentrations, but the average lifetimes of the asphaltene emission was constant.

In the present work, $MeNO_2$ was used as a quencher to quench the fluorescence emission intensity and singlet excited state lifetimes for AA-5. Quenching requires molecular contact between chromophores and quenchers. When asphaltenes form aggregates, the chromophores are distributed in different locations inside the aggregates. Some chromophores may cluster into the interior of the aggregates, and they may have lower accessibilities to the quencher compared to those chromophores that are located on the external surface of the aggregates or free in toluene. For this reason, quenching studies can be used to reveal the location of a certain chromophore in a microheterogenous solution. Different quenching efficiencies for $MeNO_2$ were expected for the emission of AA-5 as a monomer and when incorporated into AA-5 aggregates. However, the same quenching rate constants were obtained for 10 mg/L and 1 g/L AA-5 with the addition of $MeNO_2$ (Table 3.7). The lower AA-5 concentration was below the threshold for which a shortening of the average lifetime was observed and therefore the solutions only contained AA-5 monomers.

One possible explanation for the equal rate constants at different AA-5 concentrations is that the aggregation does not lead to the formation of a tight structure making it possible for small molecules, like $MeNO_2$, to easily access the interior of the aggregate. Hence, the aggregates could not offer sufficient protection for the chromophores located inside the aggregates. A second possible explanation is that only the chromophores located on the surface of the aggregates or those free in toluene emit and are readily accessible for quenching by $MeNO_2$.

Moreover, the quenching rate constants obtained from different emission wavelengths were very different. The chromophores emitting at 420 nm were quenched

more efficiently than those emitting at 520 nm (Table 3.7), indicating that $MeNO_2$ selectively quench the chromophores with higher excited state energies over those with lower excited state energies. Selective quenching by $MeNO_2$ was reported previously, where a different quenching efficiency was observed for alternant and non-alternant PAHs.[78] The basic idea was that $MeNO_2$ quenched the alternant PAHs composed only of six-membered rings more efficiently than nonalternant PAHs. This report might be helpful for the identification of the composition for AA-5 samples, indicating that the chromophores emitting at 420 nm might contain more alternant PAHs than the chromophores emitting at 520 nm.

3.3.5 The usage of TRES as a tool to study the fluorescence of asphaltene

TRES is firstly reported to be employed in the study of asphaltene aggregates. Instead of the combined emission measured in steady-state fluorescence spectra, the spectra for the species with longer lifetime can be measured as a TRES. Thus, TRES can be used to obtain information about the long lived species.

At a certain AA-5 concentration, a red shift of the TRES was observed at longer decay times (Figure 3.12 bottom panel), indicating that chromophores emitting at longer wavelengths have longer lifetimes. In Figure 3.13, the TRES for the 0-5 ns time window corresponded to the combined emission for all emitting species in the AA-5 samples and the TRES was slightly red shifted with the increase of the AA-5 concentration. The TRES for the 0-5 ns time window is not very sensitive to changes in the AA-5 concentration, which is a similar result to that obtained from the steady-state fluorescence spectra (Figure 3.4). In contrast, the TRES for the 15-20 ns time window are more

sensitive to the changes in the AA-5 concentration. These spectra corresponded to the emission for the long lived species in the AA-5 samples, they were red shifted when the AA-5 concentration was increased. This observation could indicate that the chromophores that emit at shorter wavelengths form aggregates and have shorter lifetimes because the chromophores in the aggregates have shorter lifetimes they do not emit in the 15-20 ns time window.

Moreover, the quenching of AA-5 by $MeNO_2$ was monitored by TRES (Figure 3.17), in which $MeNO_2$ quenched the fluorescence intensity of AA-5 at shorter wavelengths more efficiently than the quenching for the longer wavelengths. This result indicates that $MeNO_2$ selectively quenches the chromophores with the high excited state energies in AA-5 samples, which is in agreement with the quenching rate constants measured at different emission wavelengths.

3.4 Conclusion

Aggregation of AA-5 led to a shortening of the average lifetime for the AA-5 emission. For the chromophores excited and emitting at different wavelengths, the shortening of the average lifetimes occurred for different concentration ranges. For the chromophores with high excited state energies, the average lifetime started to decrease at a relatively low AA-5 concentration (50 mg/L), suggesting that these chromophores are more likely to form aggregates and the shortening of the average lifetime is due to intra-aggregate quenching. For the chromophores with lower excited state energies, the average lifetime decreased at high AA-5 concentrations (> 1 g/L) and this quenching is due to a bimolecular quenching process. Therefore, aggregation is found to be an

inhomogeneous process in AA-5 solutions; not all species form aggregates at the same concentration and different species have different aggregation behaviours.

Fluorescence quenching studies showed that $MeNO_2$ had equal quenching efficiency for the emission of AA-5 in diluted and concentrated solutions, but $MeNO_2$ selectively quenched the chromophores with the high excited state energies over other chromophores.

4. USE OF PYRENE AS AN EXTERNAL FLUORESCENT PROBE TO STUDY THE AGGREGATION OF ASPHALTENES

Some of the results presented in this chapter have been published in the Photochemical & Photobiological Sciences. Reproduced by permission of The Royal Society of Chemistry (RSC) on behalf of the European Society for Photobiology, the European Photochemistry Association, and RSC. This open access article can be accessed via the website (at http://pubs.rsc.org/en/content/articlelanding/2014/pp/c4pp00069b).

4.1 Objectives

Fluorescence can be used to characterize the aggregation of asphaltenes by exploring the intrinsic emission of asphaltenes as was presented in Chapter 3. A different approach is to use externally added probes, which have different fluorescence properties in different microenvironments.[25,50] Py was chosen as an external probe to study the aggregation of asphaltenes because Py might interact with a subset of the components of asphaltenes through π–π stacking interactions.

The incorporation of Py into asphaltene aggregates could lead to quenching of the fluorescence emission of Py because asphaltenes contain some components that have lower excited state energies than Py. In addition, Py might be located in different microenvironments. For example, Py could be located in the homogeneous toluene phase or inside the asphaltene aggregates, leading to different lifetimes for the singlet excited state of Py. The accessibility of small molecules to Py located in the various microenvironments could also be different, and therefore the efficiency for the quenching of the singlet excited state of Py by a quencher might be expected to be different. Such

differential quenching has been previously observed when the singlet excited state of Py was incorporated into host systems such as cyclodoextrins,[56] bile salt aggregates[55,79] or dendrocalixarenes.[57] In the present study, $MeNO_2$ was employed as a quencher for the singlet excited state of Py[78,80,81] in the presence of AA-5. The objective of the quenching studies presented in this chapter was to investigate if Py was incorporated into the AA-5 aggregates and if the aggregates alter the accessibility of small molecules, i.e. the quencher, to an aggregate incorporated probe.

4.2 Results

4.2.1 Steady-state fluorescence of pyrene

4.2.1.1 Fluorescence of pyrene in the presence of AA-5 asphaltene

AA-5 absorbs light over a wide range of the UV-visible spectrum, therefore, no wavelength is available for the exclusive excitation of Py, without concomitantly exciting the asphaltenes. The fluorescence emission spectra of Py in the presence of AA-5 were obtained using an excitation wavelength of 337 nm, and the emission spectra of Py and AA-5 overlapped. For this reason, the steady-state spectra correspond to the combined spectra for the emission of Py and AA-5. The emission from AA-5 could be subtracted from the combined emission spectrum when the AA-5 concentration was very low (top panel in Figure 4.1). The resulting spectra were those for the Py emission and a decrease in the Py fluorescence intensity was observed with the addition of AA-5. Such a decrease could be either due to the quenching of the Py emission by AA-5 or it could be due to the absorption of some of the photons of the excitation beam by AA-5 leading to a smaller fraction of photons being absorbed by Py or it could be due to different

microenvironment for Py that leads to lower quantum yield. At high AA-5 concentrations (10-100 mg/L) the AA-5 emission became prominent relative to the Py emission (bottom panel in Figure 4.1). The Py emission was visible due to its vibrational structure superimposed to the broad emission from AA-5. Such a large contribution of the AA-5 emission make it impossible to determine accurately the emission intensity of Py and any further analysis from the steady-state emission spectra is not warranted.

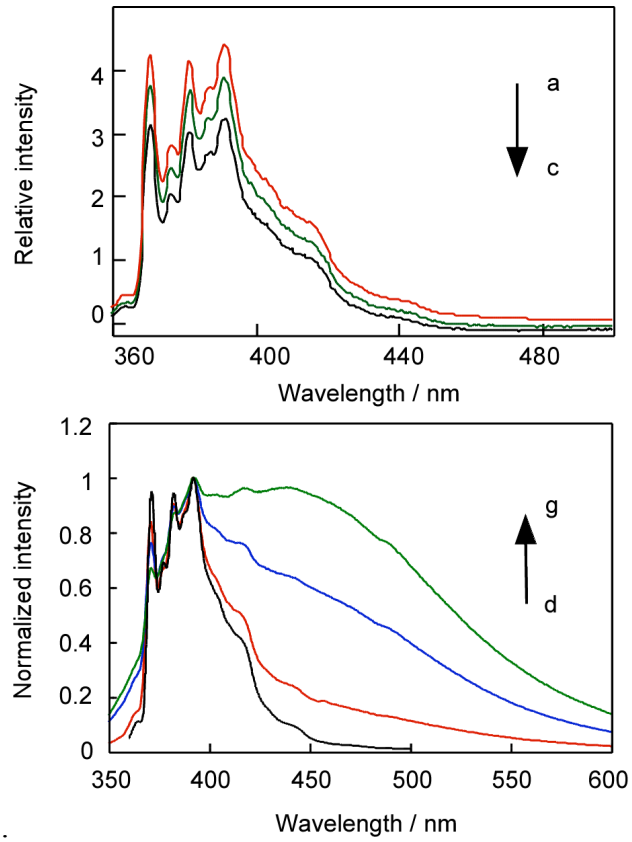

Figure 4.1 Top panel: fluorescence emission spectra for 20 μM Py in toluene (λ_{ex} = 337 nm) with the addition of (a) 0 mg/L, (b) 1 mg/L, (c) 2 mg/L AA-5 when the emission of AA-5 was subtracted from the total spectrum. Bottom panel: normalized fluorescence emission spectra of 20 μM Py in toluene (λ_{ex} = 337 nm) with the addition of (d) 0 mg/L, (e) 10 mg/L, (f) 50 mg/L and (g) 100 mg/L AA-5. The spectra were normalized at the maximum intensity. These spectra were not corrected for the Raman emission from the solvent because this emission was negligible. A 90 degree arrangement between the excitation source and detection optics was employed for all samples with the exception of the solution with 50 and 100 mg/L AA-5 for which the front face sample holder was used.

4.2.1.2 Quenching of the fluorescence of pyrene by nitromethane

The singlet excited state of Py is known to be quenched by $MeNO_2$ in methanol solutions with a rate constant of 3.6×10^9 $M^{-1}s^{-1}$.[80] The fluorescence emission intensity of Py in the absence of AA-5 was observed to decrease with the addition of $MeNO_2$ (Figure 4.2).

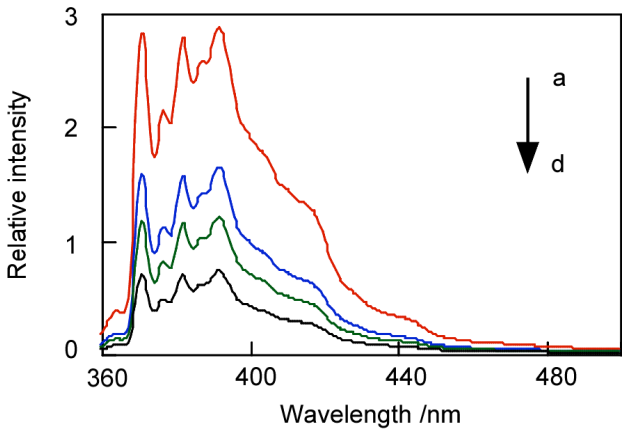

Figure 4.2 Fluorescence emission spectra of 20 μM Py in toluene (λ_{ex} = 337 nm) with the addition of (a) 0 mM, (b) 1.25 mM, (c) 2.5 mM and (d) 5 mM $MeNO_2$. A 90 degree arrangement between the excitation source and detection optics was employed.

In Chapter 3, it was shown that the excited states in AA-5 are quenched by $MeNO_2$. The fluorescence of AA-5 and Py were both quenched by $MeNO_2$. An example of the typical fluorescence emission spectra of Py in the presence of AA-5 with increasing $MeNO_2$ concentrations is shown in Figure 4.3.

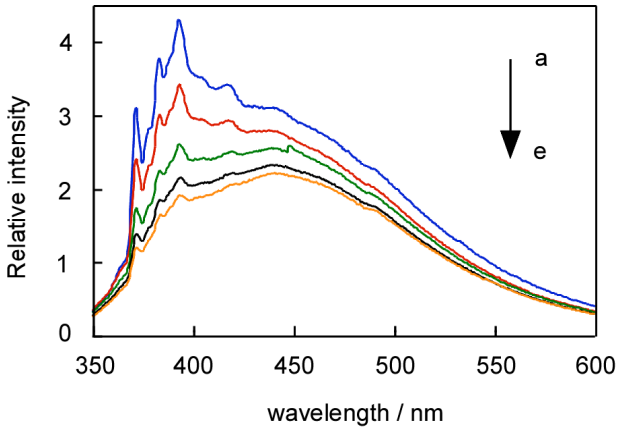

Figure 4.3 Fluorescence emission spectra of 20 μM Py (λ_{ex} = 337 nm) in the presence of 500 mg/L AA-5 quenched by (a) 0 mM, (b) 0.97 mM, (c) 2.9 mM, (d) 4.8 mM and (e) 6.73 mM $MeNO_2$. The front-face sample holder was employed for these measurements.

The fluorescence emission intensity of Py in the presence of AA-5 was observed to decrease with the addition of $MeNO_2$. Although the combined emission from Py and AA-5 was obtained, the emission of Py was quenched more efficiently than the emission from AA-5. This result is consistent with the longer excited state lifetimes for Py than for asphaltene (see below).

4.2.2 Time-resolved fluorescence studies for the pyrene emission in the presence of AA-5 asphaltene

4.2.2.1 Lifetime of pyrene in deaerated solutions

As described in Chapter 3, oxygen efficiently quenches excited states.[48,51] The singlet excited state lifetime of Py in aerated toluene was 18 ns, which was not very different from the longest lifetime (ca. 7 ns) observed for the excited states of AA-5 in aerated samples. After deaeration, an increase of the Py lifetime from 18 ns to 305 ns was observed. This lifetime is much longer than the longest lifetimes (ca. 15 ns) for the

excited states of AA-5 in deaerated samples, making it easier to differentiate the Py emission from the asphaltene emission. Therefore, all the time-resolved fluorescence decays for samples containing Py were acquired using deaerated solutions.

The time-resolved fluorescence decay for Py in toluene was a straight line in the semi-log plot and one lifetime was recovered for the Py singlet excited state. In contrast, non-exponential decays were obtained with an initial fast component for the emission decay of the Py-AA-5 solutions (Figure 4.4). The initial fast component increased as a contribution of the total intensity when the AA-5 concentration was raised. This fast component is due to the fluorescence emission from the excited states of AA-5, and/or the Py inside the AA-5 aggregates (refer to section 4.3.1).

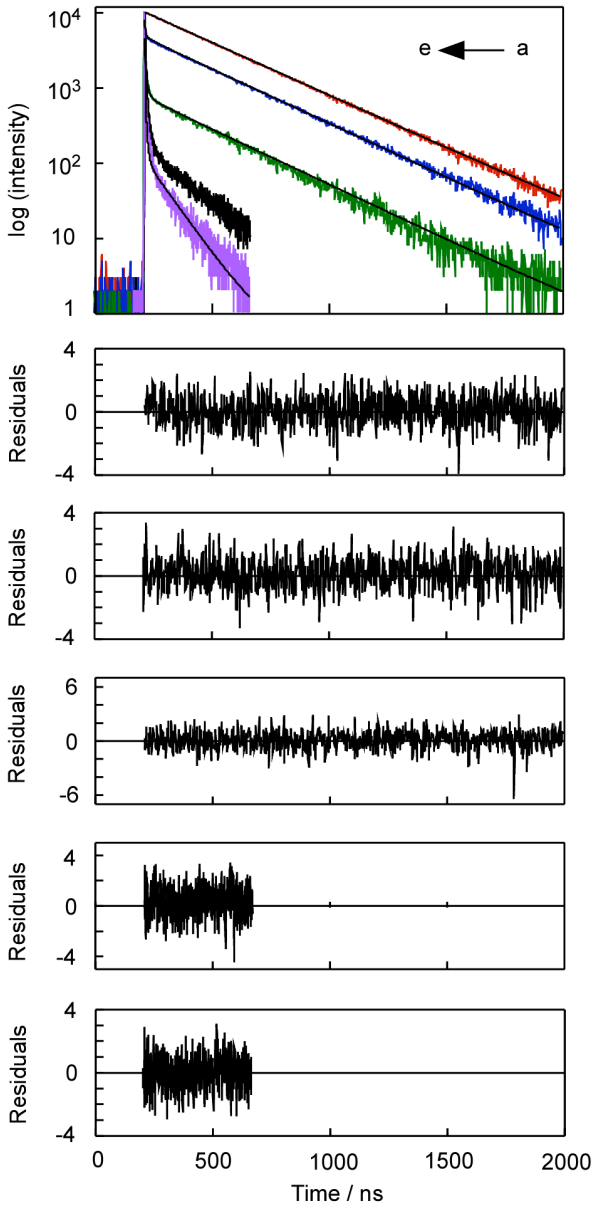

Figure 4.4 Time-resolved fluorescence decays for 20 μM Py in toluene in the presence of AA-5: (a, red) 0 mg/L, (b, blue) 10 mg/L, (c, green) 100 mg/L, (d, black) 500 mg/L and (e, purple) 1 g/L. The excitation and emission wavelengths were 335 and 391 nm, respectively. The fit of the experimental data are shown in black. The residuals between the fit for the sum of four exponentials (b-e) or for the mono-exponential function (a) and the experimental data are shown in the panels below the decays. The IRF is not shown because tail fits were employed (see 2.3.3). A 90 degree arrangement between the excitation source and detection optics was employed for all samples with the exception of the solutions with 100 and 500 mg/L AA-5 for which the front face sample holder was used.

The decays for the Py emission in the presence of AA-5 were fit to a sum of exponentials. Usually, the fit to three or four lifetimes led to adequate residuals and χ^2 values. The longest lifetime corresponds to the decay for the Py emission, while the other shorter lifetimes are related to the fluorescence decays for AA-5.

The number of counts accumulated for the Py emission was decreased as the AA-5 concentration was raised. The primary reason for this observation is that the AA-5 emission contributed more to the total emission as the AA-5 concentration increased. For example, 10,000 accumulation counts for the channel with maximum intensity were collected for the decay of Py in the absence of AA-5, and all the counts in this channel were from the Py emission. In contrast, approximately 100 counts out of the total of 10,000 counts in the channel of maximum intensity were related to the Py emission in the presence of 500 mg/L AA-5 (Figure 4.4). The low relative intensity for the Py emission decreased the reliability of the fit and therefore values for the recovered lifetimes could be less precise. A control experiment was performed with Py in the presence of 500 mg/L AA-5, in which the decay was accumulated for 100,000 counts for the channel with maximum intensity. In this case 1,000 counts were due to the Py emission. Comparison of the decays with the two accumulation times showed that the recovered Py lifetimes were the same. Therefore, for the experiments performed for Py in the presence of AA-5, the total accumulation counts for the channel with maximum intensity was increased until at least 100 counts were obtained for the longest lifetime due to Py emission.

4.2.2.2 Quenching studies of pyrene by AA-5 asphaltene

The longest lifetime in the Py-AA-5 solutions corresponds to the lifetime for the excited state of Py. The decays for the emission of 20 μM Py in the presence of 10, 100, 500, and 1000 mg/L AA-5 were collected and the recovered lifetimes for the singlet excited state of Py are shown in Table 4.1.

Table 4.1 The recovered lifetimes for the emission of 20 μM Py in toluene in the presence of AA-5. The excitation and emission wavelengths were 335 and 391 nm, respectively.[a]

AA-5 / mgL^{-1}	τ / ns
0 (6)[b, c]	305 ± 9
10 (2)[b, c]	306 ± 2
100 (3)[b, d]	276 ± 8
500 (2)[b, d]	186 ± 4
1000 (2)[b, d]	121 ± 1

a, errors for the average of two independent experiments correspond to the average deviation. Errors for more than two experiments correspond to standard deviations. b, values in parenthesis correspond to the number of independent experiments. c, experiments were performed using a 90 degree arrangement between the excitation source and the detection optics. d, experiments were performed using the front-face sample holder.

The fluorescence lifetime for the emission of 20 μM Py in toluene was found to be 305 ± 9 ns, which is shorter than the previously reported value of 337 ns for a 0.1 μM Py in toluene.[71] The shorter lifetime is probably due to an incomplete removal of oxygen when bubbling the solutions with nitrogen. The difference in the lifetimes observed corresponds to an oxygen concentration of 12.5 μM, calculated using Equation 1.9 and a quenching rate constant of 2.5×10^{10} M^{-1} s^{-1} determined previously in cyclohexane.[53]

This low oxygen concentration indicates that with nitrogen bubbling 99.4% of the total of the oxygen in the aerated toluene sample ($[O_2]_{aerated}$ = 2.1 mM)[53] is removed.

A decrease of the Py lifetime from 305 ns in the absence of AA-5 to 121 ns in the presence of 1 g/L AA-5 was observed, indicating that the singlet excited state of Py is quenched by AA-5. A linear quenching plot was obtained for this quenching (Figure 4.5). The quenching rate constant was $(3.7 \pm 0.2) \times 10^9$ $M^{-1}s^{-1}$ determined from the slope of the quenching plot.

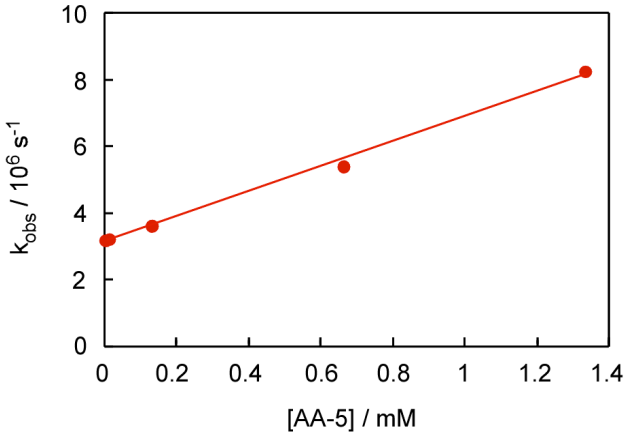

Figure 4.5 Quenching plot for the emission of 20 μM Py in toluene by AA-5, where the molecular weight of AA-5 is assumed to be 750 g/mol.[17,19] The k_{obs} values correspond to the inverse of the longest lifetimes recovered from the fluorescence decays of Py-AA-5 solutions. The line corresponds to the fit of the experimental data to Equation 1.9.

4.2.2.3 Quenching studies of pyrene by nitromethane in the absence and presence of AA-5 asphaltene

The quenching experiments for the excited state of Py by $MeNO_2$ were performed in the presence of different concentrations of AA-5. The objective of these experiments was to determine if the asphaltene aggregates provided a protection of incorporated Py towards the quenching by $MeNO_2$. Py species located in the interior of the aggregates are

expected to have a lower quenching efficiency than those excited Py species located in the homogeneous phase.

In Chapter 3, it was shown that the change in the average lifetime of AA-5 emission with AA-5 concentrations was dependent on the excitation/emission wavelengths used. For this reason, the lifetime dependence with the AA-5 concentration was investigated at the excitation and emission wavelengths employed for Py measurements (λ_{ex} = 335 nm, λ_{em} = 391 nm) (Appendix C, Table C.1). The concentration range of AA-5 investigated was between 10 mg/L and 5 g/L, and the front-face sample holder was employed to measure the emission for the concentrated samples ([AA-5] ≥ 50 mg/L; refer to section 3.2.2.2 for details on the switch between sample holders).

One can notice in Figure 4.6 where the emission wavelength was 391 nm, that the shortening of the average lifetime was more gradual in comparison to the trend shown in Figure 3.8, where the emission wavelength was 420 nm. However, the chromophores that emit at 391 nm showed the same pattern of the dependence of fluorescence lifetimes on the concentration of AA-5 as the chromophores that emit at 420 nm. In particular, for both emission wavelengths, two different regions for the shortening of the average lifetimes were observed. One was observed at low AA-5 concentrations (around 50 mg/L), and a further shortening of the average lifetime was observed at high AA-5 concentrations (above 1 g/L). Two possible quenching mechanisms might be involved as was discussed in section 3.3.2. The lifetime decrease at low AA-5 concentrations is due to intra-aggregate quenching, while the lifetime shortening at high AA-5 concentrations is due to the bimolecular quenching.

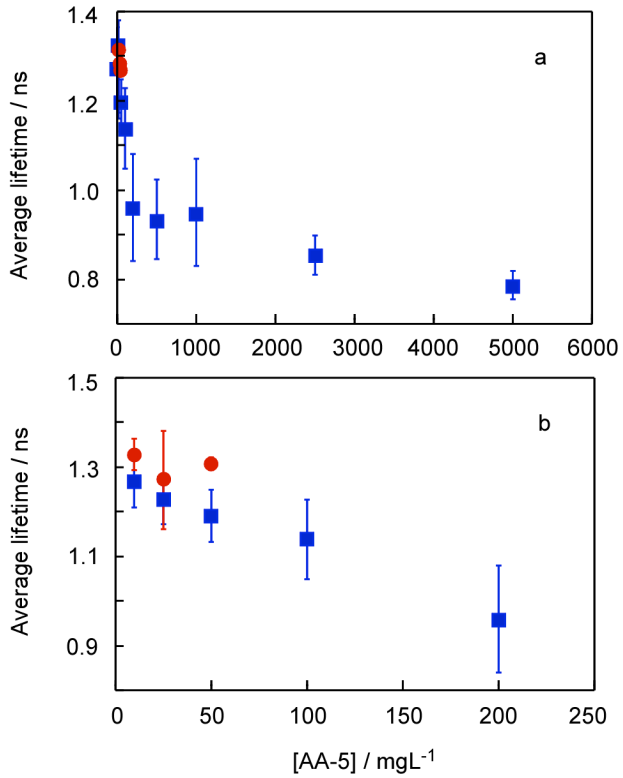

Figure 4.6 The changes of the average lifetimes for the emission of AA-5 when the excitation and emission wavelengths were 335 and 391 nm, respectively: a, [AA-5] = 10 mg/L to 5 g/L; b, [AA-5] = 10 mg/L to 200 mg/L (red dots: experiments performed using a 90 degree arrangement between the excitation beam and the detection optics, blue squares: experiments performed using the front-face sample holder).

In the presence of different concentrations of AA-5, the quenching of the fluorescence of Py by $MeNO_2$ was studied using SPC measurements. An example of the fluorescence decays for the Py-AA-5 solutions with the addition of $MeNO_2$ is shown in Figure 4.7. The simultaneous quenching of the fluorescence of Py and AA-5 was apparent in the steady-state experiments (Figure 4.3). However, in the SPC experiments the quenching of the Py fluorescence can be studied separately from the quenching of the AA-5 emission. The quenching of the Py emission was apparent as a shortening of the longest lifetime in the decay (Fig. 4.7). The shortening of the AA-5 emission lifetimes

was not observable on the time scales used to detect the Py emission because the excited state lifetimes for AA-5 are too short (< 15 ns).

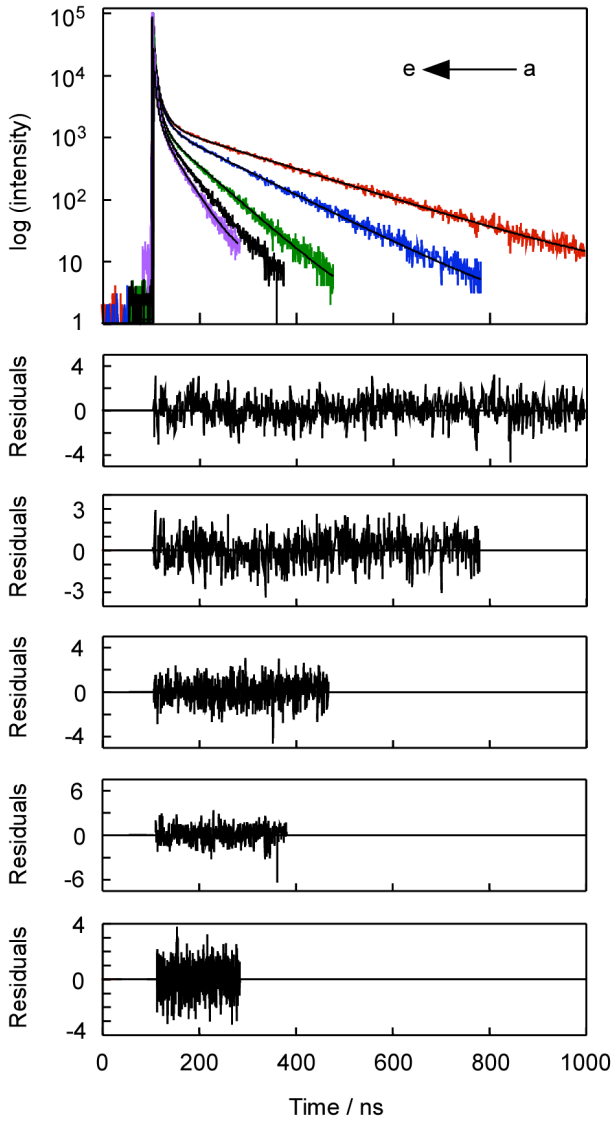

Figure 4.7 Time-resolved fluorescence decays for 20 μM Py in the presence of 500 mg/L AA-5 quenched by $MeNO_2$ when the excitation and emission wavelengths were 335 and 391 nm, respectively. The concentration of $MeNO_2$ was 0 mM (a, red), 0.97 mM (b, blue), 2.9 mM (c, green), 4.8 mM (d, black) and 6.7 mM (e, purple). The fit of the experimental data are shown in black. The residuals between the sum of four exponential fits and the experimental data are shown in the panels below the decays. The front face sample holder was employed for all measurements.

Quenching plots were obtained by plotting the observed decay rate constants against the concentrations of $MeNO_2$, where the observed decay rate constants correspond to the longest lifetimes, which are assigned to the Py emission. Figure 4.8 gives examples for the quenching plots for the quenching of the singlet excited state Py in the presence of AA-5 by $MeNO_2$.

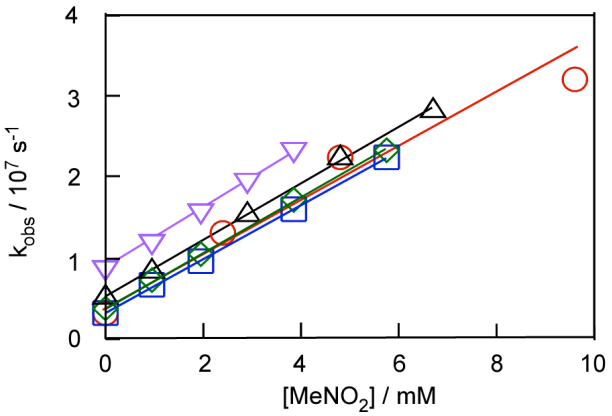

Figure 4.8 Quenching plots for the emission of 20 μM Py by $MeNO_2$ in the presence of 0 mg/L (○), 10 mg/L (□), 100 mg/L (◇) 500 mg/L (△) and 1 g/L (▽) AA-5 ($\lambda_{ex/em}$=335/391 nm). Quenching in the absence of AA-5 was studied for $MeNO_2$ concentrations up to 16 mM. This last point, which falls on the linear relationship, is not included for clarity sake.

The quenching rate constants were calculated from the slopes of the quenching plots (Equation 1.9). The quenching rate constants for the Py emission in the presence of different concentrations of AA-5 were the same within experimental errors (Table 4.2).

Table 4.2 Quenching rate constants for the emission of 20 μM Py in toluene by $MeNO_2$ in the presence of different concentrations of AA-5. The excitation and emission wavelengths were 335 and 391 nm, respectively.

[AA-5] / mgL^{-1}	k_q /10^9 $M^{-1}s^{-1}$
0 (5) [a, b]	3.2 ± 0.4
10 (1) [a, b]	3.3 ± 0.2
100 (3) [a, c]	3.5 ± 0.3
500 (2) [a, c]	3.6 ± 0.2
1000 (1) [a, c]	3.8 ± 0.2

a, values in parenthesis correspond to the number of independent experiments. Errors for the average of two independent experiments correspond to the average deviation or to the propagation of individual error values, whichever is larger. Errors for more than two independent experiments correspond to the standard deviation. Errors for one independent experiment were estimated to be ± 0.2, since the statistical error for an individual experiment was unrealistically small (± 0.01). b, experiments were performed using a 90 degree arrangement between the excitation source and the detection optics. c, experiments were performed using the front-face sample holder.

4.2.3 Effect of the addition of asphaltene and nitromethane to the time-resolved emission spectra of pyrene

The results in Figure 4.1 and Figure 4.3 showed that the steady-state fluorescence spectra for the emission for Py and AA-5 could not be separated, but provided the combined emission from both fluorophores. TRES is a useful tool to differentiate the emission spectra for Py from the spectra for the emission from AA-5 because of the large difference in their excited state lifetimes. The time-resolved fluorescence decays for Py-AA-5 solutions were collected from 360 nm to 450 nm with 5 nm increments. In addition, the bandwidth for the emission monochromator was set to 4 nm (0.5 mm slits) in order to better resolve the Py emission. An example of the TRES for Py in the presence of 100 mg/L AA-5 is shown in Figure 4.9. Similar results were obtained for Py in the presence of 10 mg/L AA-5.

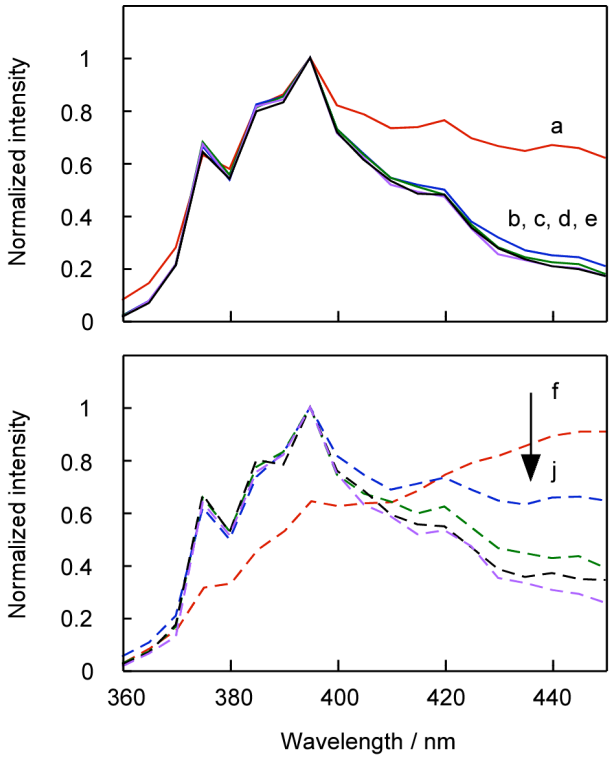

Figure 4.9 Normalized TRES for the emission of 20 μM Py in the presence of 100 mg/L AA when the excitation wavelength was 335 nm. The spectra in the top panel are those in the absence of $MeNO_2$ obtained from the integration between different time windows: 0-38 ns (a, red solid), 38-76 ns (b, blue solid), 76-114 ns (c, green solid), 114-152 ns (d, black solid) and 152-190 ns (e, purple solid). The spectra in the bottom panel are those in the presence of 3.4 mM $MeNO_2$ obtained from the integration between different time windows: 0-10 ns (a, red dash), 10-20 ns (b, blue dash), 20-30 ns (c, green dash), 30-40 ns (d, black dash) and 40-50 ns (e, purple dash). The experiments were performed using the front-face sample holder.

TRES provides more informative spectra than the steady-state fluorescence spectra. At a short delay after the excitation pulse, the TRES showed the combined emission from AA-5 and Py, which is similar to the steady-state fluorescence spectrum (Figure 4.1). This TRES showed the structured emission from Py with a maximum at 390 nm on top of broad emission for AA-5. At longer delays after excitation, the short-lived AA-5 component decayed and only the Py emission was collected in the TRES.

Similarly, in the presence of $MeNO_2$ the TRES at short delays mainly showed the emission from AA-5 where the Py emission appears as weak structured bands. As the delay was increased the Py emission became more defined. The structured spectra for Py around 370 to 400 nm became more clear and the intensities of broad band for AA-5 around 400 to 450 nm were decreased when the delay time became longer, consistent with the smaller contribution from the short lived emission of AA-5.

4.3 Discussion

4.3.1 The changes of the fluorescence lifetime of pyrene in different environments

The objective of this work was to characterize the possible binding between Py and asphaltene aggregates through π–π stacking interactions. It is known that the singlet excited state lifetime of Py changes when it is incorporated into host systems. The increase of fluorescence lifetime of Py was observed when it was incorporated into most host systems such as sodium dodecyl sulfate (SDS) micelles, bile salt aggregates and cyclodextrins.[25,59,82-85] It was also observed that the binding between Py and some host systems, such as the micelle of dendro-calixarene, led to a shortening of the fluorescence lifetime.[57] The lengthening of lifetime could be due to the increased in the rigidity around Py provided by the host system, and a reduction of collisional interactions between the excited state Py and the dissolved oxygen and other quenching impurities in the bulk solution. The shortening of lifetime of Py (from 132 ns to 18 ns) was found to be due to the interaction of the singlet excited state of Py with the dendro-calixarene when Py was complexed to this host.[57] Therefore, the measurement of Py lifetimes in the presence of

AA-5 is the tool employed to investigate the possible binding of Py to the AA-5 aggregates.

From the average lifetime studies of AA-5, it is known that some components in AA-5 form aggregates at low concentrations (< 100 mg/L) (see section 3.3.2 and section 4.2.2.3). The fluorescence lifetime of Py was collected at high AA-5 concentration (ca. 1 g/L) for which the presence of AA-5 aggregates was detected. In the present work, the fluorescence of Py showed a high sensitivity to the presence of AA-5 aggregates, the Py lifetime decreased from 305 ns to 121 ns when the concentration of AA-5 was 1 g/L. The changes of fluorescence lifetime of Py suggest an interaction between Py and AA-5. Two possibilities exist for the shortening of the Py lifetime: i) incorporation into the AA-5 aggregate or ii) bimolecular quenching of the excited state Py in the homogenous phase by AA-5.

Several studies on the incorporation of fluorescent probes into host systems showed that the excited state of the probe decayed with two different lifetimes. The difference is due to the probe partitioning between two different environments, one lifetime is assigned to the fluorescence of probe free in the solvent and the other lifetime is assigned to the fluorescence of probe located inside the host system.[25] Therefore, more than one lifetime is expected for the excited state of Py in the presence of AA-5 aggregates. In the present work, only one long lifetime assigned to the Py emission was recovered from the fluorescence decays for Py-AA-5 solutions. The other shorter lifetimes are assigned to AA-5 emission. This result suggests that all the emission come from Py located in the same environment. The possibilities to be considered are: i) all the Py molecules are located inside the AA-5 aggregates. ii) Py is partitioned into two

different environments. The long lived component corresponds to portion of Py free in toluene and the emission of Py in the aggregate cannot be detected. iii) all the Py molecules are located in toluene.

It is unlikely that all Py molecules are located inside the AA-5 aggregates. In the present work, a shortening of the Py emission lifetime from 305 ns to 276 ns was observed in the presence of 100 mg/L AA-5 solutions. If the lifetime of 276 ns is assigned to the emission of Py located inside the aggregates, a constant lifetime is expected to be obtained because further increases in the concentration of host molecules will not affect the Py located inside the host system. For example, the fluorescence lifetime of Py located inside dendro-calixarene micelles was 18 ns at different concentration of dendro-calixarene.[57] However, a continuous decrease (from 305 ns to 121 ns) in the fluorescence lifetime of Py was observed with the increase of AA-5 concentration (Table 4.1). This observation suggests that the emissive Py species is located in an environment where it senses the increase in the total AA-5 concentration. This observation is inconsistent with Py being located inside an aggregate where its lifetime should not depend on how many other aggregates are present in solution. Therefore, it is unlikely that all Py molecules are located inside the AA-5 aggregates.

It is possible that Py forms complexes with AA-5 aggregates and Py molecules are partitioned between two different environments, i.e. the aggregates and the homogenous phase. The Py molecules that are free in toluene have a long lifetime and these species are detected as the long lived component for the fluorescence decays of the Py-AA-5 solutions. On the other hand, the Py molecules incorporated into AA-5 aggregates can have a “hidden” lifetime, which could be due to two different

mechanisms. First, a tight complex can be formed between the ground state of Py and AA-5 molecules in the aggregates, in which case static quenching can occur during excitation. In this case, Py does not emit and it is not detectable in the SPC experiments. For the static mechanism, a decrease in the steady-state intensity of the fluorophore is observed (see section 1.2.1.5). However this experiment is not possible because the Py and AA-5 emission spectra overlap. Second, the Py excited state is formed in the aggregate but its lifetime is shorter than observed for Py in solution. As mentioned above the continuous decrease in the lifetime of long lived Py fluorescence species is not due to its incorporation into the aggregates. It is also reasonable to expect a shorter lifetime for the aggregate incorporated Py because of the presence of chromophores with excited state energies lower than the excited state energy for Py. However, no intermediate Py lifetime between the lifetime for Py in toluene and the lifetimes for AA-5 was recovered at any AA-5 concentrations. Therefore, if Py is incorporated into the aggregates its excited state lifetime is of the order of the lifetimes for the emission of AA-5. In any event not all Py can be incorporated into the aggregates because of the presence of the long lived Py emission which is assigned to the emission of Py in toluene.

4.3.2 The quenching of the fluorescence lifetime of pyrene in the presence AA-5 asphaltene by nitromethane

The results discussed above suggest that either Py is not incorporated into the AA-5 aggregates or that Py located inside the aggregates are not easily detected. Quenching studies provides the information about the location of emissive Py species and

supported this assignment. Usually, aggregates act as a host system that can protect the excited state of an incorporated fluorescence probe from external quenchers. A smaller quenching rate constant is expected for the excited state Py located inside the aggregates compared to Py that is free in solution. The experimental results showed that the quenching rate constants did not change within error when the concentrations of AA-5 were increased from 0 to 1 g/L (Table 4.2), indicating that the presence of AA-5 aggregates does not offer any protection for the emissive Py from quenchers. Therefore, the results of the quenching experiments are consistent with the assignment that the long lived species corresponds to Py molecules free in toluene.

One should notice that the decay rate constants calculated in the quenching studies were based on the longest lifetime recovered from the decays of Py-AA-5 solutions. Therefore the quenching studies only provide information on this species, which is not protected from quenching. Any Py that might be in the aggregates is not detectable in the SPC experiments and therefore is not involved in the quenching studies.

Based on the experimental results, the detectable Py are located in the homogeneous phase and no Py is detected inside the AA-5 aggregates. These results are probably a reflection of the fact that toluene is a good solvent for Py. In contrast, in aqueous solutions, Py is readily incorporated into host systems with hydrophobic environments, where the host system provides a protection of the excited state of Py from quenching.[25,50] In the organic phase, Py was found to interact with other aromatic systems via $\pi-\pi$ interactions.[59] The fact that a substantial amount of Py is located in the homogeneous phase in the presence of AA-5 suggests that $\pi-\pi$ stacking, if it occurs is

weak. Therefore, Py is not a good probe to study asphaltene aggregation because it could not be efficiently incorporated into the aggregates.

4.3.3 The quenching of the fluorescence lifetime of pyrene by AA-5 asphaltene

As discussed above, the emission of Py located in toluene is quenched by AA-5 via a bimolecular reaction. The quencher might be AA-5 monomers and/or AA-5 aggregates. If only the AA-5 monomers play the role of quencher, a curved quenching plot with a downward curvature is expected because the quencher concentration would not increase linearly with the AA-5 concentration as some AA-5 monomers would be incorporated into aggregates. A curved quenching plot with a downward curvature is also expected if AA-5 aggregates participate in the quenching process with an equal or lower quenching efficiency than the quenching efficiency for AA-5 monomers. However, linear quenching plots were obtained (Figure 4.5) in the present work. One possible explanation is that AA-5 aggregates quench the emission of Py with a higher quenching efficiency than AA-5 monomers, resulting in a linear quenching plot by coincidence. Another possible explanation is that the effective components in AA-5 that quench the fluorescence of Py do not form aggregates at the concentration range investigated.

In the present work, the quenching rate constant was determined to be $(3.7 \pm 0.2) \times 10^9$ $M^{-1}s^{-1}$, which is lower than the diffusion control rate constant in toluene (1.1×10^{10} $M^{-1}s^{-1}$) at 20^oC.[53] The highest possible quenching rate constant for a bimolecular process in solution is the one for a diffusion controlled process. Assuming that AA-5 quenches the excited state of Py with the highest possible rate constant, at least one third of the

AA-5 components quench Py. Any lower fraction of AA-5 would lead to a rate constant above the diffusion controlled limit, a situation that is not possible. In the early literature, Nicodem worked on the quenching of Py by petroleum.[71] The decay rate constants for the fluorescence of Py were found to be proportional in a linear fashion to the concentration of crude oil. The quenching rate constant was reported as $(3.03 \pm 0.06) \times 10^9$ petroleum fraction^{-1}s^{-1} but this unit was not defined. Since the literature value and the value reported in the present work are different in units, a direct comparison cannot be made.

4.4 Conclusion

Py was employed as an external fluorescent probe to explore the importance of π-π interactions between the Py and asphaltenes. Only one fluorescence lifetime was recovered for the Py emission, which is assigned to Py that is free in the homogeneous solvent. No evidence was observed for the complexation between Py and AA-5 aggregates, which means that either the complexes are not detectable with the techniques employed or, more likely, that Py is not incorporated into AA-5 aggregates. This result indicates that π-π interaction might not be the predominate driving force for the incorporation of small aromatic molecules into asphaltene aggregates when they are solubilized in toluene.

5. SUMMARY

The combination of the use of complementary fluorescence techniques was employed to study the aggregation of asphaltenes by exploring the intrinsic emission from asphaltene solutions at different concentrations. Intra-aggregate quenching led to the shortening of the average lifetime for the asphaltene emission. The chromophores with high excited state energies manifested to be more likely to form aggregates at low concentrations (ca. 50 mg/L). The chromophores with lower excited state energies did not aggregate for the concentration range investigated. Therefore, there is no critical concentration at which asphaltenes aggregate. Different components in asphaltene samples revealed different aggregation behaviours. The intrinsic asphaltene emission was quenched by $MeNO_2$, where the accessibility of quenchers to the asphaltene monomers and aggregates were the same. Thus, asphaltene aggregation does not lead to a tight complex and small molecules, such as $MeNO_2$, can easily access the interior of the aggregates. In addition, the selective quenching of $MeNO_2$ on asphaltene molecules could be used to differentiate between chromophores with different excited state energies.

The fluorescence of an externally added Py was investigated in the presence of asphaltenes. No emissive Py species from the interior of asphaltene aggregates were detected. When the Py emission was quenched by $MeNO_2$, the quenching efficiencies determined for Py in the absence or the presence of asphaltene aggregates were the same. These results suggest that Py is not incorporated into asphaltene aggregates and all the emissive Py species are located in the toluene phase, since the access of small molecules is not hindered. Therefore, π-π stacking is not dominant for the incorporation of small aromatic hydrocarbons into asphaltene aggregates when asphaltenes are solubilized in

toluene. Other probes that might be interact with asphaltene aggregates through acid-base interactions or hydrogen bonding might be explored to better probe the different environments in the asphaltene aggregates.

The current results provide information on that the types of components that are relevant for aggregation, and on the "compactedness" of asphaltene aggregates. This information is fundamental in the development of strategies for breaking up of the asphaltene aggregates. Furthermore, based on the current experiments, the optimum experimental conditions could be determined for which the accessibility of small molecules is enhanced, which could be very useful to designing new methods for the hydrogenation of asphaltene.

6. REFERENCES

(1) Leffler, W. L. *Petroleum Refining in Nontechnical Language-4th ed.*; Penn Well Corporation: Tulsa, 2008.

(2) Vassiliou, M. S. *The A to Z of the Petroleum Industry*; The Scarecrow Press, Inc.: Plymouth, 2009.

(3) Alboudwarej, H.; Felix, J.; Taylor, S.; R., B.; Bremner, C.; Breough, C.; Skeates, C.; Baker, A.; Palmer, D.; Pattison, K.; Beshery, M.; Krawchuk, P.; Brown, G.; Triana, J. A. C.; Hathcock, R.; Koerner, K.; Hughes, T.; Kundu, D.; Cardenas, J. L.; West, C. *Oilfield Review* **2006**, *18*, 34-53.

(4) Mullins, O. C.; Sheu, E. Y.; Hammami, A.; Marshall, A. G. *Asphaltenes, Heavy Oils, and Petroleomics*; Springer: New York, 2007.

(5) National Energy Board: Calgary, 2010.

(6) Yarranton, H. W.; Fox, W. A.; Svrcek, W. Y. *Can. J. Chem. Eng.* **2007**, *85*, 635-642.

(7) Akbarzadeh, K.; Hammami, A.; Kharrat, A.; Zhang, D.; Allenson, S.; Creek, J.; Kabir, S.; Jamaluddin, A.; Marshall, A. G.; Rodgers, R. P.; Mullins, O. C.; Solbakken, T. *Oilfield Review* **2007**, *19*, 22- 43.

(8) Long, R. B. In *Chemsitry of Asphaltenes*; Bunger, J. W., Li, N. C., Eds.; American Chemical Society: Washington, 1981, p 17.

(9) Hammami, A.; Ratulowski, J. In *Asphaltenes, Heavey Oils, and Petroleomics*; Mullins, O. C., Sheu, E. Y., Hammami, A., Marshall, A. G., Eds.; Springer: New York, 2007, p 617.

(10) Collins, C. In *Methods in Biotechnology*; Willey, N., Ed.; Humana Press Inc.: Totowa, 2007; Vol. 23, p 99.

(11) Ancheyta, J.; Trejo, F.; Rana, M. S. *Asphaltenes: Chemical Transformation during Hydroprocessing of Heavy Oils*; CRC Press: Boca Raton, 2009.

(12) Mullins, O. C. *Energy Fuels* **2010**, *24*, 2179-2207.

(13) Dechaine, G. P.; Gray, M. R. *Energy Fuels* **2010**, *24*, 2795-2808.

(14) Mullins, O. C. *Energy Fuels* **2009**, *23*, 2845-2854.

(15) Speight, J. G.; Moschopedis, S. E. In *Chemistry of Asphaltenes*; Bunger, J. W., Li, N. C., Eds.; American Chemical Society: Washington, 1981, p 1.

(16) Pinkston, D. S.; Duan, P.; Gallardo, V. A.; Habicht, S. C.; Tan, X.; Qian, K.; Gray, M. R.; Mullen, K.; Kenttamaa, H. I. *Energy Fuels* **2009**, *23*, 5564-5570.

(17) Groenzin, H.; Mullins, O. C. *J. Phys. Chem. A* **1999**, *103*, 11237-11245.

(18) Groenzin, H.; Mullins, O. C. *Energy Fuels* **2000**, *14*, 677-684.

(19) Ruiz-Morales, Y. R., Mullins, O. C. *Energy Fuels* **2008**, *23*, 1169-1177.

(20) Zajac, G. W.; Sethi, N. K.; Joseph, J. T. *Scanning Microscopy* **1994**, *8*, 423-426.

(21) Sharma, A.; Groenzin, H.; Tomita, A.; Mullins, O. C. *Energy Fuels* **2002**, *16*, 490-496.

(22) Ruiz-Morales, Y.; Wu, X.; Mullins, O. C. *Energy Fuels* **2007**, *21*, 944-952.

(23) Agrawala, M.; Yarranton, H. W. *Ind. Eng. Chem. Res.* **2001**, *40*, 4664-4672.

(24) Sheu, E. Y. *J. Phys. Condens. Matter* **1996**, *8*, 125-141.

(25) Kalyanasundaram, K. *Photochemistry in Microheterogeneous Systems*; Academic Press: Orlando, 1987.

(26) Dickie, J. P.; Yen, T. F. *Anal. Chem.* **1967**, *39*, 1847-1852.

(27) Kuznicki, T.; Masliyah, J. H.; Bhattacharjee, S. *Energy Fuels* **2008**, *22*, 2379-2389.

(28) Makhonin, G. M.; Petrov, A. A. *Chem. Technol. Fuels Oils* **1975**, *11*, 942-946.

(29) Shirokoff, J. W.; Siddiqui, M. N.; Ali, M. F. *Energy Fuels* **1997**, *11*, 561-565.

(30) Strausz, O. P.; Mojelsky, T. W.; Lown, E. M. *Fuel* **1992**, *71*, 1355-1363.

(31) Murgich, J.; Abanero, J. A.; Strausz, O. P. *Energy Fuels* **1999**, *13*, 278-286.

(32) Yarranton, H. W. *J. Dispersion Sci. Technol.* **2005**, *26*, 5-8.

(33) Long, J.; Xu, Z.; Masliyah, J. H. *Langmuir* **2007**, *23*, 6182-6190.

(34) Rogel, E.; Leon, O.; Torres, G.; Espidel, J. *Fuel* **2000**, *79*, 1389-1394.

(35) Monte, M. B. M.; Coelho, R. R.; Middea, A. *Pet. Sci. Technol.* **2004**, *22*, 991-1001.

(36) Mostowfi, F.; Indo, K.; Mullins, O. C.; McFarlane, R. *Energy Fuels* **2008**, *23*, 1194-1200.

(37) Andreatta, G.; Goncalves, C. C.; Buffin, G.; Bostrom, N.; Quintella, C. M.; Arteaga-Larios, F.; Perez, E.; Mullins, O. C. *Energy Fuels* **2005**, *19*, 1282-1289.

(38) Zeng, H.; Song, Y. Q.; Johnson, D. L.; Mullins, O. C. *Energy Fuels* **2009**, *23*, 1201-1208.

(39) Betancourt, S. S.; Ventura, G. T.; Pomerantz, A. E.; Viloria, O.; Dubost, F. X.; Zuo, J.; Monson, G.; Bustamante, D.; Purcell, J. M.; Nelson, R. K.; Rodgers, R. P.; Reddy, C. M.; Marshall, A. G.; Mullins, O. C. *Energy Fuels* **2009**, *23*, 1178-1188.

(40) Freed, D. E.; Lisitza, N. V.; Sen, P. N.; Song, Y. Q. In *Asphaltenes, HeaVy Oils and Petroleomics*; Mullins, O. C., Sheu, E. Y., Hammami, A., Marshall, A. G., Eds.; Springer: New York, 2007, p 279.

(41) Pietraru, G.-M.; Cramb, D. T. *Langmuir* **2003**, *19*, 1026-1035.

(42) Ghosh, A. K.; Srivastava, S. K.; Bagchi, S. *Fuel* **2007**, *86*, 2528-2534.

(43) Schneider, M. H.; Andrews, A. B.; Mitra-Kirtley, S.; Mullins, O. C. *Energy Fuels* **2007**, *21*, 2875-2882.

(44) Goncalves, S.; Castillo, J. A.; Fernandez, A.; Acevedo, S. In *19th Congress of the International Commission for Optics: Optics for the Quality of Life*; 1 ed.; SPIE: 2004; Vol. 4829, p 829-830.

(45) Goncalves, S.; Castillo, J.; Fernandez, A.; Hung, J. *Fuel* **2004**, *83*, 1823-1828.

(46) Souza, R. S.; Nicodem, D. E.; Garden, S. J.; Correa, R. J. *Energy Fuels* **2010**, *24*, 1135-1138.

(47) Wang, X.; Mullins, O. C. *Appl. Spectrosc.* **1994**, *48*, 977-984.

(48) Lakowicz, J. R. *Principles of Fluorescence Spectroscopy, Third Edition*; Springer: New York, 2006.

(49) Kalyanasundaram, K.; Thomas, J. K. *J. Am. Chem. Soc.* **1977**, *99*, 2039-2044.

(50) Bohne, C.; Redmond, R. W.; Scaiano, J. C. In *Photochemistry in Organized and Constrained Media*; Ramamurthy, V., Ed.; VCH Publishers: New York, 1991, p 79.

(51) Wardle, B. *Principles and Applications of Photochemistry*; John Wiley, 2009.

(52) Hollas, M.; Chung, M.-A.; Adams, J. *J. Phys. Chem. B.* **1998**, *102*, 2947-2953.

(53) Murov, S. L.; Carmichael, I.; Hug, G. L. *Handbook of Photochemistry*; Marcel Dekker, INC.: New York, 1993.

(54) Xu, W.; Demas, J. N.; DeGraff, B. A.; Whaley, M. *J. Phys. Chem.* **1993**, *97*, 6546-6554.

(55) Ju, C.; Bohne, C. *Photochem. Photobiol.* **1996**, *63*, 60-67.

(56) Dyck, A. S. M.; Kisiel, U.; Bohne, C. *J. Phys. Chem. B* **2003**, *107*, 11652-11659.

(57) Yihwa, C.; Kellermann, M.; Becherer, M.; Hirsch, A.; Bohne, C. *Photochem. Photobiol. Sci.* **2007**, *6*, 525-531.

(58) Kobayashi. N.; Saito, R. H., H.; Hino, Y.; Ueno, A. Osa, T. *J. Chem. Soc. Perkin Trans. 2* **1983**, 1031.

(59) Leyton, P.; Sanchez-Cortes, S.; Garcia-Ramos, J. V.; Domingo, C.; Campos-Vallette, M.; Saitz, C.; Clavijo, R. E. *J. Phys. Chem. B* **2004**, *108*, 17484-17490.

(60) Downare, T. D.; Mullins, O. C. *Appl. Spectrosc.* **1995**, *49*, 754-764.

(61) Mullins, O. C.; Mitra-Kirtley, S.; Zhu, Y. *Appl.Spectrosc.* **1992**, *46*, 1405-1411.

(62) Ralston, C. Y.; Mitra-Kirtley, S.; Mullins, O. C. *Energy Fuels* **1996**, *10*, 623-630.

(63) Ryder, A. G. *Appl. Spectrosc.* **2002**, *56*, 107-116.

(64) Wade, D. A.; Torres, P. A.; Tucker, S. A. *Anal. Chim. Acta* **1999**, *397*, 17-31.

(65) Albuquerque, F. C.; Nicodem, D. E.; Rajagopal, K. *Appl. Spectrosc.* **2003**, *57*, 805-810.

(66) Merino-Garcia, D.; Andersen, S. I. *Pet. Sci. Technol.* **2003**, *21*, 507-525.

(67) Al-Muhareb, E.; Morgan, T. J.; Herod, A. A.; Kandiyoti, R. *Pet. Sci. Technol.* **2007**, *25*, 81-91.

(68) Ryder, A. G. *Appl. Spectrosc.* **2004**, *58*, 613-623.

(69) Ghosh, A. K.; Bagchi, S. *Energy Fuels* **2008**, *22*, 1845-1850.

(70) Ryder, A. G.; Glynn, T. J.; Feely, M.; Barwise, A. J. G. *Spectrochim. Acta, Part A* **2002**, *58*, 1025-1037.

(71) Nicodem, D. E.; da Cunha, M. F. V.; Guedes, C. L. B. *Appl. Spectrosc.* **2000**, *54*, 1409-1411.

(72) Arteaga-Larios, F. C., Ana; Perez, Elias *Energy Fuels* **2005**, *19*.

(73) Yarranton, H. W.; Alboudwarej, H.; Jakher, R. *Ind. Eng. Chem. Res.* **2000**, *39*, 2916-2924.

(74) Yin, C.-X.; Stryker, J. M.; Gray, M. R. *Energy Fuels* **2009**, *23*, 2600-2605.

(75) Ware, W. R. *J. Phys. Chem.* **1962**, *66*, 455-458.

(76) In *EPL-Series Picosecond Pulsed Diode Lasers*; Edinburgh Instruments Ltd.: Livingston, 2008; Vol. Issue 5, December 2008.

(77) In *EPLED 320- EPLED 360 Picosecond Pulsed Light Emitting Diodes*; Edinburgh Instruments Ltd.: Livingston, 2008; Vol. Issue 1, March 2008.

(78) Pandey, S.; Acree, W. E.; Cho, B. P.; Fetzer, J. C. *Talanta* **1997**, *44*, 413-421.

(79) Chen, M.; Gratzel, M.; Thomas, J. K. *J. Am. Chem. Soc.* **1975**, *97*, 2052-2057.

(80) Kleinman, M. H.; Bohne, C. In *Molecular and Supramolecular Photochemistry*; Ramamurthy, V., Schanze, K. S., Eds.; Marcel Dekker Inc.: New York, 1997; Vol. 1, p 391.

(81) Fletcher, K. A.; Pandey, S.; Storey, I. K.; Hendricks, A. E.; Pandey, S. *Anal. Chim. Acta* **2002**, *453*, 89-96.

(82) Meyerhoffer, S. M.; McGown, L. B. *Anal. Chem.* **1991**, *63*, 2082-2086.

(83) Ju, C.; Bohne, C. *J. Phys. Chem.* **1996**, *100*, 3847-3854.

(84) Zhang, Y.; Liu, C.; Shi, W.; Wang, Z.; Dai, L.; Zhang, X. *Langmuir* **2007**, *23*, 7911-7915.

(85) Yin, C.-X.; Tan, X.; Müllen, K.; Stryker, J. M.; Gray, M. R. *Energy Fuels* **2008**, *22*, 2465-2469.

Appendix A

Table A.1 Recovered lifetimes and pre-exponential factors for the emission of AA-5 in toluene at different concentrations ($\lambda_{ex/em}$ = 335/520 nm).[a]

[AA-5] mg/L	τ_1 / ns (A_1)	τ_2 / ns (A_2)	τ_3 / ns (A_3)	$<\tau>$ / ns
1 (4)[b, c]	1.27 ± 0.04 (0.55± 0.01)	3.53 ± 0.09 (0.39 ± 0.01)	9.3 ± 0.2 (0.059 ± 0.009)	2.62 ± 0.04
10 (6)[b, c]	1.26 ± 0.04 (0.54 ± 0.01)	3.52 ± 0.08 (0.39 ± 0.01)	9.4 ± 0.2 (0.063 ± 0.006)	2.65 ± 0.04
10 (2)[b, d]	1.22 ± 0.02 (0.57 ± 0.01)	3.54 ± 0.08 (0.38 ± 0.02)	9.7 ± 0.2 (0.054 ± 0.002)	2.55 ± 0.05
25 (2)[b, c]	1.24 ± 0.04 (0.55 ± 0.02)	3.58 ± 0.09 (0.40 ± 0.01)	9.7 ± 0.2 (0.060 ± 0.006)	2.66 ± 0.02
25 (2)[b, d]	1.19 ± 0.03 (0.54 ± 0.01)	3.45 ± 0.06 (0.40 ± 0.01)	9.4 ± 0.2 (0.060 ± 0.005)	2.58 ± 0.02
50 (2)[b, c]	1.23 ± 0.03 (0.52 ± 0.01)	3.51 ± 0.08 (0.41 ± 0.01)	9.5 ± 0.2 (0.069 ± 0.005)	2.74 ± 0.05
50 (2)[b, d]	1.12 ± 0.06 (0.53 ± 0.01)	3.41 ± 0.08 (0.40 ± 0.02)	9.4 ± 0.2 (0.066 ± 0.009)	2.58 ± 0.08
100 (2)[b, d]	1.06 ± 0.05 (0.51 ± 0.02)	3.4 ± 0.1 (0.42 ± 0.02)	9.2 ± 0.2 (0.071 ± 0.001)	2.60 ± 0.05
250 (2)[b, d]	1.03 ± 0.06 (0.50 ± 0.01)	3.35 ± 0.09 (0.43 ± 0.01)	9.2 ± 0.2 (0.072 ± 0.004)	2.62 ± 0.04
500 (2)[b, d]	1.08 ± 0.05 (0.51 ± 0.02)	3.4 ± 0.1 (0.42 ± 0.01)	9.2 ± 0.2 (0.070 ± 0.006)	2.63 ± 0.03
1000 (4)[b, d]	1.07 ± 0.03 (0.50 ± 0.01)	3.41 ± 0.03 (0.43 ± 0.01)	9.2 ± 0.1 (0.072 ± 0.003)	2.66 ± 0.05
2500 (2)[b, d]	1.02 ± 0.06 (0.50 ± 0.01)	3.3 ± 0.1 (0.42 ± 0.01)	9.1 ± 0.2 (0.076 ± 0.006)	2.61 ± 0.03
5000 (2)[b, d]	0.95 ± 0.07 (0.50 ± 0.01)	3.21 ± 0.07 (0.43 ± 0.01)	8.7 ± 0.1 (0.076 ± 0.006)	2.50 ± 0.05
10000 (2)[b, d]	0.90 ± 0.06 (0.51 ± 0.01)	3.08 ± 0.09 (0.42 ± 0.01)	8.3 ± 0.2 (0.073 ± 0.005)	2.35 ± 0.04

a, errors for the average of two independent experiments correspond to the average deviation or the propagation of individual error values, whichever is larger. Errors for more than two independent experiments correspond to the standard deviation. b, values in parenthesis correspond to the number of independent experiments. c, experiments were performed using a 90 degree arrangement between the excitation source and the detection optics. d, experiments were performed using the front-face sample holder.

Appendix B

Table B.1 Recovered lifetimes and pre-exponential factors for the emission of 10 mg/L AA-5 in toluene with the addition of $MeNO_2$ ($\lambda_{ex/em}$= 335/420 nm).[a, b]

[$MeNO_2$] /mM	τ_1 / ns (A_1)	τ_2 / ns (A_2)	τ_3 / ns (A_3)	$<\tau>$ / ns
0	0.80 ± 0.03 (0.69± 0.01)	2.7 ± 0.1 (0.27 ± 0.01)	8.3 ± 0.2 (0.042 ± 0.001)	1.63 ± 0.04
9.6	0.78 ± 0.02 (0.71 ± 0.01)	2.57 ± 0.05 (0.26 ± 0.01)	7.7 ± 0.1 (0.027 ± 0.001)	1.43 ± 0.02
19.0	0.75 ± 0.02 (0.72 ± 0.02)	2.32 ± 0.08 (0.26 ± 0.01)	7.4 ± 0.3 (0.023 ± 0.006)	1.31 ± 0.03
37.2	0.70 ± 0.03 (0.76 ± 0.01)	2.1 ± 0.1 (0.22 ± 0.01)	7.6 ± 0.4 (0.0122 ± 0.0001)	1.11 ± 0.03
54.8	0.66 ± 0.04 (0.78 ± 0.03)	1.9 ± 0.1 (0.21 ± 0.03)	7.2 ± 0.3 (0.0116 ± 0.0003)	1.00 ± 0.03
79.9	0.61 ± 0.01 (0.81 ± 0.01)	1.84 ± 0.05 (0.17 ± 0.01)	7.1 ± 0.2 (0.0108 ± 0.0001)	0.891 ± 0.006
111.4	0.59 ± 0.02 (0.87 ± 0.02)	1.9 ± 0.1 (0.12 ± 0.02)	7.5 ± 0.5 (0.0103 ± 0.0002)	0.82 ± 0.03

a, errors correspond to the standard deviation. b, experiments were performed using a 90 degree arrangement between the excitation source and the detection optics.

Table B.2 Recovered lifetimes and pre-exponential factors for the emission of 1 g/L AA-5 in toluene with the addition of $MeNO_2$ ($\lambda_{ex/em}$= 335/420 nm).[a, b]

[$MeNO_2$] /mM	τ_1 / ns (A_1)	τ_2 / ns (A_2)	τ_3 / ns (A_3)	$<\tau>$ / ns
0	0.67 ± 0.02 (0.68 ± 0.01)	2.52 ± 0.05 (0.27 ± 0.01)	7.9 ± 0.2 (0.042 ± 0.005)	1.48 ± 0.03
9.6	0.62 ± 0.04 (0.69 ± 0.01)	2.24 ± 0.09 (0.28 ± 0.01)	6.9 ± 0.3 (0.033 ± 0.006)	1.28 ± 0.03
19.0	0.57 ± 0.04 (0.69 ± 0.01)	2.00 ± 0.08 (0.28 ± 0.01)	6.6 ± 0.3 (0.024 ± 0.001)	1.12 ± 0.04
37.2	0.56 ± 0.02 (0.74 ± 0.01)	1.84 ± 0.05 (0.25 ± 0.01)	6.6 ± 0.2 (0.018 ± 0.006)	0.99 ± 0.04
54.8	0.53 ± 0.02 (0.76 ± 0.02)	1.69 ± 0.06 (0.23 ± 0.02)	6.5 ± 0.2 (0.015 ± 0.006)	0.88 ± 0.02
79.9	0.49 ± 0.01 (0.79 ± 0.01)	1.57 ± 0.02 (0.20 ± 0.01)	6.24 ± 0.08 (0.0100 ± 0.0001)	0.760 ± 0.006
111.4	0.46 ± 0.02 (0.83 ± 0.01)	1.57 ± 0.07 (0.16 ± 0.01)	6.3 ± 0.2 (0.0093 ± 0.0002)	0.68 ± 0.02

a, Errors correspond to the standard deviation. b, experiments were performed by front-face arrangements between the excitation source and the detection optics.

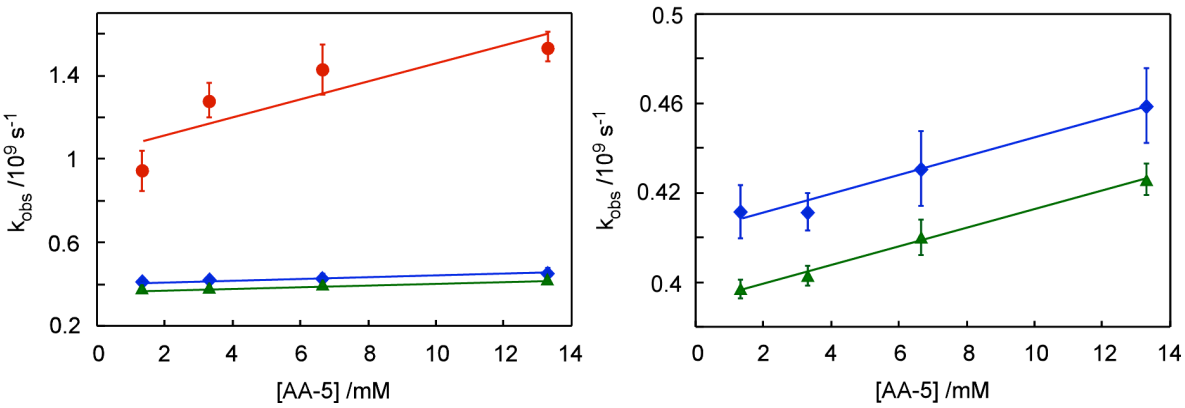

Figure B.1 Bimolecular quenching plots for the emission of AA-5 quenched by ground state AA-5 in toluene, where molecular weight for AA-5 is assumed as 750 g/mol.[14,17] The lines correspond to the fits of the experimental data to Equation 1.9 (red: $\lambda_{ex/em}$ = 335/ 420 nm, blue: $\lambda_{ex/em}$ = 405/ 520 nm, green: $\lambda_{ex/em}$ = 335/ 520 nm).

Appendix C

Table C.1 Recovered lifetimes and pre-exponential factors for the emission of AA-5 in toluene at different concentrations ($\lambda_{ex/em}$ = 335/391 nm).[a]

[AA-5] mg/L	τ_1 / ns (A_1)	τ_2 / ns (A_2)	τ_3 / ns (A_3)	τ_4 / ns (A_4)	$<\tau>$ / ns
10 (3)[a, b]	0.46 ± 0.04 (0.53 ± 0.03)	1.4 ± 0.1 (0.34 ± 0.02)	3.8 ± 0.2 (0.11 ± 0.01)	9.3 ± 0.2 (0.020 ± 0.001)	1.33 ± 0.04
10 (3)[a, c]	0.43 ± 0.04 (0.52 ± 0.03)	1.30 ± 0.08 (0.34 ± 0.02)	3.7 ± 0.3 (0.11 ± 0.01)	9.2 ± 0.4 (0.022 ± 0.002)	1.27 ± 0.06
25 (1)[a, b]	0.4 ± 0.1 (0.49 ± 0.06)	1.2 ± 0.2 (0.37 ± 0.05)	3.5 ± 0.4 (0.12 ± 0.01)	8.9 ± 0.7 (0.023 ± 0.008)	1.3 ± 0.1
25 (1)[a, c]	0.39 ± 0.03 (0.55 ± 0.01)	1.31 ± 0.09 (0.323 ± 0.008)	3.6 ± 0.4 (0.108 ± 0.008)	10 ± 1 (0.022 ± 0.006)	1.22 ± 0.05
50 (3)[a, b]	0.451 ± 0.006 (0.541 ± 0.007)	1.40 ± 0.01 (0.328 ± 0.006)	3.84 ± 0.05 (0.110 ± 0.002)	9.4 ± 0.3 (0.021 ± 0.003)	1.31 ± 0.01
50 (3)[a, c]	0.39 ± 0.06 (0.56 ± 0.02)	1.3 ± 0.1 (0.32 ± 0.01)	3.8 ± 0.2 (0.102 ± 0.006)	9.3 ± 0.3 (0.019 ± 0.001)	1.19 ± 0.06
100 (2)[a, c]	0.36 ± 0.06 (0.585 ± 0.002)	1.36 ± 0.07 (0.307 ± 0.004)	4.0 ± 0.2 (0.093 ± 0.001)	9.6 ± 0.4 (0.015 ± 0.002)	1.14 ± 0.09
200 (1)[a, c]	0.25 ± 0.05 (0.61 ± 0.02)	1.2 ± 0.1 (0.28 ± 0.01)	3.4 ± 0.3 (0.096 ± 0.009)	8.8 ± 0.3 (0.018 ± 0.002)	1.0 ± 0.1
500 (1)[a, c]	0.24 ± 0.04 (0.60 ± 0.02)	1.13 ± 0.07 (0.29 ± 0.02)	3.4 ± 0.2 (0.095 ± 0.008)	8.6 ± 0.2 (0.017 ± 0.001)	0.94 ± 0.09
1000 (2)[a, c]	0.27 ± 0.07 (0.61 ± 0.02)	1.17 ± 0.08 (0.28 ± 0.01)	3.5 ± 0.1 (0.091 ± 0.007)	8.7 ± 0.2 (0.017 ± 0.002)	1.0 ± 0.1
2500 (2)[a, c]	0.23 ± 0.03 (0.61 ± 0.02)	1.08 ± 0.09 (0.29 ± 0.02)	3.2 ± 0.3 (0.090 ± 0.007)	8.2 ± 0.5 (0.015 ± 0.004)	0.85 ± 0.04
5000 (2)[a, c]	0.25 ± 0.02 (0.64 ± 0.01)	1.05 ± 0.05 (0.264 ± 0.008)	3.0 ± 0.2 (0.085 ± 0.004)	7.4 ± 0.4 (0.014 ± 0.003)	0.79 ± 0.03

a, values in parenthesis correspond to the number of independent experiments with 5 repeated measurements each time. Errors for the average of two independent experiments correspond to the average deviation or the propagation of individual error values, whichever is larger. Errors for more than two independent experiments correspond to the standard deviation. b, experiments were performed by using the sample in the 90 degree arrangement between the excitation beam and the detection optics. c, experiments were performed using the front-face sample holder.